The anatomy and relationships of *Piscobalaena nana* (Cetacea, Mysticeti), a Cetotheriidae *s.s.* from the early Pliocene of Peru

Virginie BOUETEL
Christian de MUIZON
Département Histoire de la Terre, UMR 5143 (MNHN, CNRS, UPMC),
Muséum national d'Histoire naturelle, case postale 38,
57 rue Cuvier, F-75231 Paris cedex 05 (France)
muizon@mnhn.fr

Bouetel V. & Muizon C. de 2006. — The anatomy and relationships of *Piscobalaena nana* (Cetacea, Mysticeti), a Cetotheriidae *s.s.* from the early Pliocene of Peru. *Geodiversitas* 28 (2) : 319-395.

ABSTRACT
Piscobalaena nana Pilleri & Siber, 1989 is a small fossil baleen-bearing mysticete from the early Pliocene of the Pisco Formation, Peru. The holotype of this species is an incomplete skull (lacking the vertex) with associated tympanics. The description of five remarkably preserved new specimens of this taxon (three of them associated with partial post-cranial skeletons) provides the opportunity to understand the intraspecific variation within one single fossil mysticete species. These specimens constitute a partial ontogenetic series including one sub-adult animal, three adults and one old individual. *Piscobalaena nana* is compared to *Nannocetus eremus* Kellogg, 1929, *Cetotherium rathkei* Brandt, 1843, *Herpetocetus sendaicus* (Hatai, Hayasaka & Masuda, 1963) and *Metopocetus durinasus* Cope, 1896, which are similar in morphology and age to the Peruvian species. A parsimony analysis of 101 morphological characters of the skull, auditory area and dentary tested on 23 taxa confirms the paraphyly of the Cetotheriidae as traditionally defined. It also suggests that six (*Piscobalaena*, *Herpetocetus*, *Metopocetus*, *Cetotherium*, *Nannocetus*, *Mixocetus*) of the 12 studied fossil baleen mysticetes constitute a clade: the Cetotheriidae *s.s.* Its monophyly is supported by 10 characters of the skull (e.g., ascending processes of the maxillae contacting medially or very approximated at apex; lateral edges of nasals strongly convergent posteriorly; supraorbital process of the frontal anteriorly oriented), and five characters of the auditory area (e.g., anterior edge of facial foramen on the internal acoustic meatus is notched [slightly to deeply] for the passage of the greater petrosal nerve). The Cetotheriidae share with the Balaenopteridae the presence of an interdigitation of the rostral and cranial bones such as the posteriorly elongated ascending process of the maxilla. This condition reinforces the cranial architecture and could suggest a similar engulfment way of feeding as observed in the Balaenopteridae.

KEY WORDS
Mammalia,
Cetacea,
Mysticeti,
Cetotheriidae,
Piscobalaena nana,
early Pliocene,
Peru,
anatomy.

RÉSUMÉ
Anatomie et affinités de Piscobalaena nana *(Cetacea, Mysticeti), un Cetotheriidae* s.s. *du Pliocène inférieur du Pérou*.
Piscobalaena nana Pilleri & Siber, 1989 est un petit mysticète à fanons du Pliocène inférieur de la Formation Pisco, Pérou. L'holotype de cette espèce est un crâne incomplet (dont manque le vertex) avec les tympaniques associés. La description de cinq nouveaux spécimens remarquablement préservés de ce taxon (trois d'entre eux associés à un squelette post-crânien partiel) permet de considérer la variation individuelle au sein d'une seule espèce de mysticète fossile. Ces spécimens constituent une série ontogénétique partielle incluant un individu sub-adulte, trois adultes et un vieil adulte. *Piscobalaena nana* est comparé à *Nannocetus eremus* Kellogg, 1929, *Cetotherium rathkei* Brandt, 1843, *Herpetocetus sendaicus* (Hatai, Hayasaka & Masuda, 1963) et *Metopocetus durinasus* Cope, 1896 qui ont une morphologie et un âge proches de ceux de l'espèce péruvienne. L'analyse de parcimonie de 101 caractères morphologiques du crâne, de la région auditive et du dentaire, testés sur 23 taxons confirme la paraphylie des Cetotheriidae tels qu'ils sont traditionnellement définis. En outre, l'analyse suggère également que six (*Piscobalaena*, *Herpetocetus*, *Metopocetus*, *Cetotherium*, *Nannocetus*, *Mixocetus*) des 12 mysticètes à fanons fossiles pris en compte constituent un clade : les Cetotheriidae *s.s.* La monophylie de ce clade est soutenue par 10 caractères crâniens (e.g., les processus ascendants des maxillaires sont en contact médialement à leur apex ou sur toute leur longueur ; les bords latéraux des nasaux sont extrêmement convergents postérieurement ; le supraorbitaire du frontal est orienté antérieurement) et cinq caractères de la région auditive (e.g., au niveau du méat auditif interne, le bord antérieur du foramen facial présente une échancrure, plus ou moins profonde, pour le passage du grand nerf pétrosal). Les Cetotheriidae ont en commun avec les Balaenopteridae la présence d'une interdigitation des os rostraux et crâniaux, matérialisée, entre autres, par une élongation postérieure des processus ascendants des maxillaires. Cette condition renforce l'architecture du crâne et pourrait suggérer un mode alimentaire par engouffrement semblable à celui observé chez les Balaenopteridae.

MOTS CLÉS
Mammalia,
Cetacea,
Mysticeti,
Cetotheriidae,
Piscobalaena nana,
Pliocène inférieur,
Pérou,
anatomie.

INTRODUCTION

Although they become diversified during the Oligocene, mysticetes are known since the late Eocene (Fordyce 1989, 1992; Fordyce & Watson 1998; Fordyce & Muizon 2001; Mitchell 1989). The first mysticetes (Eocene and Oligocene) still retain functional teeth in contrast with the derived representative of the group (mostly Neogene, and Recent), which bear baleen only. Toothed mysticetes Llanocetidae (Mitchell, 1989), Aetiocetidae (Emlong, 1966), Mammalodontidae (Mitchell, 1989) are known in the Eocene of Antarctica, and in the late Oligocene of New Zealand, Japan, and North America. Since *Eomysticetus* Sanders & Barnes, 2002, which is late Oligocene in age, lacks teeth but already has baleen, baleen-bearing mysticetes, the group to which the modern mysticetes belong, probably appeared during the early Oligocene (Fordyce & Muizon 2001). The morphology of their maxilla indicates that they had replaced teeth by baleen and developed the filter-feeding system observed in the Recent mysticetes (Fordyce 1980). Toothed mysticetes are absent in the Miocene, whereas baleen mysticetes

encompass a major diversification and have been found in marine deposits of all continents.

The systematics of the early baleen mysticetes is still poorly understood. Most fossil baleen-bearing mysticetes have generally been included in the "Cetotheriidae" *sensu lato* (*sensu* Simpson 1945; McKenna & Bell 1997; Rice 1998) a diverse and heterogeneous family, the monophyly of which has never been established. In practice, all fossil mysticetes lacking the synapomorphies of the Recent families have been included in the "Cetotheriidae", a taxon therefore diagnosed with symplesiomorphies. The "Cetotheriidae" range from the late Oligocene to the early Pliocene and include more than 27 genera (Ichischima 1997; McKenna & Bell 1997; Rice 1998) from most continents (North and South America, New Zealand, Australia, Europe, and Japan).

Piscobalaena nana Pilleri & Siber, 1989 is a small mysticete from the early Pliocene of Peru. This taxon has already been mentioned as Cetotheriidae n. gen., n. sp. (Muizon 1984; Muizon & DeVries 1985; Marocco & Muizon 1988). The holotype of *Piscobalaena nana* is an incomplete skull (lacking the vertex) with associated tympanics. The specimen is from the Pisco Formation at the locality of Sud-Sacaco (Muizon 1981, 1984, 1988; Muizon & DeVries 1985), on the coast of Peru approximately 500 km south of Lima. Since its discovery, by R. Hoffstetter in the early 1970s, this locality has provided an abundant fauna of marine vertebrates including fishes, reptiles, birds and mammals (Muizon 1981, 1984, 1988; Muizon & DeVries 1985). Mammals are represented by numerous pinnipeds, cetaceans, and aquatic xenarthans (Muizon & McDonald 1995; McDonald & Muizon 2002). Abundant mysticetes remains from this site include, besides the holotype, five specimens referred to *Piscobalaena nana* (three remarkably preserved partial skulls and skeletons, and two isolated skulls). They constitute one of the best samples of fossil mysticetes from the same locality and vertebrate horizon.

The original description of *Piscobalaena nana* by Pilleri & Siber (1989) is extremely short and based on a single incomplete specimen. In the following study, the unique completeness of the new specimens allows a thorough description of the anatomy of this taxon. Furthermore, because little is known about intraspecific variation in fossil mysticetes, the sample under study, although too small for statistics, offers at least the chance to record variation. The five specimens present various stages of bone fusion and hyperostose of their skeletons (indicating individuals of distinct ontogenetic ages, cf. Skull description) and therefore constitute an ontogenetic series.

GEOLOGICAL SETTING

The Pisco Formation marks an important marine transgression (Adams 1908), which affected the southern coast of Peru in the Neogene of approximately 350 km from Pisco to Yauca. This formation includes hundreds of meters of detrital marine deposits (tuffaceous sandstone, siltstone and shelly sandstone) (Muizon 1984, 1988; Muizon & DeVries 1985). The Sacaco area is located approximately 550 km south of Lima and extends 25 to 30 km along the coast. This area corresponds to the upper part of the Pisco Formation and its age spans from late Miocene (*c.* 10 Ma) to late Pliocene (*c.* 2 Ma) (see Muizon & DeVries 1985 for further details). Based on radiometric datings as well as mollusks and vertebrate faunas, Muizon (1981, 1984, 1988) and Muizon & DeVries (1985) identified five vertebrate horizons, which bear distinct faunal assemblages. The three oldest horizons are Miocene in age: El Jahuay (ELJ, *c.* 10 to 9 Ma); Aguada de Lomas (AGL, *c.* 8 to 7 Ma); Montemar (MTM, *c.* 6 Ma). The two youngest are early Pliocene in age: Sud-Sacaco (SAS, *c.* 5 to 4 Ma); Sacaco (SAO, *c.* 4 to 3 Ma). The vertebrate fauna of the Pliocene beds is contemporaneous and shows similarities with that of the Yorktown Formation at the Lee Creek Mine of North California (USA) (Muizon & DeVries 1985).

An updated mammal faunal list of Sud-Sacaco horizon is presented below:

Carnivora
- Phocidae Gray, 1821
  - *Acrophoca longirostris* Muizon, 1981
  - *Piscophoca pacifica* Muizon, 1981
  - Monachinae n. gen., n. sp. 1
  - Monachinae n. gen., n. sp. 2

Xenarthra
Tardigrada
Nothrotheriidae Ameghino, 1920
Thalassocnus littoralis McDonald & Muizon, 2002
Cetacea
Odontoceti
Pontoporiidae Gray, 1870
Pliopontos littoralis Muizon, 1983
Phocoenidae Gray, 1825
Piscolithax longirostris Muizon 1983
Delphinidae Gray, 1821
Globicephalinae n. gen., n. sp.
Odobenocetopsidae Muizon, 1993
Odobenocetops peruvianus Muizon, 1993
Hyperoodontidae Gray, 1846
Ninoziphius platyrostris Muizon, 1983
Mysticeti
Cetotheriidae Brandt, 1872
Piscobalaena nana Pilleri & Siber, 1989
Balaenopteridae Gray, 1864
Balaenoptera sp.

Abbreviations

Institutional abbreviations

CGM	Cairo Geological Museum, Cairo, Egypt;
ChM	Charleston Museum, Charleston, South Carolina;
CMUO	Condon Museum, University of Oregon, Eugene, Oregon;
LACM	Los Angeles County Museum, Los Angeles;
MNHN	Muséum national d'Histoire naturelle, Paris;
NSMT-PV	Section of Vertebrate Paleontology, Department of Geology, National Science Museum, Tokyo;
SMNK	Staatliches Museum für Naturkunde, Karlsruhe;
UCMP	Museum of Paleontology, University of California, Berkeley;
USNM	United States National Museum of Natural History, Smithsonian Institution, Washington, DC.

Anatomical abbreviations

Skull

ag	alveolar groove;
apM	ascending process of the maxilla;
bbPth	broken base of the pterygoid hamulus;
bcf	basicapsular fissure;
Bo	basioccipital;
Bop	basioccipital process;
ch	choanae;
eam	external auditory meatus;
fm	foramen magnum;
fpo	foramen pseudovale;
Fr	frontal;
fsg	fossa in the squamosal for the sigmoid process of the tympanic;
fTy	fossa for tympanohyal ligament;
ifo	infra-orbital foramen;
iopM	infra-orbital plate of maxilla;
iPa	interparietal;
jn	jugular notch;
La	lacrimal;
Mth	mesethmoid;
Mx	maxilla;
Na	nasal;
occ	occipital condyle;
Pa	parietal;
Pal	palatine;
pap	paroccipital process of the squamosal;
pgp	postglenoid process of squamosal;
pmc	postmeatal crest;
PMx	premaxilla;
popFr	postorbital process of frontal;
prnM	preorbital notch of maxilla;
prpFr	preorbital process of frontal;
prpM	preorbital process of maxilla;
Pt	pterygoid;
Pts	pterygoid sinus;
Soc	supraoccipital;
sop	supraorbital process of frontal;
Sq	squamosal;
stf	sternomastoid fossa;
tf	temporal fossa;
Vo	vomer;
zyp	zygomatic process of squamosal.

Tympanic

all	anterolateral lip;
a.sp	anterior spine of the tympanic;
ca	conical apophysis;
dl	dorsal lobe;
et	notch for eustachian tube;
iv	involucrum;
map	mallear pedicle;
medk	medial keel;
mf	median furrow;
ppp	pedicle of posterior process of petrotympanic;
sg	sigmoid process;
ty	tympanic;
vl	ventral lobe.

Petrosal

ap	anterior process;
app (br)	pedicle of anterior process (broken);
ct	crista transversa;
ctpp	caudal tympanic process of petrosal;
elf	endolymphatic foramen;
fc	fenestra cochleae;
fhm	fossa for head of malleus;
fs	sulcus for the facial nerve;
fsm	fossa for stapedial muscle;

fv	fenestra vestibuli;
gtt	groove for tensor tympani;
hf	hiatus fallopii;
IAM	internal auditor meatus;
pc	pars cochlearis;
plf	perilymphatic foramen;
pp	posterior process of petrotympanic;
pyd	pyramidal process;
sff	secondary facial foramen;
smf	suprameatal fossa;
VII	facial nerve canal.
Malleus	
ah	articular head;
al	anterior lamina;
ma	manubrium;
ped (br)	pedicle of malleus (broken);
pm	processus muscularis.
Incus	
cb	crus breve;
cl	crus longum (stapedial process);
fs	facet for stapes.
Stapes	
fai	facet for articulation with the incus;
sf	stapedial foramen;
sfp	stapedial foot plate.
Dentary	
ap	angular process;
co	mandibular condyle;
cp	coronoid process of the mandible;
fipt	fossa for the internal pterygoid muscle;
mdf	mandibular foramen;
mdfo	mandibular fossa;
mf	mandibular foramina;
pfap	posterior fossa of angular process;
po.cr	posterior crest of the coronoid process;
sl	notch for the symphyseal ligament;
vag	vestigial alveolar groove.

SYSTEMATICS

Order CETACEA Brisson, 1762
Suborder AUTOCETA Haeckel, 1866
Infraorder MYSTICETI Cope, 1891

Family CETOTHERIIDAE Brandt, 1872

DIAGNOSIS. — See p. 376.

Genus *Piscobalaena* Pilleri & Siber, 1989

TYPE SPECIES. — *Piscobalaena nana* Pilleri & Siber, 1989.

DIAGNOSIS. — As for the only included species, *Piscobalaena nana*.

INCLUDED SPECIES. — The type species only.

Piscobalaena nana Pilleri & Siber, 1989

HOLOTYPE. — SMNK PAL 4050, a partial skull lacking the vertex and left tympanic (Figs 1; 2).

LOCALITY. — Sud-Sacaco, approximately 540 km of the Pan-American Highway, southern coast of Peru (see Muizon 1981 for locality map).

HORIZON AND AGE. — Pisco Formation, SAS horizon (*sensu* Muizon & DeVries 1985), early Pliocene.

REFERRED SPECIMENS. — Most referred specimens (MNHN SAS 892, 1616-1618, 1623, 1624) are from the early Pliocene of Sud-Sacaco, but one isolated petrotympanic (MNHN PPI 259) and a right scapula (MNHN PPI 260) are from the late Miocene of Aguada de Lomas.
MNHN SAS 892: sub-complete skeleton including skull (lacking extremity of supraorbital process of left frontal and apex of premaxillae), right tympanic and petrosal *in situ*, left tympanic and petrosal removed from the skull, 3 left auditory ossicles, both dentaries, atlas, axis, 4 posterior cervical vertebrae, 4 thoracic vertebrae, 1 lumbar vertebra, left scapula lacking the apex of coracoid process, fragmentary right scapula, complete right humerus, complete right and left radii, complete right ulna, fragmentary left ulna, vertebral head of one rib.
MNHN SAS 1616: skull lacking both premaxillae, mesethmoid and right tympanic and petrosal, left tympanic and petrosal *in situ*.
MNHN SAS 1617: sub-complete skeleton with complete skull, left tympanic broken and *in situ*, left petrosal *in situ*, right tympanic removed from the skull, right petrosal *in situ*, right malleus, right incus, hyoid, 7 cervical vertebrae, 11 thoracic vertebrae, 11 lumbar vertebrae, 2 caudal vertebrae, 10 left ribs (1-10), 11 right ribs (1-11), fragmentary left scapula, complete left humerus, radius and ulna, carpals, metacarpals and phalanges.
MNHN SAS 1618: partial skeleton with complete skull lacking the mesethmoid, both dentaries complete, both tympanics prepared, right and left petrosals *in situ*, 5 auditory ossicles prepared, right lacrimal prepared, left lacrimal *in situ*, hyoid, 7 cervical vertebrae, 12 thoracic vertebrae, 2 lumbar vertebrae, 7 left ribs (1-4, 7-9), 9 right ribs (1-8, 10), 1 fragmentary pelvis.
MNHN SAS 1623: partial skull lacking premaxillae and apices of maxillae, left tympanic and petrosal *in situ*,

FIG. 1. — *Piscobalaena nana*, holotype (SMNK Pal 4050), skull: **A**, dorsal view; **B**, ventral view. Scale bar: 10 cm.

fragmentary right tympanic removed from the skull, right petrosal *in situ*.
MNHN SAS 1624: 7 cervical vertebrae, 5 dorsal vertebrae.
MNHN PPI 259: isolated complete petrotympanic.
MNHN PPI 260: right scapula. These two specimens are from late Miocene beds at Aguada de Lomas but are referred to *Piscobalaena nana*.

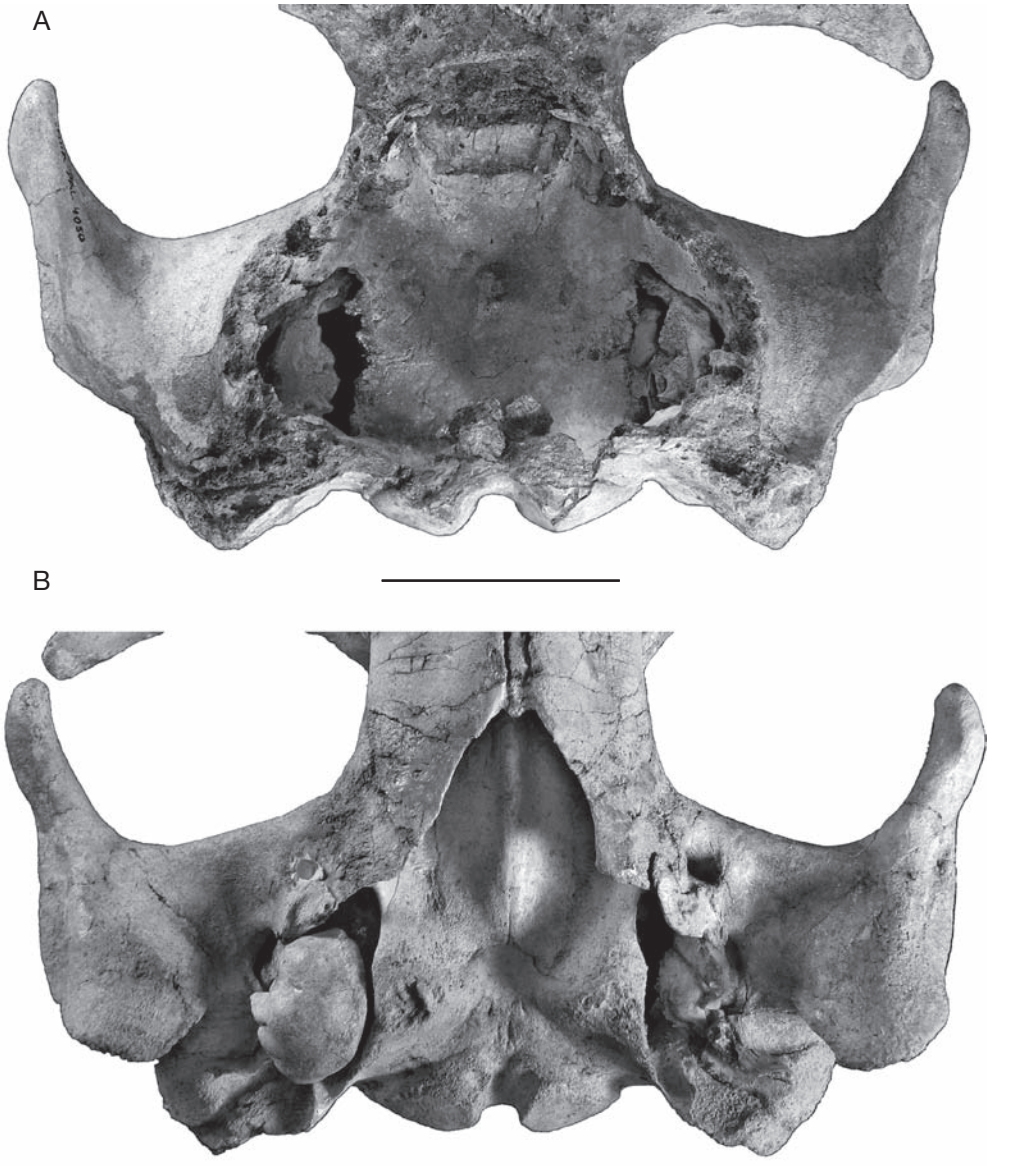

FIG. 2. — *Piscobalaena nana*, holotype (SMNK Pal 4050), basicranium: **A**, dorsal view; **B**, ventral view. Scale bar: 10 cm.

DIAGNOSIS

Small-sized fossil mysticete (condylobasal length of skull close to 1000 mm), preorbital process of maxilla laterally developed and dorsomedially prolonged as a crest expanding until mid-length of the maxillo-frontal suture; ascending process of maxilla elongated posteriorly almost until vertex; sigmoid maxillo-palatine suture (anteriorly convex in its lateral half and posteriorly convex in its medial half); pear-shaped tympanic (anterior third narrower than posterior two thirds); ventral lobe more posteriorly projected than dorsal and medi-

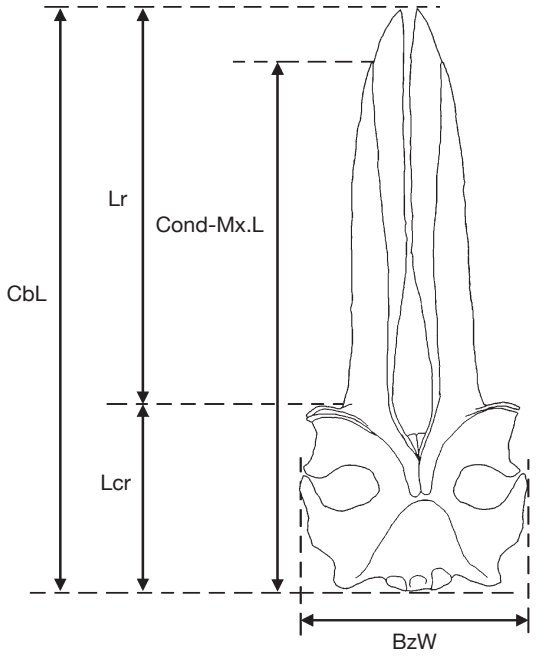

FIG. 3 — Measurements of the skull of *Piscobalaena nana* as used in text and other figures. Abbreviations: **BzW**, bizygomatic width; **CbL**, condylobasal length; **Cond-Mx.L**, condylo-maxillary length; **Lcr**, length of cranium; **Lr**, length of rostrum.

ally keeled from anteromedial spiny protuberance to posterior apex of tympanic; ventral lip strongly convex ventrally (particularly at sigmoid process level); spiny process at anteromedial extremity of tympanic; short anterior process of petrosal; confluence of facial nerve and greater superficial petrosal nerve foramina into a long single teardrop foramen; short and thick posterior process of petrotympanic; hook-like, short and outwardly bent coronoid process of the dentary; angular process posteriorly projected behind the level of the mandibular condyle; groove for insertion of internal pterygoid muscle present medially and posteriorly between the mandibular condyle and the angular process; scapula trapezoid (transversely elongated).

DIFFERENTIAL DIAGNOSIS

Piscobalaena nana differs from *Nannocetus eremus* Kellogg, 1929 in:

– ventrolateral orientation (in posterior view) of the postglenoid process (ventral in *Nannocetus* Kellogg, 1929);
– postglenoid process parallel (in ventral view) to the anteroposterior axis of the skull (process twisted medially in *Nannocetus*);
– greater posterior projection of the ventral lobe of the tympanic than the dorsal lobe (they equally project in *Nannocetus*);
– deeper notch separating the two lobes of the tympanic;
– pyriform morphology of the tympanic in ventral view (reniform in *Nannocetus*);
– ventral lip of the tympanic strongly inflated (little inflated in *Nannocetus*);
– medial edge of the involucrum with a step in its anterior third (sub-rectilinear in *Nannocetus*);
– anterior process of the petrosal quadrangular (sub-triangular in *Nannocetus*);
– thick crista transversa of the petrosal (thin in *Nannocetus*);
– pars cochlearis flattened anteriorly (hemispherical in *Nannocetus*).

Piscobalaena nana differs from *Herpetocetus sendaicus* (Hatai, Hayasaka & Masuda, 1963) in:
– ascending processes contact behind the nasals for approximately one fourth of their length (for two thirds in *Herpetocetus* (Van Beneden, 1872));
– posterior limit of narial fossa is approximately at the same level as or posterior to the line joining the preorbital processes of the frontals (distinctly anterior in *Herpetocetus*);
– postglenoid process ventrolaterally oriented (in posterior view) (ventrally oriented in *Herpetocetus*);
– postglenoid process parallel (in ventral view) to the anteroposterior axis of the skull (process twisted medially in *Herpetocetus*);
– supraoccipital roughly semicircular (triangular in *Herpetocetus*);
– low dorsal crest of the zygomatic process with a shallow squamosal fossa (the crest is elevated and the fossa is deep in *Herpetocetus*);
– basioccipital processes low and shallow fossa between the processes (they are prominent and the fossa is deep in *Herpetocetus*);
– sigmoid (concavo-convex) maxillo-palatine suture

TABLE 1. — Measurements (in mm) of condylo-maxillary length (Cond-Mx.L) of SMNK PAL 4050, MNHN SAS 892, 1616, 1617, 1618 and 1623. Condylobasal length (CbL) is extrapolated (**ex**) from Cond-Mx.L.

	SMNK PAL 4050	MNHN SAS 892	MNHN SAS 1616	MNHN SAS 1617	MNHN SAS 1618	MNHN SAS 1623	Mean
Cond-Mx.L (measured)	953	920	765	947	966	–	910
CbL	1037 ex	1002 ex	833 ex	1033	1050	–	991

TABLE 2. — Measurements (in mm) of bizygomatic width (BzW) of SMNK PAL 4050, MNHN SAS 1616, 1617, 1618 and 1623. Condylobasal length of the skull (CbL) is extrapolated (**ex**) from BzW.

	SMNK PAL 4050	MNHN SAS 1616	MNHN SAS 1617	MNHN SAS 1618	MNHN SAS 1623	Mean
BzW (measured)	410	327	405	417	433	398
CbL	1039 ex	828 ex	1033	1050	1097 ex	1009 ex

(convex anteriorly in *Herpetocetus*);
– presence of an anterior spine on the tympanic (absent in *Herpetocetus*);
– anterior notch of the hiatus fallopii short and limited to the anterior edge of the pars cochlearis (extremely developed anteriorly on the anteromedial edge of the anterior process in *Herpetocetus*);
– anterior process of the petrosal thick and quadrangular without lateral blade-like projection (well developed projection in *Herpetocetus*);
– angular process of the dentary projecting posteriorly to the condyle to a much smaller extent than in *Herpetocetus*;
– cervical vertebrae free (Axis, C3 and C4 are fused in *Herpetocetus*).

Piscobalaena nana differs from *Cetotherium rathkei* (Brandt, 1843) in:
– lateral and medial edges of the ascending process of the maxilla sub-parallel (convergent in *Cetotherium* (Brandt, 1843));
– ascending processes of the maxillae elongated posteriorly and contacting on most of their length postrerior to the nasals (converging and very close, but not contacting, at apex in *Cetotherium*);
– preorbital process of the maxilla sub-vertical and anteriorly convex lamina of bone (thick at apex and antero-laterally oriented – not convex – in *Cetotherium*);
– postglenoid process parallel (in ventral view) to the anteroposterior axis of the skull (process twisted medially in *Cetotherium*);
– semi-circular dorsal angle of the supraoccipital (sharp angle in *Cetotherium*).

Piscobalaena nana differs from *Metopocetus durinasus* (Cope, 1896) in:
– lateral and medial edges of the ascending process of the maxilla sub-parallel (convergent in *Metopocetus* (Cope, 1896));
– semi-circular supraoccipital (sub-triangular in *Cetotherium*).

DESCRIPTION

Skull

General features. The most obvious characteristic of *Piscobalaena nana* is its extremely small size relatively to most other mysticetes. Although not all the specimens of the available sample are equally preserved, it is interesting to evaluate the average cranial length of this taxon. The total length of the skull (condylobasal length: CbL, Fig. 3) can be measured on two skulls only, those on which the apex of the premaxillae is preserved (Fig. 4). The condylobasal length, measured from the posterior extremity of the occipital condyle to the apex of the premaxilla is 1050 mm in MNHN SAS 1618 and 1033 mm in MNHN SAS 1617 (mean: 1041.5 mm). The apices of the premaxillae are damaged on MNHN SAS 892, and these bones are missing on MNHN SAS 1616 and MNHN SAS 1623. However, the condylobasal length of the skull of these specimens can be extrapolated from the distance between the occipital condyles and the anterodorsal edge of the

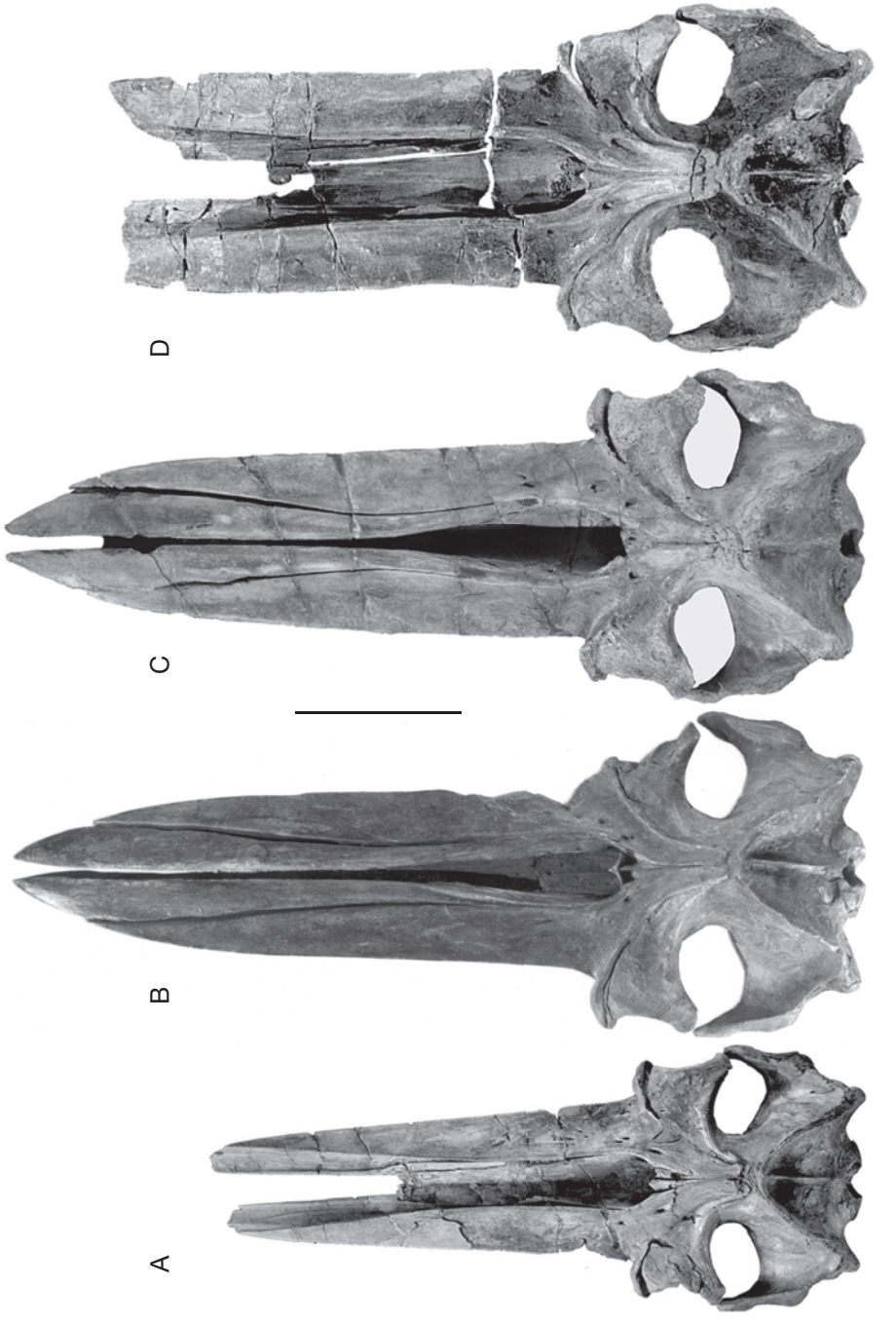

FIG. 4. — *Piscobalaena nana*, dorsal view of the skull of four individual to show the size individual variation within the species: **A**, "old juvenile" or sub-adult (MNHN SAS 1616); **B**, adult (MNHN SAS 1617); **C**, adult (MNHN SAS 1618); **D**, old adult (MNHN SAS 1623). Scale bar: 20 cm.

TABLE 3. — Relative lengths of the rostrum and cranium in *Piscobalaena nana*. Abbreviations: **ex**, extrapolated; **Lcr**, length of the cranium measured from the preorbital notch to the posterior limit of the occipital condyles; **Lr**, length of the rostrum measured from the preorbital notch to the apex of the premaxilla (Fig. 3); **CbL** = Lr + Lcr. For the skulls in which the rostrum is not completely preserved (SMNK PAL 4050, MNHN SAS 892, 1616 and 1623) the length of the rostrum is calculated from the measured Lcr and the extrapolated CbL obtained with the condylo-maxillary length (Cond-Mx.L, Table 1) or with the bizygomatic width (BzW, Table 2) for MNHN SAS 1623.

	SMNK PAL 4050	MNHN SAS 892	MNHN SAS 1616	MNHN SAS 1617	MNHN SAS 1618	MNHN SAS 1623
Lr	708 ex	675 ex	556 ex	729	723	732 ex
Lcr (measured)	330	327	277	316	327	366
Lcr/Lr	0.466	0.484	0.498	0.433	0.452	0.501

maxillo-premaxilla suture, the condylo-maxillary length (Cond-Mx.L, Fig. 3), which is 920 mm for MNHN SAS 892 and 765 mm for MNHN SAS 1616. Compared with the mean of the measurements in the two complete specimens MNHN SAS 1617 and 1618, the extrapolated condylobasal length of the two skulls is 1002 mm for MNHN SAS 892 and 833 mm for MNHN SAS 1616 (see Table 1).

In MNHN SAS 1623, the premaxillae are missing and the anterior extremity of the maxilla is not preserved. However, the condylobasal length of this skull can be extrapolated (CbL of MNHN SAS 1623 = 1098 mm ex) from the bizygomatic width (BzW, Fig. 3) of the skull (see Table 2).

In this case, the extrapolation obtained with the condylo-maxillary length for MNHN SAS 1616 can be tested with the bizygomatic width measured on the most complete skulls MNHN SAS 1617 and 1618 (average CbL = 1041.5 mm; average BzW = 411 mm). The length obtained for MNHN SAS 1616 from the bizygomatic width is 828.6 mm, an approximation close to that obtained from the condylo-maxillary length (833 mm). However, MNHN SAS 1616 is a sub-adult individual and an allometric growth of the rostrum is likely to have occurred as is observed in Recent balaenopterids. Therefore, it is possible that the actual condylobasal length of the skull was slightly smaller than the result obtained above. However, SMNK PAL 4050 is a full adult specimen and the extrapolation obtained from the Bizygomatic width (1039 mm) is almost identical to that obtained from the condylo-maxillary length (1037 mm). This indicates that the bizygomatic width is also a reliable measurement to extrapolate the condylobasal length of the skull.

Hence, the average length of the skull of *Piscobalaena nana* on the basis of five specimens approaches 1 m with a maximum variation of approximately 25% between MNHN SAS 1616 and 1623.

As in all mysticetes, the skull of *Piscobalaena* has an elongated rostrum and a massive cranium. In *Piscobalaena*, the line joining the preorbital processes of the maxillae limits the rostrum posteriorly. The relative proportions of the cranium-rostrum lengths are shown in Table 3 and indicate that the rostrum of *Piscobalaena* is approximately twice as long as the cranium.

Because it has unfused sutures, the small skull of MNHN SAS 1616 probably belongs to an old juvenile or sub-adult individual. The sutures are not clearly visible in any of the other specimens, which are thus regarded as full adults. The skull of MNHN SAS 1623, the largest of the five specimens, presents hyperostosis of crests and sutures with small exostoses, which suggests that it was an old individual. Hyperostosis and exostoses are also present in MNHN 1618, but they are absent in MNHN SAS 892 and 1617. In extant mysticetes, females are generally more massive and approximately 5% larger than males (Ralls & Mesnick 2002). Therefore, and according to the measurements shown in Tables 1 and 2, MNHN SAS 892 could be referable to a male, MNHN 1618 to an old male, and MNHN 1623 to an old female. MNHN SAS 1617 could be a young female (Fig. 4).

In adult specimens of *Piscobalaena nana*, the lateral edges of the rostrum are sub-parallel on their posterior two thirds and then converge anteriorly. The cranium is approximately square-shaped. The temporal fossa is transversely oval-shaped. The narial opening occupies the posterior third of the

mesorostral groove. The posterior limit of the nares is approximately at the same level or slightly posterior to the line joining the preorbital processes of the maxillae.

In lateral view, the rostrum is sub-rectilinear and the dorsal border of the orbit is at the same level as the lateral edge of the maxilla. The vertex is high and located just above the centre of the temporal fossa on the sub-adult individual and slightly behind on the other specimens.

Premaxilla. On the dorsal side of the skull (Fig. 5), the maxillo-premaxilla suture ends anteriorly on the lateral edge of the rostrum approximately 100 mm posterior to the apex of the premaxilla. The deep groove on the skulls of MNHN SAS 1617 and 1618 between the maxilla and the premaxilla is probably an artefact due to a displacement of the two bones during fossilisation. Anteriorly, the premaxillae widen, their largest width being at the same level as the anterior extremity of the maxillo-premaxilla suture in dorsal view. The posterior extremities of the premaxillae are often not preserved but the mark of the sutures on the maxillae indicates that they did not extend posteriorly as far as the ascending processes of the maxillae. The posterior extremity of the premaxilla is wedged between the nasal and the maxilla and does not extend further posteriorly than mid-length of the lateral edge of the nasals.

Maxilla. The ventral surface of the maxilla is concavo-convex: concave ventrally in its lateral half and convex ventrally in its medial half. On the ventrolateral edge of the maxilla (Fig. 6B), the well defined and long alveolar groove extends posteriorly until the infraorbital plate-like expansion of the maxilla. This groove is the vestige of the dental alveoli, observed in toothed mysticetes (Barnes *et al.* 1994). Absent in adults of extant mysticetes, this groove is present during the foetal development of baleen mysticetes and carries teeth buds, which are resorbed in the gum before birth (Schulte 1916; Slijper 1979).

The ventral surface of the rostral portion of the maxilla is concavo-convex, rather flat laterally, distinctly concave in its median area and convex on its medial edge. Mostly on the flat and median regions of the ventral face of each maxilla, several grooves (*c.* 50 to 200 mm long by *c.* 5 mm wide) anteroposteriorly oriented and diverging anteriorly are present on the posterior two thirds of the rostrum. The number of these grooves is variable from one maxilla to the other. In extant mysticetes, these grooves receive the blood vessels and nerves which supply the palatal epithelium producing the baleen.

On the dorsal side of the skull (Figs 4; 5), the maxilla extends posteromedially in a long and massive ascending process (Kellogg 1929), which reaches the vertex and almost contacts the anterior edge of the supraoccipital. The ascending processes of the maxillae rest on the frontal posteriorly; they border the premaxillae and the nasals laterally and contact each other posterior to the nasals. In dorsal view, the apices of the maxillae expand posterior to the line joining the apices of the zygomatic processes and reach the level of the posterior edge of the temporal fossa.

On the dorsal face of the maxilla, the arrangement, size, and number (5 to 10) of the maxillary foramina are variable. Posteriorly, one large maxillary foramen is consistently present, approximately at the level of the anterior edge of the nasals. But the size and position of this foramen may vary in the same individual from one maxilla to the other.

On the dorsal face of the skull, the posterior edge of the maxilla (fronto-maxillar suture) is oblique. It faces posterolaterally and is markedly concave posteriorly. As a consequence, both fronto-maxillar sutures form an anteriorly-open V from the preorbital processes of the maxillae to the vertex posteriorly. Laterally, at the anterior edge of the orbit, the preorbital process of the maxilla is adjacent to the preorbital process of the frontal and is separated from the latter by a deep fissure, which receives a leaf-like lacrimal as shown in MNHN SAS 1617. The preorbital process of the maxilla is thick and salient and projects laterally almost perpendicular to the lateral border of the rostral portion of the maxilla. It extends medially along the posterior edge of the maxilla in a thick rim, which tapers posteriorly and progressively merges with the lateral edge of the ascending process of the maxilla, midway from the apex of the ascending process. The preorbital

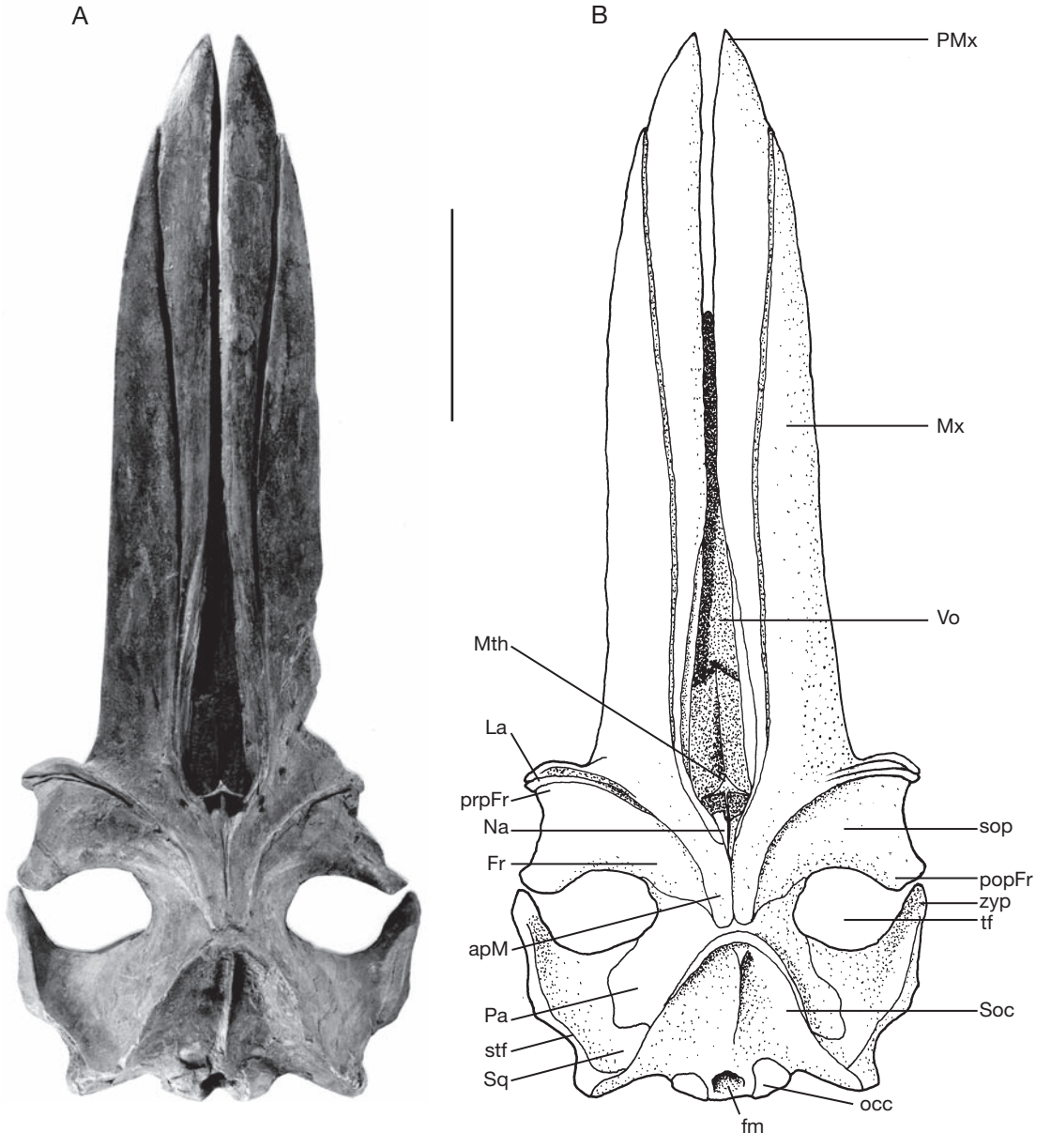

FIG. 5. — *Piscobalaena nana*: **A**, dorsal view of the skull MNHN SAS 1617; **B**, reconstruction. Abbreviations: see p. 322. Scale bar: 20 cm.

notch is a deep saddle-shaped groove excavated in the maxilla anterior to the preorbital process and which extends on the ventral face of the maxilla. The term preorbital notch is used here to avoid confusion with the antorbital notch of odontocetes. In odontocetes, the antorbital notch is excavated in the maxilla and the jugal and a true antorbital process of the maxilla is not present although an

antorbital tubercle may be observed. In odontocetes, the maxilla projects posteriorly over the supraorbital process of the frontal toward the vertex.

In mysticetes, the maxilla does not overlap the supraorbital process of the frontal and presents two distinct processes: the ascending process and the preorbital process. The former projects posteromedially toward the vertex, as in terrestrial mammals. The latter is anterior to the preorbital process of the frontal, and separated from it by the lacrimal. In some taxa, this process is separated from the lateral edge of the rostral portion of the maxilla by a deep sulcus, which receives the facial nerve on its way to the dorsal side of the head. On the lateral edge of the preorbital process of the maxilla is a very narrow and short horizontal notch, which could receive part of the insertion of the superficial branch of the masseter muscle (Schulte 1916).

In its posteroventral region, the maxilla projects posteriorly and ventrally, and forms a well developed infraorbital plate-like expansion. The lateral edge of this expansion thickens and projects laterally to form the preorbital process of the maxilla.

Nasal. The nasals (Figs 4; 5) are triangular and anteroposteriorly elongated. They strongly narrow posteriorly, and are wedged between the ascending processes of the maxillae. The posterior extremity of the nasal does not reach the posterior edge of the maxilla (i.e. the maxillae contact each other behind the nasals and hide the nasofrontal suture). The anteromedial angle of the nasal is elevated and projects anteriorly against the sub-vertical, plate-like mesethmoid.

Lacrimal. In MNHN SAS 1618, the left lacrimal (Fig. 8) is preserved but dissociated from the skull. The bone is a thin plate, longer than wide and strongly concave posteriorly. In MNHN SAS 1617, the left lacrimal is still *in situ* on the skull (Fig. 7), encased between the preorbital process of the maxilla and the preorbital process of the frontal.

Frontal. The frontals (Figs 4; 5; 7) are almost excluded from the vertex and are almost completely overlaid medially by the ascending processes of the maxillae. Lateral to the posterior extremity of the ascending process is a small and sharp crest, which is apressed against the parietal. This crest is the posteromedial part of the temporal crest, which runs along the posterior edge of the supraorbital process (Barnes *et al.* 1994). It is anteriorly convex, relatively salient and developed from the medial part of the frontal (ventral to the posterior extremity of the ascending process of the maxilla) to the apex of the postorbital process of the frontal.

The supraorbital process is moderately developed and gently slopes laterally from the median axis of the skull with no step from the maxilla to the frontal as in Recent balaenopterids and eschrichtiids. The anteromedial area of the supraorbital process is partly covered by the ascending process of the maxilla, which gives it a triangular outline in dorsal view. The preorbital process of the frontal is relatively short compared to that of balaenopterids and the postorbital process is massive and posterolaterally oriented. The posterior edge of the supraorbital process is markedly concave posteriorly and the temporal fossa is transversely elliptical. The lateral margins of the orbits (i.e. the line joining the preorbital and postorbital processes) are slightly convergent anteriorly.

On the anteromedial wall of the temporal fossa, the fronto-parietal suture is vertical and runs ventrally towards the posterior base of the optic nerve sulcus. Anteriorly to the anterior edge of the orbit, the supraorbital process has a plane area against which the posterodorsal face of the lacrimal is apressed.

Parietal. On the vertex, the exposure of the parietals is very reduced, the bones being tightly wedged between the frontals and the supraoccipital. The interparietal is not visible on the dorsal surface of the skull but in internal view only, tightly wedged between the parietal anteriorly and the supraoccipital posteriolry (cf. below Internal view of the cranium). From the vertex, the fronto-parietal suture (Figs 4; 5) is oriented anteriorly and runs along the temporal crest for 5 to 8 cm. At the level of the anterior edge of the temporal fossa, the suture turns ventrally toward the medial base of the posterior edge of the optic groove, where the parietal partially covers the frontal and extends slightly anteriorly.

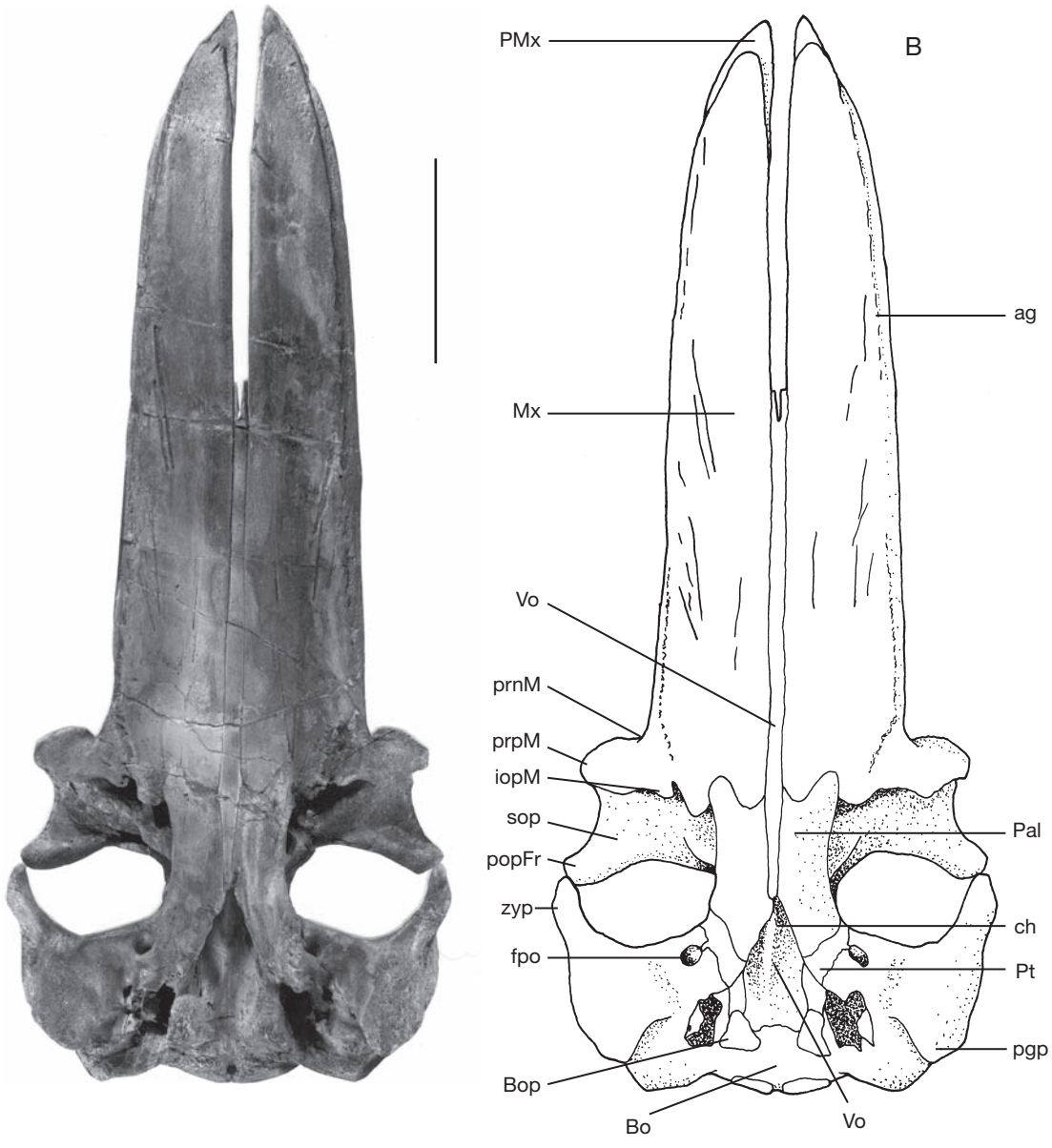

FIG. 6. — *Piscobalaena nana*: **A**, ventral view of the skull (MNHN SAS 1618); **B**, reconstruction. Abbreviations: see p. 322. Scale bar: 20 cm.

Posteromedially to the fronto-parietal suture, the parieto-squamosal suture starts on the posterodorsal edge of the alisphenoid fenestra in MNHN 1616 (cf. below Alisphenoid section) then it extends posterodorsally and passes on an elongated and anteroventrally oriented ridge of the braincase wall for the origin of the temporalis muscle. Dorsal to this crest, the suture turns anterodorsally on 4 or 5 cm and then abruptly shifts posteriorly to contact the lambdoid crest at mid-height. Then, the

FIG. 7. — *Piscobalaena nana*, lateral view of the skull (MNHN SAS 1617). Scale bar: 20 cm.

parietal is apressed against the lambdoid crest up to the vertex.

Mesethmoid. The mesethmoid (Figs 4; 5) consists in two parts. The dorsal portion is a sub-vertical plate, V-shaped and posteriorly open. The base of the V extends anteriorly and forms a median septum between the bony nares. The ventral portion of the mesethmoid is fully preserved in MNHN SAS 1617 only. It is a bony plate of spongy bone, which expands anteriorly and forms the floor of the nares. This plate bears a sharp crest which is the ventral portion of the narial septum and which was connected to the septum of the dorsal portion by the nasal cartilage. The ventral portion of the mesethmoid is approximately 100 mm long and 50 mm wide.

Vomer. Dorsally (Figs 4; 5), the vomer is a long gutter-like bone, which occupies most of the mesorostral groove for approximately half the length of the rostrum. In ventral view (Figs 6; 9), the vomer presents a carina wedged between the maxillae and the palatines and which is 10 to 20 mm in width. This carina extends from mid-length of the rostrum to the posterior edge of the choanae dorsally. Medially, between the palatines, the vomer forms the medial portion of the ventral edge of the choanae. The posterodorsal portion of the vomer is distinctly concave ventrally and presents, in the sagittal plane, a median crest, which widens dorsally. This part of the vomer forms most of the dorsal edge of the choanae. It covers the basisphenoid and basioccipital ventrally and is laterally bordered by the lateral lamina of the pterygoids, which it partly covers too.

Palatines. In ventral view (Fig. 6), the palatines are anteroposteriorly elongated and extend from the preorbital process of the frontal anteriorly to the level of the foramen pseudovale posteriorly. The maxillo-palatine suture has a distinctive sigmoid shape: it is anteriorly concave in its medial half and convex in its lateral half. The lateral edge of the palatine is rectilinear and ventrally borders the ventral face of the base of the supraorbital process of the frontal. In some specimens (e.g., MNHN SAS 1617), the anterior portion of the palatine is distinctly depressed.

Pterygoid. In ventral view (Figs 6; 9), the lateral part of the pterygoid is a small narrow portion of bone wedged between the palatine and the squamosal. A very reduced part of the pterygoid contributes to the anteromedial edge of the foramen pseudovale. The pterygoid expands dorsally on the lateral wall of the braincase, where it articulates with the parietal and the alisphenoid. Medially, this same portion of the pterygoid forms the lateral wall of the pterygoid sinus.

The pterygoid is excavated posteriorly by a deep sinus, which splits the bone into a medial and a lateral lamina (Fig. 9). Most of the sinus is excavated in the pterygoid but its posterior portion is made of the basioccipital. The pterygoid sinus extends posteriorly as far as the two thirds of the cranial hiatus. The medial lamina of the pterygoid articulates posteriorly with the basioccipital just anterior to the basioccipital process and medially with the vomer. Most of the pterygoid sinus is excavated in the medial lamina and, therefore, deeply excavates the basicranium medially. Ven-

trally, the medial lamina forms the dorsolateral part of the roof of the choanae. The lateral lamina is almost totally overlapped by the squamosal laterally and does not extend further posteriorly than the anterior edge of the cranial hiatus. The sinus is largely open ventrally and a deep notch separates the lateral and medial laminae. As a consequence, the ventral lamina of the pterygoid is restricted to the anteriormost portion of the sinus (Fig. 9). The dorsal lamina of the pterygoid forms the roof of the sinus and its posterior edge is the anterior edge of the cranial hiatus (basicapsular fissure of Luo & Gingerich 1999).

The hamular process of the pterygoid is short and faces posteriorly.

FIG. 8. — *Piscobalaena nana*, left lacrimal (MNHN SAS 1618): **A**, anterior view; **B**, dorsal view. Scale bar: 2 cm.

Alisphenoid. In adult mysticetes, the alisphenoid is partially or totally covered by the parietal and the pterygoid. Therefore, its contribution to the outer surface of the braincase is either very reduced or totally absent. When present at the surface of the lateral wall of the braincase, it is not perforated by the foramen ovale (see below). However, in juveniles and in sub-adult individuals, the parietal and pterygoid have not totally developed and the alisphenoid is visible through a small window between the two bones. Such a condition is present in MNHN SAS 1616; a sub-adult individual. No alisphenoid is visible on the lateral wall of the braincase of the four other specimens of *Piscobalaena*.

Squamosal. In dorsal view (Figs 4; 5), the large zygomatic and postglenoid processes form most of the squamosal. The zygomatic processes are robust and diverge anteriorly. Their medial face is straight to slightly concave medially and their apex is recurved medially and ventrally. On the lateral and ventral edges of the apex of the process is a rugose surface for the origin of the masseter profundus (Schulte 1916). The lateral edge of the processes is deeply excavated. In lateral view, the zygomatic process increases in height anteroposteriorly and is approximately three times higher at its base than at its apex. In fact the posterior end of the zygomatic process is difficult to define because its ventral edge is aligned with the anterior side of the postglenoid process. Therefore, the posterior region of the zygomatic process is continuous with the postglenoid process (Fig. 7). The lateral side of the zygomatic-postglenoid complex bears a rugose convex surface for the origins of (from dorsal to ventral) the splenius, trachelo-mastoideus, mastohumeralis and sternomastoideus muscles, while more ventrally is the insertion area for the sternomandibularis muscle (based on Schulte 1916). The dorsal edge of the zygomatic process bears a thick sigmoid crest, which runs all along its length and merges with the lambdoid crest posteriorly. In dorsal view (Figs 4; 5), the two crests converge posteriorly in all the specimens except in MNHN SAS 1623, in which they are roughly parallel. Above the postglenoid process, the crest is thin, distinctly everted and overhanging the sternomastoid fossa. The latter (Fig. 30) is a deep depression, anterodorsal to the posterior process of the tympanic and dorsal to the external auditory meatus. According to Schulte's (1916) observation on *Balaenoptera borealis*, it probably receives the origins of the splenius, and trachelo-mastoideus muscles (Schulte 1916).

The postglenoid process (Figs 6; 7; 9-11) is thick and oriented posteroventrally. Its anterior edge faces anteroventrally (it is at an angle of *c.* 30° with the horizontal plane). Its posterior edge is sub-vertical (it is at an angle of *c.* 10° with the vertical plane), slightly concave, and receives the origin of the depressor mandibulae muscle, according to Schulte's observation on *Balaenoptera borealis*. The apex of the postglenoid process is thin and blade-like; it is

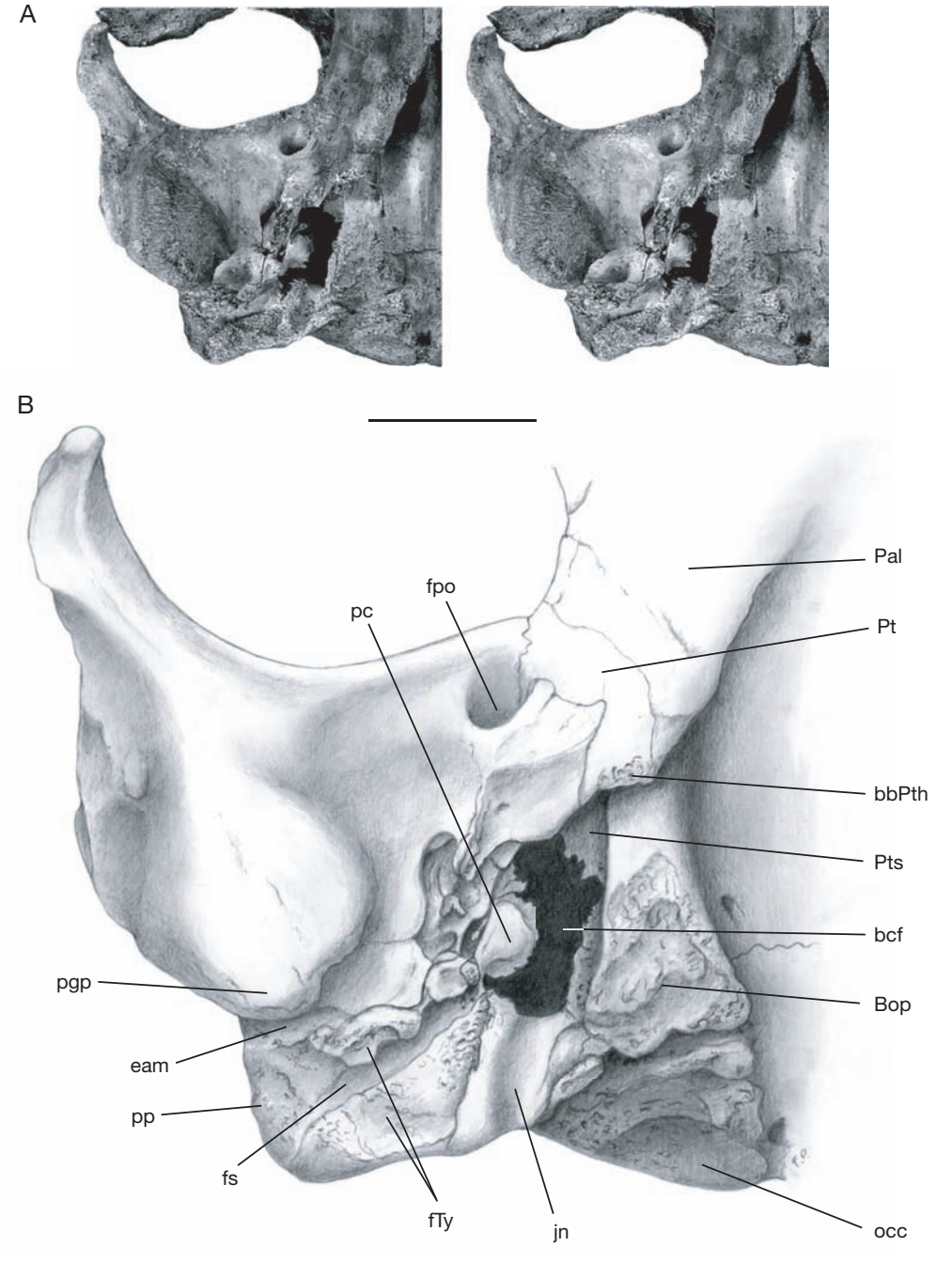

FIG. 9. — *Piscobalaena nana*, skull, right basicranium: **A**, stereo pair of MNHN SAS 1618; **B**, schema. Abbreviations: see p. 322. Scale bar: 10 cm.

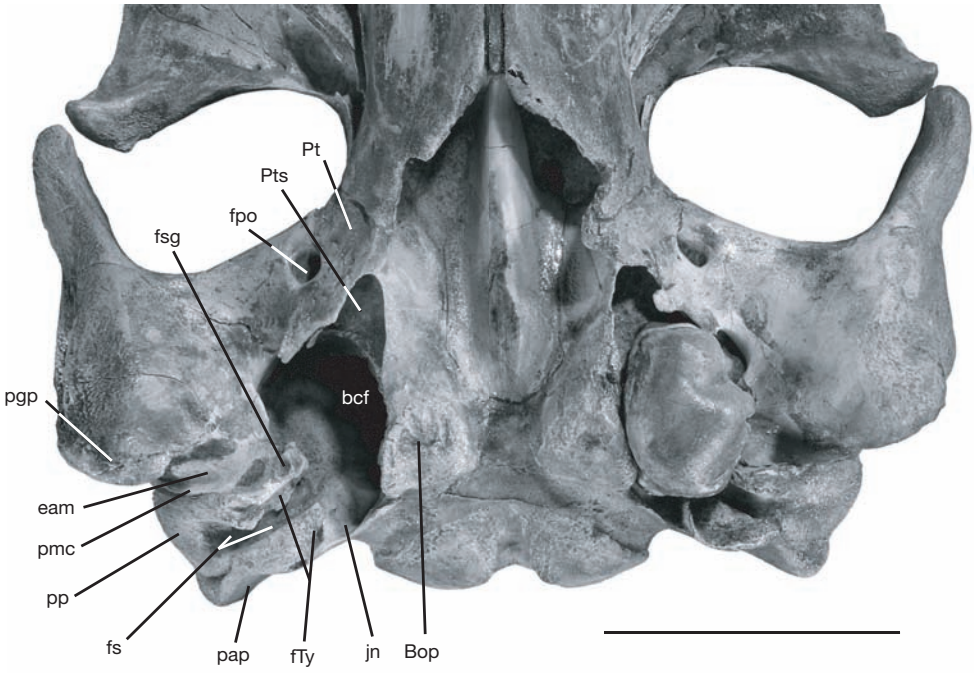

FIG. 10. — *Piscobalaena nana*, basicranium of MNHN SAS 1616. Abbreviations: see p. 322. Scale bar: 10 cm.

transversely oriented.

Between the base of the zygomatic process and the foramen pseudovale is a shallow glenoid fossa (Figs 9; 10), which is almost continuous with the anteroventral side of the postglenoid process. Anteromedial to the fossa, the wide foramen pseudovale opens slightly anterolaterally. Geisler & Luo (1998) and Luo & Gingerich (1999) used the term "foramen ovale" referring to the foramen through which the mandibular branch of the trigeminal nerve (V_3) exit the cranium. However, strictly speaking, this foramen is not homologous to the foramen ovale of placentals mammals, which is primitively perforated in the alisphenoid only (McIntyre 1967). In adult mysticetes, the alisphenoid is either very reduced or not visible at the surface of the lateral wall of the skull and is covered laterally by the squamosal and the pterygoid. When visible on the external side of the braincase, it is not perforated by the foramen ovale. The alisphenoid is visible on the internal side of the lateral wall of the skull. The exit of the mandibular nerve from the skull is not through a foramen but via a groove in the alisphenoid, located at the anterior edge of the basicapsular fissure. This condition is present in all mysticetes (including aetiocetids [Barnes *et al*. 1994]) and in some archaeocetes (basilosaurids), but absent in pakicetids, which do not have a basicapsular fissure (Luo & Gingerich 1999). The formation of the basicapsular fissure of mysticetes from a *Pakicetus* morphotype has reduced the bones adjacent to the petrosal anteriorly, essentially the alisphenoid, including the posterior edge of the foramen ovale. The foramen at the surface of the lateral wall of the braincase of mysticetes through which the V_3 exits the skull is therefore not homologous to the primitive foramen ovale and for this reason we follow Sanders & Barnes (2002) in the use of the term foramen pseudovale. In odontocetes, the alisphenoid is not covered laterally by the squamosal and outcrops at the surface of the lateral wall of the braincase. The foramen through which the V_3 of odontocetes exits the skull is perforated in the alisphenoid and is therefore homologous to the

FIG. 11. — *Piscobalaena nana*, MNHN SAS 1623, skull, posterior view. Scale bar: 10 cm.

foramen ovale of early placental mammals (Luo & Gingerich 1999).

The foramen pseudovale is slightly posterior to or at the level of the line joining the posterior edges of the temporal fossae.

The peribullary fossa (Figs 9; 10) is a wide opening in the braincase which surrounds the petrosal and the tympanic. It is located between the basioccipital and the squamosal and limited anteriorly by the pterygoid. This hiatus in the squamosal is called basicapsular fissure by Luo & Gingerich (1999), a term that is retained here. It is sub-triangular, and extends anteroposteriorly from the pterygoid sinus to the jugular notch (i.e. posterior lacerate foramen, Luo & Gingerich 1999) and transversely from the medial lamina of the pterygoid to the median lacerate foramen. The latter is formed dorsolaterally by the squamosal and ventromedially by the anterolateral lip of the tympanic. The capsuloparietal emissary vein exits the skull through the median lacerate foramen.

Posterior to the postglenoid process is a deep groove, which forms the dorsal edge of the external auditory meatus. The posterior edge of this groove is a thin crest fused or closely apressed against the compound posterior process of the tympanic and petrosal: the posterior meatal crest (Fordyce 1994). On the lateral edge of the cranial hiatus, at the anteromedial edge of the squamosal canal of the external auditory meatus and slightly posterior to the medial base of the postglenoid process is a tiny fossa, which receives the apex of the sigmoid process of the tympanic (Geisler & Luo 1998). The sigmoid process of the tympanic forms the anterior edge of the opening for the tympanic ligament, homologous to the tympanic membrane (Luo & Gingerich 1999). The compound posterior process of the petrosal and tympanic is wedged between the posterior meatal crest of the squamosal anteriorly and the paroccipital crest of the exoccipital posteriorly. This crest receives the origin of the obliquus superior. Dorsally to the posterior process of the petrotympanic, the squamosal contacts the exoccipital. At this point, the squamosal-exoccipital suture is fused but still visible.

Tympanic. The description of the tympanic and petrosal below is based on the bones of the five skulls described here all from the SAS horizon (5 Ma) at Sud-Sacaco. However, a remarkably preserved isolated petrotympanic (MNHN PPI 259, Fig. 12) has been discovered in the AGL horizon (7 to 8 Ma) at Aguada de Lomas. Two skulls of *Piscobalaena* have also been recovered at Aguada de Lomas and are regarded here as referable to the same species as *P. nana*. They are the property of the Museo de Historia Natural de la Universidad Nacional Mayor de San Marcos (Lima, Peru). Therefore, we also refer the petrotympanic of Aguada de Lomas to this species and include it in the following description. This specimen includes a complete petrotympanic and attached malleus. Because the bone is very smooth and bears no exostoses as generally observed in adult ear bones, and because of the small size of the compound posterior process, it belongs to a juvenile individual.

The tympanic of *Piscobalaena* will be described in anatomical position and its orientation will follow Oishi & Hasegawa (1994a: fig. 3). In Recent mysticetes, the tympanic has suffered a 90° rotation relatively to its position in archaeocetes, odontocetes and toothed mysticetes. The condition of fossil baleen-bearing mysticetes is similar to that in Recent mysticetes, except in *Eomysticetus*. Therefore, in almost all baleen mysticetes, the outer lip of the tympanic faces ventrally, the lateral lobe is ventral and the medial lobe is dorsal.

In ventral view (Figs 10; 12; 13), the tympanic (ectotympanic *sensu* Luo 1998) is pear-shaped, wider posteriorly than anteriorly. Its greatest width

FIG. 12. — *Piscobalaena nana*, MNHN PPI 259, petro-tympanic: **A**, ventral view; **B**, cerebral (dorsal) view; **C**, medial view; **D**, lateral view. Scale bar: 2 cm.

is located at the level of the sigmoid process and its longest axis is parallel to the sagittal axis of the skull. In adults, at the anterior end of the involucrum and located anteroventrally to the notch for the Eustachian tube, is a small anterior spine.

The involucrum (Figs 10; 12; 13) is thick, depressed in its median area and presents numerous transverse striae. The posterior two thirds of the involucrum are much thicker (i.e. wider) than the anterior third. The posterior extremity of the involucrum is a globulous hemispherical mass, facing dorsally and which constitutes the dorsal lobe of the tympanic. In its posterolateral portion, at the medial base of the dorsal lobe, the involucrum bears a thick spiny crest (well developed in MNHN SAS 1616, 1618, and 1623), which protrudes dorsomedially. It is absent in PPI 259. The ventral lobe of the tympanic is the posterior extremity of a thick keel, which surrounds the bone from the posteroventral angle of the external auditory meatus to its anterior apex, running along the basioccipital and the medial lamina of the pterygoid in its medial portion. The two lobes are separated by a shallow notch on the posterior half of the tympanic on its medial side. The ventral lobe extends further posteriorly than the dorsal lobe.

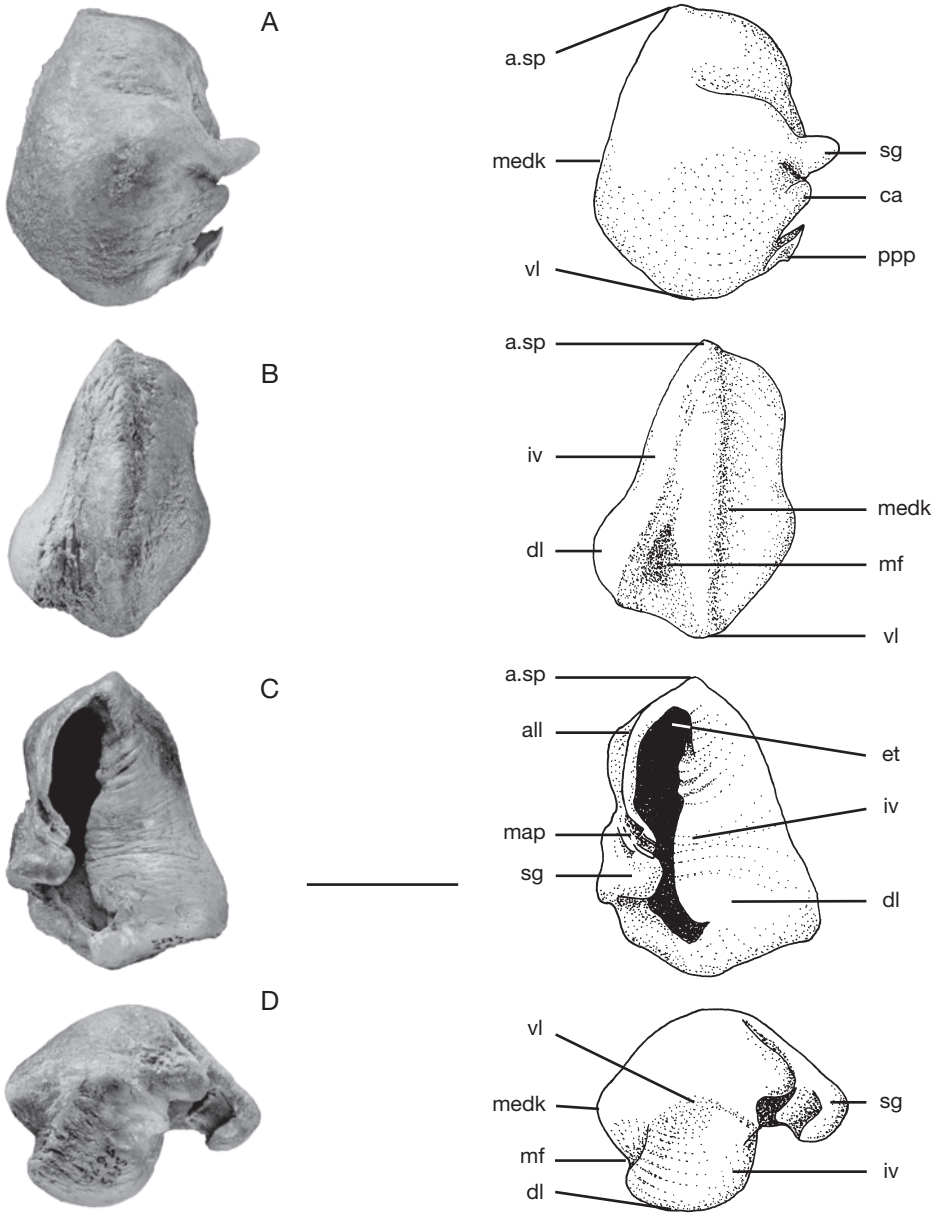

FIG. 13. — *Piscobalaena nana*, left tympanic: **A**, MNHN SAS 892, in ventral view; **B**, MNHN SAS 1618, in medial view; **C**, MNHN SAS 1618, in cerebral (dorsal) view; **D**, MNHN SAS 1618, in posterior view. Abbreviations: see p. 322. Scale bar: 2 cm.

The ventral lip (Figs 12D; 13B) of the tympanic is distinctly bilobate. A posterior strongly convex eminence is located medial to the sigmoid and conical processes. It forms the posterior two thirds of the lip. A smaller convexity forms the anterolateral region of the tympanic. Both eminences are

separated by a deep and wide transverse sulcus, medial to the anterior pedicle and anterior to the sigmoid process.

The sigmoid process is well developed and limited anteriorly by a wide sulcus and posteriorly by a thin slit. The posterior edge of the process is semicircular and forms the anterior half of the opening for the tympanic ligament. Posterior to the sigmoid process, the conical apophysis is low and closely apressed against the sigmoid process. Because the conical apophysis protrudes dorsolaterally in the opening for the tympanic ligament (the external auditory meatus), the latter is bilobate ventrally and anteroposteriorly elongate.

Anterior to the sigmoid process, on the lateral edge of the outer lip, is an elongated eminence, which is fused with the anterior process of the malleus. Dorsolateral to this eminence is a very thin and anteroposteriorly directed groove for the passage of the chorda tympani. The anterior pedicle of the malleus for attachment to the petrosal is lateral to the groove for the chorda tympani.

The compound posterior process of the tympanic and petrosal (Figs 7; 8; 10) is short and triangular. Its lateral side faces ventrolaterally. The medioventral side of the posterior process is excavated by two grooves. The anterior one has a rugose surface and is probably the anterior part of the attachment area for the stylohyal ligament. The posterior groove is smooth and is for the facial nerve, which exits the skull at this point, and, therefore, corresponds to the stylomastoid notch. On the dorsolateral edge of the posterior process is a rugose surface, which probably receives part of the origins of the sternomastoideus and mastohumeralis muscles (Schulte 1916).

Measurements of the tympanic, see Appendix 4 (Table 9). The width of the tympanic is measured at the level of the apex of the sigmoid process, perpendicularly to the longest sagittal axis of the bone. The longest sagittal axis of the tympanic is measured from the anterior spiny protuberance to the posteriormost edge of the bone.

Petrosal. (Figs 12; 14). The left petrosal of MNHN SAS 892 (Fig. 14) has been removed from the skull but the compound posterior process is still *in situ*. The ventral face of the petrosal is exposed in MNHN SAS 1617 and 1618, and MNHN PPI 259 is an isolated petrotympanic of a juvenile individual.

In dorsal view, the anterior process of the petrosal is short and thick. It is transversely compressed and its apex is tapered, sharp, and dorsoventrally straight. The lateral face of the process is regularly convex and smooth.

The suprameatal fossa is deep and narrow. The structure of the bone on its surface is vesicular and rugose. Its lateral margin is a thick rim, which represents a relict of the dorsal part of the superior process (tegmen tympani in Luo & Gingerich 1999). The internal auditory meatus is sub-circular and isolated anteriorly from the facial nerve foramen by a thick and prominent crista transversa and posteriorly from the perilymphatic foramen by a thin but salient pyramidal process (Geisler & Luo 1996). The endocranial facial foramen is a wide teardrop opening. The posterior main part of the opening is a circular foramen for the facial nerve. The anterior part of the teardrop opening is a fissure for the passage of the palatine branch of the facial nerve (the greater petrosal nerve *sensu* Geisler & Luo 1996 and Luo & Gingerich 1999: 53; or the major petrosal nerve of Miller *et al.* 1964: 557; see also Wible 1990: 188), which is located at the anterodorsal contact between the anterior process and the pars cochlearis. It is homologous to the hiatus fallopii (Luo & Gingerich 1996: 53). This teardrop-shaped double foramen is approximately 15 mm long. The palatine branch of the facial nerve enters the pars cochlearis through the same foramen as the facial nerve but within its proper anterior fissure, the hiatus fallopii (Geisler & Luo 1996).

In ventral view, the pars cochlearis is a smooth half-sphere. Lateral to the pars cochlearis, the secondary facial foramen (the tympanic aperture of the facial nerve canal in Wible 1990: 188) is small and located slightly anterior to the fenestra vestibuli. From it, the facial nerve sulcus runs posteriorly slightly beyond the fenestra vestibuli (Geisler & Luo 1996).

Anterolateral to the secondary facial foramen is a large and shallow fossa for the head of the malleus. Posteriorly, the facial sulcus is bordered laterally by the crista parotica, which is high and well developed. Lateral to the crista petrosa is a deep fossa incudis.

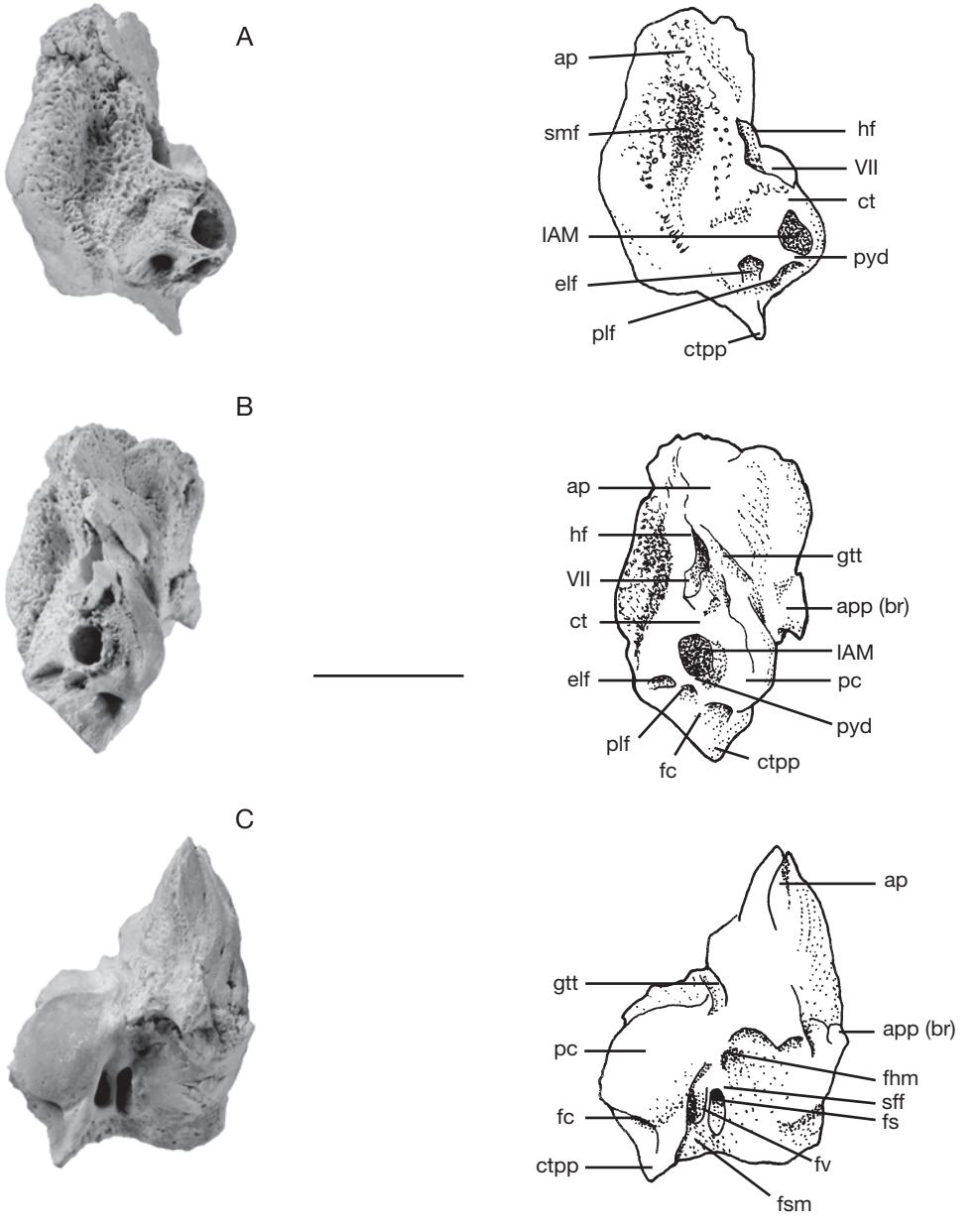

FIG. 14. — *Piscobalaena nana*, MNHN SAS 892, left petrosal: **A**, cerebral (dorsal) view; **B**, medial view; **C**, ventral view. Abbreviations: see p. 322. Scale bar: 2 cm.

Posteriorly, the crista petrosa turns into a thick and elevated bony mass that is the base of the posterior pedicle (i.e. the base of the posterior process of the petrosal fused to that of the tympanic). Posterior to the facial sulcus is a wide excavation at the posterior base of the pars cochlearis and at the base of the posterior process. This cavity is a large semicircular fossa for the stapedial muscle, located dorsally

and medially to the facial nerve. The surface of the fossa is very rugose and excavated by numerous small alveoli, thus indicating a powerful muscle. In some specimens (MNHN 1618 and 1616) the edges of the conical excavation formed by the facial nerve sulcus and the stapedial fossa almost contact ventrally, mainly because of a medial expansion of the posterior process.

The medial edge of the fenestra cochleae, just ventral to the endo- and perilymphatic foramina is greatly expanded in a large shelf, which receives the medial part of the stapedial fossa on its lateral side. This shelf is the caudal tympanic process, which is apparently remarkably developed in *Piscobalaena*.

Anteriorly, the groove for the insertion of the tensor tympani muscle (Geisler & Luo 1996) is deep and sub-rectilinear. It is a well defined sulcus, which separates the anterior base of the pars cochlearis and the anterior process. It extends from the anteroventral edge of the pars cochlearis to the ventral edge of the hiatus fallopii.

Laterally, at the base of the anterior process pedicle, there is no distinct lateral projection nor squamosal fossa as is observed in Balaenidae and in *Herpetocetus* (Geisler & Luo 1996). Posteriorly, lateral to the base of the posterior process is an elevated squamosal flange. It is separated from the posterior pedicle by a deep fossa, which communicates with the fossa incudis.

Malleus. The description of the malleus is based on the malleus of MNHN SAS 892 (Fig. 15A-C). The pedicle of the malleus (i.e. anterior process of the malleus) is fused to the anterior lamina and to the anterior edge of the sigmoid process of the tympanic. It is robust and bears two parallel columns separated by a deep groove. In this groove runs the chorda tympani, the nerve of the tympanic membrane partly modified into a ligament in cetaceans (Fraser & Purves 1960). On its posterior side, the head bears the articular facet for the incus. It is made of two semi-circular facets, which are at an angle of approximately 90°. The dorsal facet is the largest (approximately twice as large as the ventral one). Both facets are slightly convex. At the medial extremity of the line between the two facets is a tiny foramen through which the chorda tympani passes.

The column (body) of the malleus is the portion of the bone medial to the head. It bears two processes: the manubrium and the processus muscularis. The manubrium is the process on which the tympanic ligament attaches. It is greatly reduced in cetaceans relatively to land mammals. The manubrium of *Piscobalaena* is relatively long for a cetacean, hook-like and bent ventrally. The processus muscularis is prominent anteriorly and protrudes anterolaterally over the edge of the ventral facet for the incus. In posterior view, the manubrium is distinctly medial to the processus muscularis.

Measurements of the malleus, see Appendix 4 (Table 10). The length is measured between the posteriormost point of the manubrium and the anteriormost point of the processus muscularis. The width of the head is the largest width of the manubrium at the level of the facets for the incus.

Incus. The description of the incus is based on the incus of MNHN SAS 892 (Fig. 15D-F). The two facets for the articulation with the malleus are semi-circular and their surfaces are slightly concave. They form an angle of approximately 90° with each other. The ventral facet is approximately twice the size of the other facet.

The body of the incus is relatively massive and its cross-section is round. Its apex is thinner and bears the facet for the stapes, which faces anteriorly. This facet is oval-shaped: its longest axis is mediov-entrally-laterodorsally oriented. The surface of the facet is concave. The crus breve is relatively long with a thick base and a thin apex.

Stapes. The description of this bone is based on the stapes of MNHN SAS 892 (Fig. 15G). The stapedial foramen occupies the posterior half of the stapes. It is slightly oval-shaped: its longest axis oriented mediolaterally. The stapedial footplate is oval-shaped, concave and articulates with the fenestra ovale. The facet for the articulation with the incus is oval-shaped and is one third smaller than the facet for the fenestra ovale. On the posterior edge of the bone, dorsal to the margin of the facet

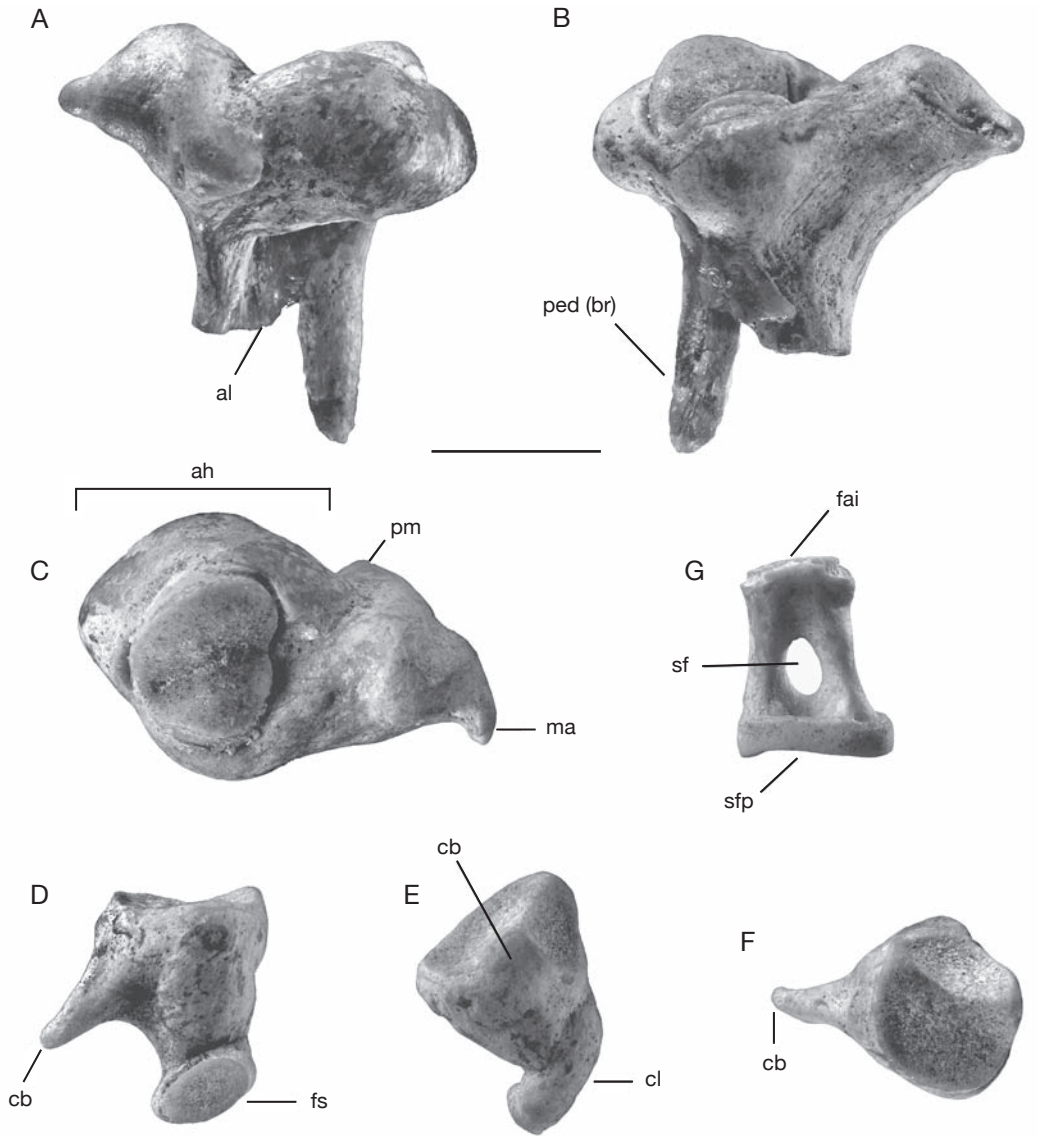

FIG. 15. — *Piscobalaena nana*, MNHN SAS 892, left auditory ossicles: **A**-**C**, malleus; **A**, dorsal view; **B**, ventral view; **C**, posterior view; **D**-**F**, incus; **D**, dorsal view; **E**, medial view; **F**, anterior view; **G**, stapes, in posterior view. Abbreviations: see p. 322. Scale bar: 5 cm.

is a small process for the insertion of the stapedial muscle.

Supraoccipital. The supraoccipital (Figs 4; 11) is sub-triangular, its anteriormost edge regularly convex anteriorly. The supraoccipital bears a thin and elevated sagittal crest in the midline. The crest is variably developed, being extremely pronounced in MNHN SAS 1618 and 1623. In the five specimens, it almost reaches the dorsal edge of the foramen magnum ventrally and occupies at least 80% of the length of the supraoccipital. The sagittal crest divides the bone into two fossae, which are deeper at their anterodorsal level. These fossae receive the

origin of the semispinalis muscle (Schulte 1916). In dorsal view, the lambdoid crests are laterally convex. They contact anteriorly at the vertex in an anteriorly convex and regular curve. In MNHN SAS 1623, the lambdoid crests bear thick exostosis, related to the old age of the individual.

Basioccipital. In its anterior part (Figs 6; 9; 10), the basioccipital is partially covered by the posterior expansion of the vomer. Its lateral borders consist of the basioccipital crests, which form the medial edges of the peribullary fossa. The basioccipital crest bears a massive, bulging, rugose and sub-triangular tubercle: the basioccipital process, which receives the origin of the longus colli muscle. Between the basioccipital processes, the basioccipital is smooth and concave. It bears a narrow medial depression, which is narrower than the largest width of one process.

Exoccipital. The foramen magnum (Fig. 11) is dorsoventrally oval-shaped. The occipital condyles are kidney-shaped and wide (maximum width: 55 mm in MNHN SAS 1623). A wide and shallow groove for the insertion of the scalenus and recti capitis antici muscles (Schulte 1916) separates the ventral edge of the condyle from the posterior extremity of the basioccipital crest.

Between the occipital condyle and the paroccipital process of the exoccipital (*sensu* Schulte 1916), the bone is smooth. In dorsal view (Figs 4; 5; 11), this area is posteriorly concave in MNHN SAS 1616 (juvenile) whereas it is sub-rectilinear or slightly posteriorly convex in the other specimens. The paroccipital process (Fig. 11) is very large and forms a posterior wall behind the posterior process of the petrotympanic and articulates with the squamosal dorsal to the process. Its lateral edge is a sub-vertical, thick, and rugose rim for the insertion of the rectus posticus, longissimus dorsi, trachelo-occipitalis and obliquus superior muscles (Schulte 1916). The posterior surface of the paroccipital processes face posteromedially and the lateral crests strongly protrude posteriorly, being slightly posterior to the occipital condyles.

Ventrally (Figs 6; 9; 10), the exoccipital constitutes the posterior crest-like wall of the peribullary

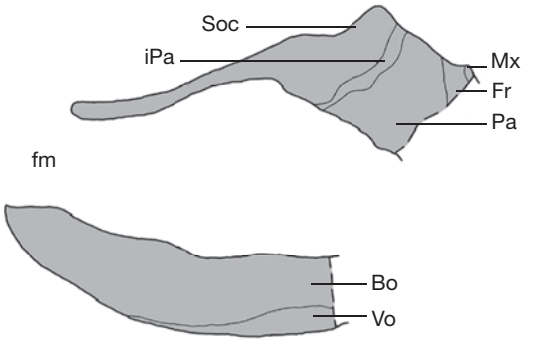

FIG. 16. — *Piscobalaena nana*, MNHN SAS 1623, schema of sagittal section of skull. Abbreviations: see p. 322.

fossa. The jugular notch excavates the exoccipital, in front of the posteromedial angle of the tympanic, lateral to the basioccipital process. Its posterior and lateral borders are thin and crest-like. The jugular vein, the internal carotid and the hypoglossal, glossopharyngeal, vagus and spinal nerves exit the skull through this notch. Lateral to the jugular notch is a deep fossa excavated in the exoccipital and adjacent to the facial nerve sulcus in the posterior process of the petrotympanic. The structure of the bone in the fossa is rugose and irregular as well as that of the fossa in the posterior process of the petrotympanic, anterior to the facial nerve sulcus. The two fossae are for the attachment of the stylohyal ligament, which floors the facial nerve.

Internal view of the cranium. The cranium of MNHN SAS 1623 was sectioned parasagitally, approximately 10 mm off the sagittal plane on the right, which allows observation of the internal sutures of the skull (Fig. 16).

At the vertex, in cross-section, the skull roof is approximately 50 mm thick. The maxillo-frontal and fronto-parietal sutures are sub-vertical. Although not visible externally, the sutures of the interparietal with the parietal anteriorly and the supraoccipital posteriorly are distinctly visible. In cross-section, the bone is reduced to a very thin stripe (2 to 4 mm) wedged between the parietal and the supraoccipital. At the vertex, the parietal is massive and the supraoccipital is slightly thinner and tapers posteriorly toward the foramen magnum.

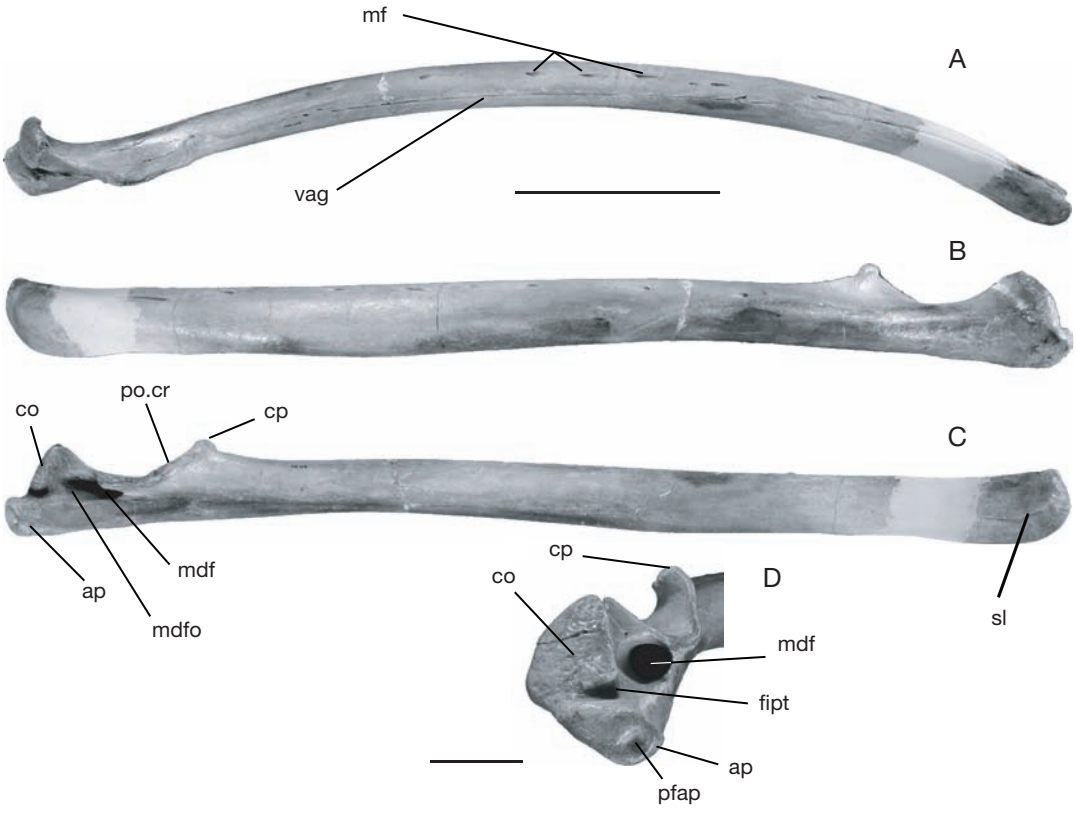

FIG. 17. — *Piscobalaena nana*, MNHN SAS 1618, left dentary: **A**, dorsal view; **B**, lateral view; **C**, medial view; **D**, posterior view. Abbreviations: see p. 322. Scale bars: A-C, 20 cm; D, 5 cm.

The frontal forms most of the anterior part of the skull roof. The fronto-parietal suture starts just anteriorly to the vertex level and is sigmoid: anteriorly concave in its dorsal part and convex in its ventral part. Ventrally, the suture runs down until the basioccipital and merges with the dorsal wall of the optic nerve canal.

The parietal consists of a very large band of bone (70 mm) between the frontal and the supraoccipital. The interparietal appears at the vertex only. The parietal and supraoccipital constitute the dorsal and lateral walls of the endocranial cavity. The parieto-squamosal suture is partly obliterated because of the old age of the specimen. The parieto-supraoccipital suture starts approximately 100 mm anteriorly to the foramen magnum. It is sigmoid: anteriorly convex in its dorsal half and posteriorly convex in its ventral half. Ventrolaterally, the suture merges with the alisphenoid. Identification of this bone is difficult because of the advanced ossification of the skull. The posterodorsal region of the endocranial cavity consists in the supraoccipital. None of the supraoccipital-exoccipital and exoccipital-basioccipital sutures are visible.

Ventrally, the basioccipital constitutes the floor of the endocranial cavity. In cross-section, it is thick (*c.* 40 mm). The sutures of the alisphenoid with the other bones are obliterated. But the groove for the passage of the mandibular nerve is well pronounced at the anterior edge of the basicapsular fissure. Measurements of the skull, see Appendix 4 (Table 11).

Dentary. The horizontal ramus of the dentary (Fig. 17) is strongly bent medially as generally in baleen mysticetes. It is constant in width and height on its posterior two thirds. It progressively tapers transversely and increases in height toward its apex. There, the ventral edge of the dentary is ventrally expanded into a very thin and smoothly convex crest, which is approximately 200 mm long. The anterior extremity of the bone is twisted (anticlockwise for the left dentary and clockwise for the right one) in such a way that the ventral edge of the apex of each dentary is shifted medially. A short sub-horizontal notch (Fig. 17C) where the ligamentous symphysis inserts is present on the medial face of the apex. The dorsal edge of the horizontal ramus bears a thin rim and medially to this rim is a vestigial alveolar groove, which reaches the apex of the dentary. Lateral to the dorsal rim, the mandibular surface bears several mental foramina, which become more broadly separated anteriorly and give passage to epithelial vessels and nerves. In the median portion of the dentary, the lateral edge of the horizontal ramus is strongly convex, while the medial edge is only slightly convex, thus providing a roughly semicircular cross-section of the bone. The ventral edge of the ramus forms a distinct angulous carina. This ridge receives the attachment of the mylohyoid muscle (Pivorunas 1977; Lambertsen 1983; Kimura 2002). This muscle is involved in engulfment feeding and plays an important role in expelling the water through the baleens (Lambertsen 1983; Orton & Brodie 1987).

The vertical ramus constitutes the posterior fifth of the dentary. The mandibular foramen opens in the dorsal half of the vertical ramus just posterior to the lowest part of the posterior ridge of the coronoid process. It opens posteriorly and extends in a deep and wide mandibular fossa until the inferior portion of the condyle. The coronoid process is low but wide and triangular in lateral view. Dorsally, its posterior crest is strongly concave laterally. It is long and reaches the dorsal edge of the condyle. The temporalis muscle, which inserts on the coronoid process and on its posterior crest, was therefore a powerful muscle. The short and thick apex of the process is hook-like and strongly bent laterally. The condyle is very large. In posterior view, it is roughly

FIG. 18. — *Piscobalaena nana*, MNHN SAS 1617, hyoid in ventral view. Scale bar: 2 cm.

oval-shaped, higher than wide, and narrower in its dorsal part than in its ventral part. Its long axis is oriented dorsomedially-ventrolaterally. The condyle is only slightly lower than the coronoid process and clearly expanded laterally. In lateral view, the articular surface of the condyle is oblique at an angle of approximately 50° with the horizontal plane. The angular process is thick, oval-shaped and its greater axis is medioventrally-laterodorsally oriented thus forming approximately a right angle (in posterior view) with the orientation of the condyle. In lateral view the angular process is developed posteriorly and extends well posterior to the condyle although to a lesser extent than in *Herpetocetus sendaicus*. The ventral half of the angular process bears a small and shallow fossa, which is approximately 15 mm in diameter. The angular process receives the depressor mandibulae, which was powerful (because of the size of the process) and efficient (because of the length of the process and the lever arm of the action). It has not been possible to elucidate which muscle or ligament attaches in the small fossa. On the medial side of the dentary, the condyle and the angular process are separated by a deep notch for the insertion of the internal pterygoid muscle (Kellogg 1968). Measurements of the dentary, see Appendix 4 (Table 12).

Post-cranial skeleton

Hyoid apparatus. None of the stylohyoids are preserved. The co-ossified basihyals and thyrohyals (Fig. 18) are dorso-ventrally thin and bear two little cornuas anterodorsally, which are short anteroposteriorly but wide transversely. Posterolaterally, the two long cornuas progressively increase in width

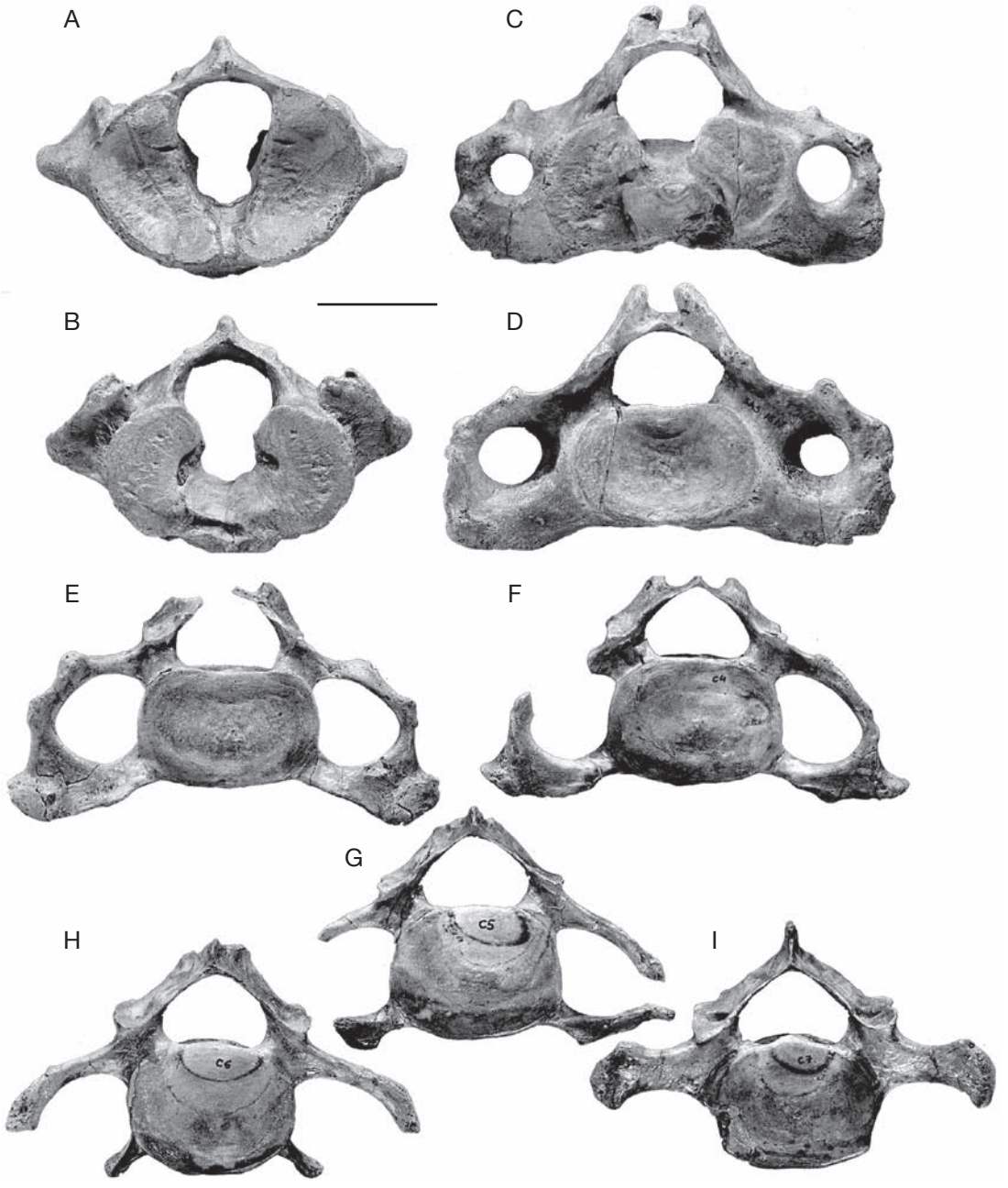

FIG. 19. — *Piscobalaena nana*, MNHN SAS 1617, cervical vertebrae: **A**, atlas, in anterior view; **B**, atlas, in posterior view; **C**, axis, in anterior view; **D**, axis, in posterior view; **E-I**, C3, C4, C5, C6, C7 in anterior view. Scale bar: 5 cm.

toward their apices and their thickness is relatively constant all along their length. Measurements of the hyoid, see Appendix 4 (Table 13).

Vertebrae. Three of the skulls (MNHN SAS 892, 1617, and 1618) are associated with axial skeleton and one isolated set of articulated cervical and

dorsal vertebrae (MNHN SAS 1624) has been referred to a juvenile or sub-adult *Piscobalaena nana* (Table 4).

Cervical vertebrae. The seven cervical vertebrae (Figs 19; 20) of *Piscobalaena nana* are free as is observed in balaenopterids and eschrichtiids but contrary to the condition observed in Recent balaenids. Their centra are relatively thick anteroposteriorly. The table below (Table 4) compares the ratio of the total length of the cervical segment to the width of the centrum of the last cervical in some Recent and fossil mysticetes. Measurements of fossil mysticetes other than *Piscobalaena* are from Kellogg (1965, 1968, 1969). All species are from the middle Miocene of the Calvert Formation. The length of the cervical segment for these four specimens has been estimated because some vertebrae were either missing or were lacking one or two epiphyses. It is noteworthy that the cervical segment of *Piscobalaena* (from the early Pliocene of the Pisco Formation) is significantly shorter (therefore probably more derived) than in the other fossil taxa, although none of the five fossil species have fused cervical vertebrae (Table 5).

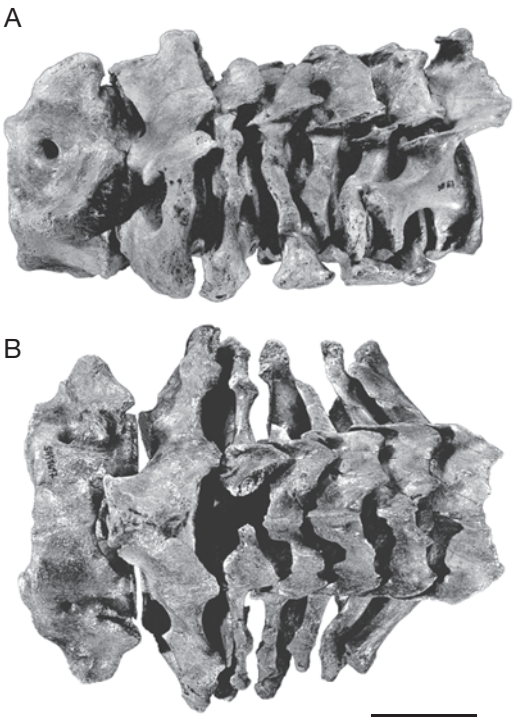

FIG. 20. — *Piscobalaena nana*, MNHN SAS 1617, cervical vertebrae: **A**, lateral view; **B**, dorsal view. Scale bar: 5 cm.

Atlas. The atlas (Figs 19A, B; 20) is anteroposteriorly long for a mysticete. The neural arch has a small but distinct neural spine. On its posterior edge, the neural arch bears two small articular facets for the articular facets of the prezygapophyses of the axis. On each side the neural arch is pierced by a large intervertebral foramen for the cerebrospinal artery and the first intervertebral vein. This foramen is located in the anterior half of the neural arch. The transverse process is short and thick. It has no transverse foramen and is made of a dorsal and a ventral tubercle separated by a thick crest. The dorsal tubercle is located slightly below the intervertebral foramen and extends from the posterior edge of the latter to the dorsal edge of the posterior articular facet for the axis. It projects posteriorly. The ventral tubercle is 30 to 40 mm ventral to the dorsal and distinctly anterior to it. Its anterior border is just ventral to the anterior edge of the intervertebral foramen. It is salient laterally and projects horizontally. The neural canal significantly narrows at mid-height, which gives it a characteristic mushroom-like morphology.

The articular surfaces for the occipital condyles are roughly semicircular and obliquely oriented. Although approximated they do not contact ventrally. They are widely separated dorsally. They are strongly concave when compared to those of Recent mysticetes.

In posterior view, the articular surfaces for the axis are kidney-shaped, relatively flat to slightly convex and their ventral edges contact the articular facet for the odontoid process of the axis. The latter is concave, faces posterodorsally at an angle of approximately 45° with the horizontal plane, and expands on the ventral edge of the neural canal.

The ventral arch of the atlas is massive and thick. It bears a large and low ventral tubercle, which is approximately twice wider than long.

Axis. The axis (Figs 19C, D; 20) is twice wider than high mainly because of the great size of the

TABLE 4. — Number of preserved vertebrae in the Sud-Sacaco specimens.

MNHN SAS specimen	892	1617	1618	1624
Cervicals	6	7	7	7
Thoracics	4	11	12	5
Lumbars	1	11?	2	–
Caudals	–	2	–	–

TABLE 5. — Comparison of the relative length of the cervical segment in *Piscobalaena* to four other fossil mysticetes from the Calvert Formation and to a Recent balaenopterid and balaenid (in mm). Abbreviation: **e**, estimated.

	Length cervical (LCS)	Width of centrum C7 (WCC7)	WCC7/LCS
Piscobalaena nana (MNHN SAS 1617)	197	76	0.385
Piscobalaena nana (MNHN SAS 1618)	208	80	0.385
Parietobalaena palmeri (USNM 23203)	262e	84	0.320
Pelocetus calvertensis (USNM 11976)	349e	114	0.326
Halicetus ignotus (USNM 23636)	350e	96	0.274
Thinocetus arthritus (USNM 23794)	351e	104e	0.296
Balaenoptera borealis	522	205	0.392
Eubalaena glacialis	257	245	0.953

transverse processes. As for the atlas, it is anteroposteriorly long in lateral view and its centrum is 30 mm long at the base of the odontoid process. The neural arch is robust and bears a small and low bifid neural spine. On the centrum, the articular facets for the atlas are kidney-shaped and slightly concave. Their medial and ventral edges contact the odontoid process, except in MNHN SAS 1617. The odontoid process is conical, wide and anteriorly reduced. At mid-height, the odontoid process bears a sub-horizontal thin crest, which marks the dorsal edge of the articular facet with the atlas. The transverse process is wide, wing-like and roughly quadrate. It is pierced by a very large transverse process (vertical diameter: 25 mm; horizontal diameter: 30 mm). On the dorsal border of the process is a small tuberosity just dorsal to the transverse foramen and which bears a poorly defined articular facet for the transverse process of the C3. The ventrolateral angle of the transverse process also bears a small articular facet for the C3. This facet is poorly marked except in MNHN SAS 1617.

In lateral view (Fig. 20A), the neural arch is anteriorly developed, and particularly in MNHN SAS 1617. It presents two anterolaterally projecting angles, which are rudimentary prezygapophyses. On their ventral face, at the apex, they present a small articular facet, which articulates with the small facet on the posterior edge of the neural arch of the atlas. The postzygapophyses are small but present well defined, oval-shaped articular facets for C3.

On the centrum, the articular surface for C3 is oval-shaped and deeply concave with its dorsal and ventral edges slightly concave dorsally. Measurements of the atlas and the axis, see Appendix 4 (Table 14).

C3-C7. The neural arch of C3-C7 (Figs 19C-G; 20) is V-shaped, decreasingly opened ventrally from C3 to C7. The arch also increases in height and anteroposterior length from C3 to C7. The neural spine is small but slightly increases in size from C3 to C7. The prezygapophyses are large and widely separated, a condition that increases from C3 to C7. They bear a distinct tiny fossa at the posterior angle of the articular facet. This fossa increases in size posteriorly and becomes a real pit on C6 and C7 (Fig. 19E-I). The postzygapophyses are large and divide posteriorly into a "proper" postzygapophysis (which bears the articular facet) and a medial tubercle. From C4 to C6 the medial tubercle migrates medially and increases in size. It almost disappears on C7.

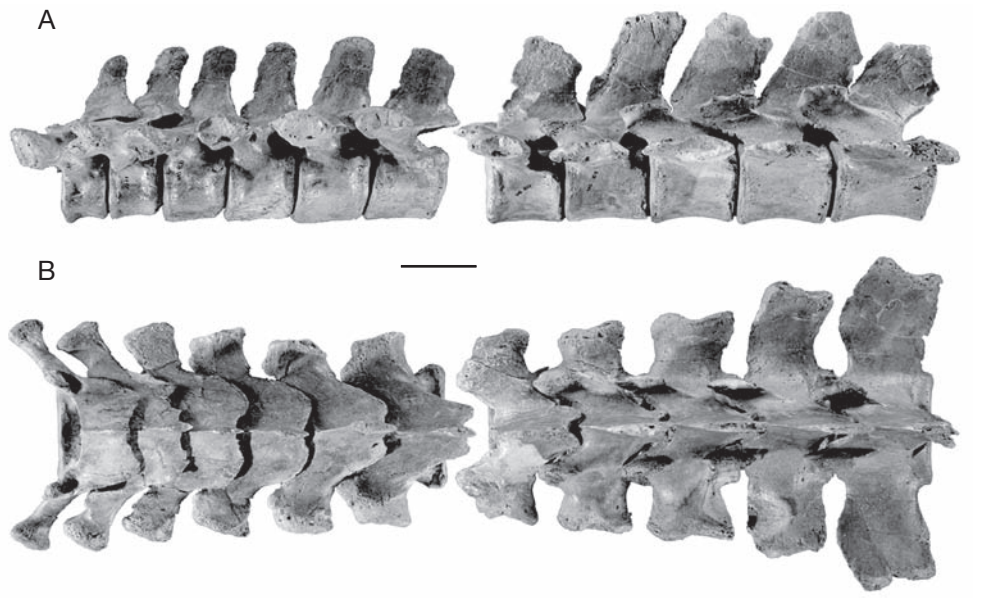

FIG. 21. — *Piscobalaena nana*, MNHN SAS 1617, thoracic vertebrae: A, D1-D11, in lateral view; B, D1-D11, in dorsal view. Scale bar: 5 cm.

On C3-C4, the transverse foramen is unusually large (at least twice larger than on the axis) and closed. It occupies almost the whole of the transverse process, which is reduced to a bony arch. The transverse foramen is open on C5-C6 and the transverse process is divided into thin ventral and dorsal branches. The branches are similar in length on C5 but on C6 the dorsal branch is distinctly larger than the ventral, which is reduced to a small process. On C7, the ventral process is absent and the dorsal is much thicker than on C3-C6. The apex of the transverse process of C7 is expanded and bears the articulation of the tuberculum of the first rib. The dorsal branch of the transverse process of C3 and C4 bears two small tuberosities, which are faint on C4 and disappear on C5 and C6.

The transverse process of C3 projects laterally (in the same plane as the centrum), while the dorsal branches are anteriorly oriented on C4 to C7, a condition which is incipiently developed on C4 and C5 but which strongly increases on C6 and C7. The cross-section of the ventral half of the transverse process is roughly triangular on C3 and C4 and dorsoventrally flattened on the posterior cervical vertebrae. The ventral branch of the transverse process of C3-C4 bears a thick ventrolateral tuberosity, which progressively reduces in size until C6. On C4, the posterior edge of the ventral branch has a small sub-horizontal tuberosity, which becomes a large rim on C5 and disappears on C6.

On C3 to C7, the centra are much wider than high and have a roughly oval to rectangular shape.

Thoracic vertebrae. *Piscobalaena nana* has 11 thoracic vertebrae (Fig. 21). In anterior view, the neural arch is V-shaped, increasingly opening from T1 to T4 and then progressively closing up to the last thoracic vertebra. Its anteroposterior length progressively increases from the first to the last thoracic vertebra. The neural apophysis is small, anteroposteriorly short and distinctly shorter at apex than at base. From T1 to T11, the neural apophysis increases in size. It is approximately three to four times higher on the posterior thoracics than on T1. Furthermore, the neural apophysis, triangular on T1, becomes progressively rectangular on the posterior thoracics and is as long at apex than at base. They are slightly inclined posteriorly, a condition which increases from T1 to T11.

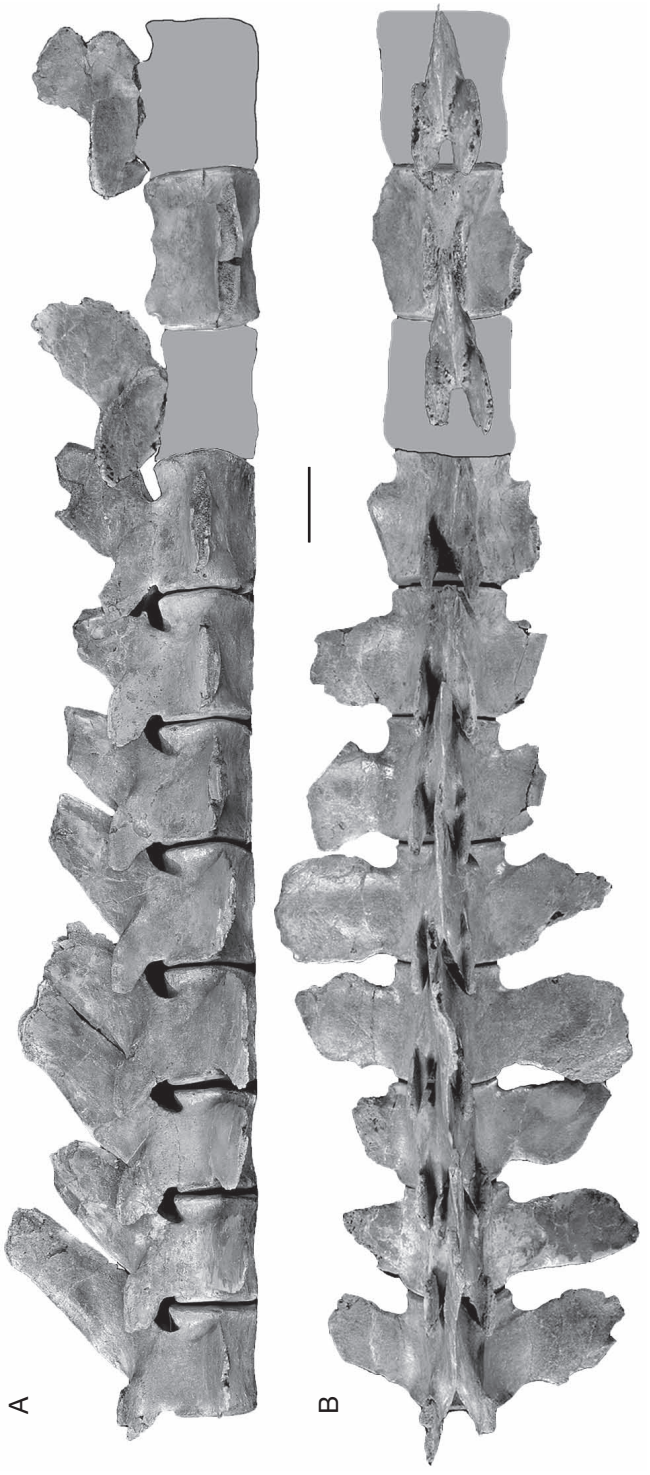

FIG. 22. — *Piscobalaena nana*, MNHN SAS 1617, lumbar vertebrae: **A**, L1-L11, in lateral view; **B**, L1-11, in dorsal view. Scale bar: 5 cm.

The prezygapophyses cannot be strictly defined as apophyses and are in fact reduced to prezygapophyseal facets. From T1 to T3, the prezygapophyseal facet is slightly salient dorsally and anteriorly and bears a deep and dorsally oriented fossa at its posterior extremity on T1. The fossa decreases in size from T1 to T4, on which it almost disappears. On the next vertebrae, the facet is long and narrow and located at the anterior edge of the neural arch. The facets are widely separated on T1 to T4, approximate on the next vertebrae, and almost contact at the anterior base of the neural spine from T8 to T11. On T4, at the anterior edge of the transverse process and lateral to the prezygapophyseal facet is a small tubercle, which develops on the following thoracics in well pronounced mammillary processes (metapophyses). From T4 to T11, the mammillary processes greatly increase in size and migrate medially. They progressively approximate to the base of the transverse process from T5 to T8 and are located on the neural arch from T9 to T11.

The postzygapophyses progressively reduce in size from T1 to T11 and are almost absent on T10 and T11 of MNHN SAS 1617. Large and widely separated on the anterior thoracics, the postzygapophyses approximate to the neural spine medially on the posterior vertebrae and almost contact on T9 and T10.

The transverse processes of the anterior thoracics are long, narrow, and anteroposteriorly oriented in the first three thoracics. They progressively increase in anteroposterior length and decrease in dorsoventral thickness from T1 to T11. Their transverse lengths decrease from T1 to T4, are constant from T5 to T7 and strongly increase from T7 to T11. In anterior view, the apex of the transverse process is at the level of the dorsal edge of the centrum on T1 and T2, above this plane from T3 to T7, at the level of the dorsal edge of the centrum on T8 and T9 and below this level on T10 and T11. The anteroposterior length of the centrum progressively increases from the first to the last thoracic vertebra. The articular semi-facets for the rib capitulum on the centrum are present until T7, on which the anterior semi-facet only is present. From T8 to T11, the ribs articulate only with the apex of the transverse process.

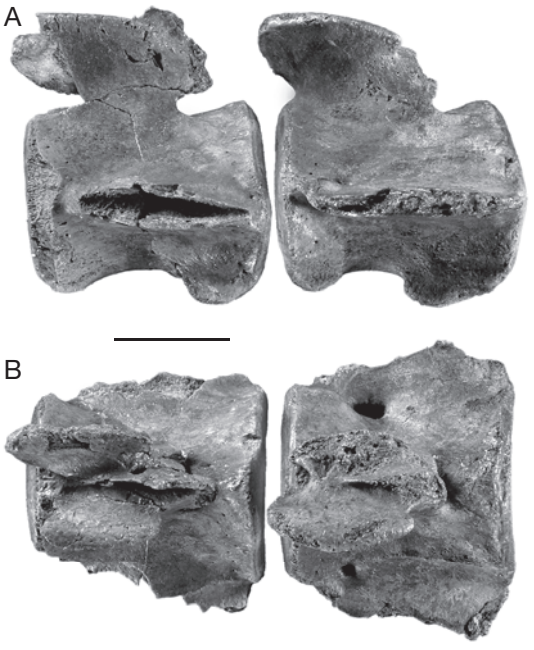

FIG. 23. — *Piscobalaena nana*, MNHN SAS 1617, caudal vertebrae: **A**, ?CA3-?CA4, in lateral view; **B**, ?CA3-?CA4, in dorsal view. Scale bar: 5 cm.

Lumbar vertebrae. Eleven lumbar vertebrae are preserved on MNHN SAS 1617 (Fig. 22). L1 to L8 are almost complete. L10 is a centrum and L9 and L11 are represented by their neural arch. The vertebrae are very similar to each other. Their neural spines are posterodorsally oriented and their transverse processes are long anteroposteriorly, blade-like and slightly inflected ventrally. The mammillary processes (metapophyses) are very large and increase in size posteriorly. They are transversely flattened, protrude anterodorsally, and enclose the posterior edge of the neural spine of the preceding vertebra, which prevent the lumbar column from horizontal (lateral) movements. Their centra increase in length from the first to the last lumbar vertebra.

Caudal vertebrae. The only preserved caudal vertebrae are ?CA3 and ?CA4 of MNHN SAS 1617 (Fig. 23). The anterior vertebra ?CA3 is smaller than the posterior. Their centra are distinctly wider and longer than those of the lumbar vertebrae. On the posteroventral edge of the

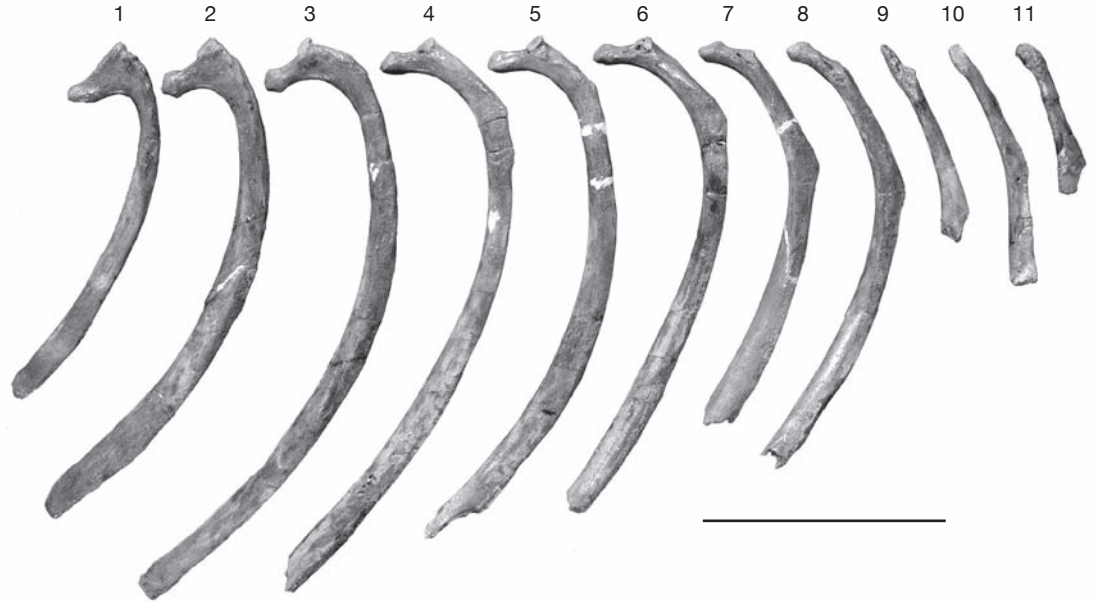

FIG. 24. — *Piscobalaena nana*, MNHN SAS 1617, right ribs. Scale bar: 20 cm.

TABLE 6. — Number of preserved ribs in specimens of *Piscobalaena nana*.

	MNHN SAS 1617	MNHN SAS 1618
Number of left ribs	10 (11 is not preserved)	7 (1-2-3-4-7-8-9)
Number of right ribs	11	9 (1-2-3-4-5-6-7-8-10)

centrum of ?CA3 are two thick articular knobs for the chevron bones. On the other, more posterior caudal vertebra, the articular processes for the chevrons are larger and the anterodorsal edge of the centrum also presents a small tubercle for ligamentous attachment of the chevron. The neural arch is lower than on the last lumbars and the mammillary processes are shorter. The transverse processes are broken on both vertebrae. It is however possible to observe the condition of the passage for the spinal artery. On ?CA3, the artery passes in a groove at the anterior base of the transverse process. On ?CA4, the process is perforated by a foramen for the artery, the right being three times larger than the left. On ?CA4, on the lateral edges of the centrum, dorsal to the posterior base of the transverse process, is a low but sharp crest for muscular attachment.

Ribs. MNHN SAS 1618 ribs are more massive and slightly shorter than those of MNHN SAS 1617 (Fig. 24). This confirms the probable referral of MNHN SAS 1618 to a female. In MNHN SAS 1617, 11 right ribs are preserved. The articular facet of the capitulum and the tuberculum are distinct on the first eight ribs. On the last three ribs, the capitulum disappears and the articulation with the vertebrae is with the tuberculum only. The first rib is the shortest and the angle between the vertebral portion of the rib (capitulum, neck and tuberculum) and the body is always inferior to 90°. On the next two ribs, this angle is wider. The next ribs (4 to 8) are regularly curved and the last three ribs (9 to 11) are sub-rectilinear. The tuberosity present on the posterior edge of the first rib migrates ventrally on the body of the next ribs so that it is located approximately on the

dorsal third of the last ribs. Number of preserved ribs, see Table 6.

Pelvis. The preserved part of the pelvis (MNHN SAS 1618, Fig. 25) is 70 mm long and forms a thick and slightly curved bony spine terminated by a small rim behind which the bone is not preserved.

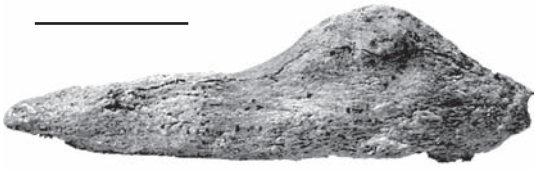

FIG. 25. — *Piscobalaena nana*, MNHN SAS 1618, pelvic bone (vestigial). Scale bar: 2 cm.

Scapula. The scapula of MNHN SAS 892 and 1617 are preserved. An isolated scapula from Aguada de Lomas has also been referred to *Piscobalaena nana* (MNHN PPI 260). As mentioned above, the small cetothere of the AGL Horizon (at Aguada de Lomas) is regarded, on the basis of two skulls, as belonging to the same species as that of Sud-Sacaco (i.e. *Piscobalaena nana*). The scapula of *Piscobalaena* (Fig. 26A, B) has a unique trapezoidal and elongated morphology, which contrasts with the triangular shape generally observed in the other mysticetes: the greatest proximodistal length of the bone is approximately twice shorter than the width. The angle formed by the cranial and caudal edges of the scapula is of approximately 125° in MNHN SAS 1617 and 155° in MNHN SAS 892.

On the lateral side of the scapula, the infraspinatus fossa forms most of the surface of the bone. It receives the deltoideus origin in its anterior third and the infraspinatus muscle origin posteriorly on most of the remaining surface. The supraspinatus fossa is restricted to a narrow anteroventral groove limited laterally by the scapular spine. The acromion is a long and spatulated process, medially concave. It projects anteriorly and is approximately parallel to the length of the scapula. At the anterior base of the glenoid cavity is a long finger-like coracoid process, which is parallel to the acromion. In proximal view, the coracoid process is strongly oriented medially at an angle of approximately 35° with the plane of the bone. The glenoid cavity is oval-shaped with a medial edge less convex than the lateral. The medial face of the scapula is a large fossa for the subscapularis muscle. It is smooth but bears several ridges for attachment of the muscle radiating from the glenoid cavity. On the posteroventral edge of the bone, at mid-length between the posterior edge of the glenoid cavity and the posterior angle, is a distinct crest for the origin of the teres major muscle, which probably occupied part of the posterior area of the lateral face of the scapula, posterior to the infraspinatus muscle origin. The posterior third of the posterior border of the scapula bears another ridge, which extends on the medial face of the bone. This muscle scar is for the origin of the serratus muscle. Measurements of the scapula, see Appendix 4 (Table 15).

Humerus. The humerus of *Piscobalaena* (Fig. 26C, D) is short and massive and transversely flattened. The head is hemispherical and posterolaterally oriented. It is large, protrudes posteriorly and its diameter is greater than the anteroposterior length of the distal epiphysis. The greater tubercle is anteromedial to the head. It is stout and massive and, although salient, it is lower than the head. It extends on the anterior edge of the diaphysis in a short and thick deltopectoral crest, which remains on the proximal half of the bone. The lesser tubercle is a small tuberosity on the medial side of the epiphysis, approximately at the level of the centre of the head. It is much lower than the greater tuberosity. On the distal epiphysis, the elbow articulation is ankylosed as in all mysticetes and odontocetes. The facets for the radius and ulna are relatively flat. The radial facet, however, is slightly concave and the ulnar facet presents a posterior extension on the posterior edge of the diaphysis for the olecranon of the ulna. The radial facet faces anteroproximally and the ulnar facet faces posteroproximally and both facets are at an angle of approximately 130°. Measurements of the humerus, see Appendix 4 (Table 16).

Radius. The radius (Fig. 26E) is approximately 50% to 33% longer than the humerus. It is spatulate and

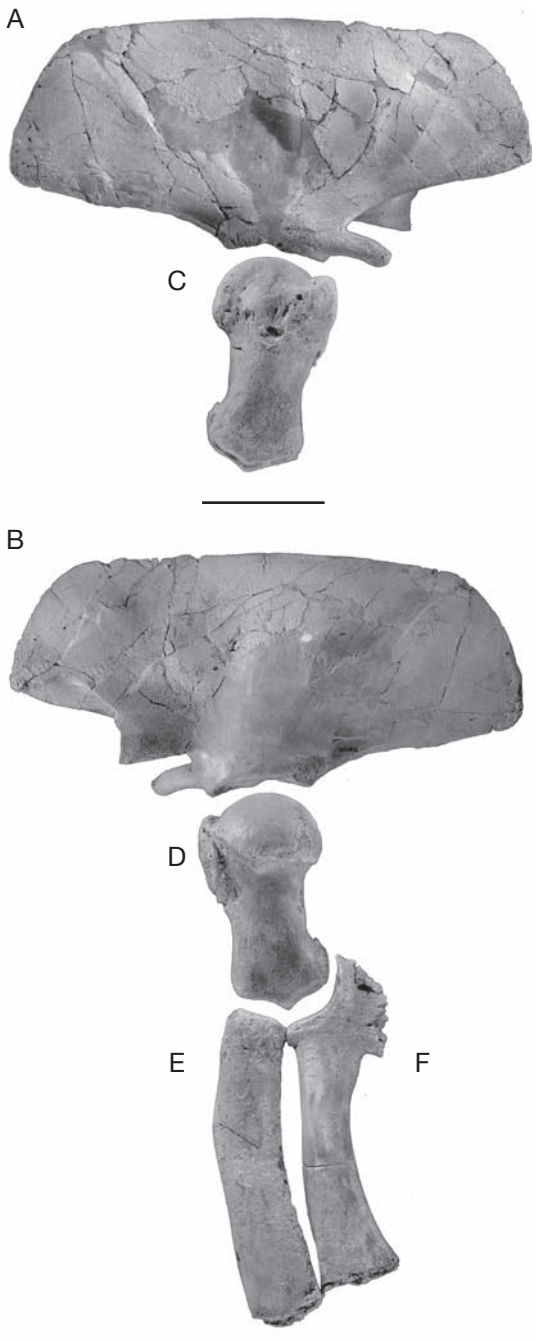

FIG. 26. — *Piscobalaena nana*: **A**, **B**, left scapula (MNHN SAS 892); **A**, medial view; **B**, lateral view; **C**, **D**, left humerus (MNHN SAS 1617); **C**, medial view; **D**, lateral view; **E**, left radius, in lateral view; **F**, left ulna, in lateral view. Scale bar: 10 cm.

transversely flattened as in all mysticetes. The humeral facet is oval-shaped with a straight posterior edge corresponding to the straight contact between the ulnar and radial facets on the humerus. On the posterior edge of the humeral facet is a small facet for the ulna. The diaphysis is markedly bent posteriorly in the proximal third of the bone. At this point, the anterior edge of the radius is salient anteriorly. On this structure and on the anteroproximal angle of the lateral face of the bone is the insertion of the deltoideus, an abductor of the arm. The distal epiphysis has no articular facet but a rugose and irregular surface of bone for attachment of cartilage. It is oval-shaped with a straight posterior border. Measurements of the radius, see Appendix 4 (Table 17).

Ulna. As for the humerus and radius, the ulna (Fig. 26F) is transversally flattened. Its proximal extremity bears the concavoconvex humeral facet, which expands ventrally as a small vertical facet for the radius. Posterior to the humeral facet is a small olecranon with a convex posterior edge. In its distal region, the bone is rugose and irregular posteriorly for cartilage attachment. Its proximal apex is pointed. The diaphysis is bent posteriorly and widens distally. Its anterior edge is a relatively sharp crest while its posterior edge is wide and rounded. The distal epiphysis is rugose and irregular for attachment of the cartilage in which the carpals are embedded. Measurements of the ulna, see Appendix 4 (Table 18).

Carpals, metacarpals and phalanges. The left limb of MNHN SAS 1617 only is preserved (Fig. 27). Because no elements of the proximal right limb have been recovered, it is supposed that the several hand bones (including six carpals, four metacarpals and seven phalanges) of the specimen belong to the same limb. Three carpals and four metacarpals of MNHN SAS 892 have also been collected. The carpus of *Dorudon* Gibbes, 1845 contains six carpals and one accessory element, the pisiform (Uhen 2004). It is therefore probable that the carpus of *Piscobalaena* also had the same composition, a condition found in most Recent mysticetes. The carpals of *Piscobalaena* are globose and sesamoid-like. Their surface is rugose

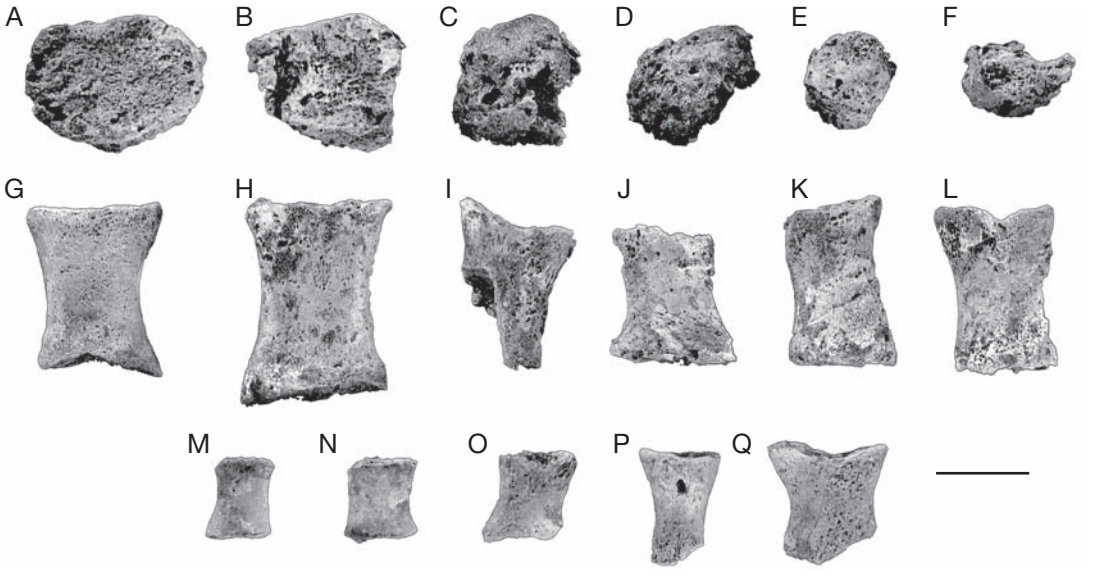

FIG. 27. — *Piscobalaena nana*, left(?) flipper (MNHN SAS 1617): **A**, ?lunar; **B**, ?unciform; **C**, ?cuneiform; **D**, ?trapezoid; **E**, ?scaphoid; **F**, ?pisiform; **G**, **H**, metacarpals; **I**-**Q**, phalanges. Scale bar: 2 cm.

and irregular corresponding to their embedment in cartilage. The largest two carpals however have a smooth and flat side (possibly external) and by comparison with the relative size of the carpals in *Dorudon*, could be the lunar (the largest) and the unciform (the smallest). The two largest of the remaining four could be the cuneiform and the trapezoid. One of the two smallest is possibly the scaphoid and the other one because it is slightly elongated and not nodular as the scaphoid could be the pisiform.

MNHN SAS 1617 has 11 digit bones preserved. Half of them are very likely to be metacarpals because of their large size and their flattened shape.

COMPARISONS

Material used for comparison

Piscobalaena nana will be extensively compared below to four species traditionally included in the "Cetotheriidae" (McKenna & Bell 1997): *Nannocetus eremus*, *Herpetocetus sendaicus*, *Cetotherium rathkei* and *Metopocetus durinasus*. The four species are morphologically very similar to *Piscobalaena nana* and are from localities of similar geological ages (late Miocene-early Pliocene).

Nannocetus is known by one species only, *Nannocetus eremus*, and apparently one single described specimen (UCMP 26502) (Kellogg 1929) from the late Miocene of the Towsley Formation of California, USA. The holotype is a poorly preserved partial skull lacking the upper portion of the braincase, the nasals, the lacrimals, the jugals and the rostrum. The left tympanic and petrosal have been recently prepared and isolated from the skull. *Nannocetus* is a small "cetothere", which could be within the range of individual size variation of *Piscobalaena*.

Herpetocetus (= *Erpetocetus*) Van Beneden, 1872 is from the early Pliocene of Europe, North America (Geisler & Luo 1996) and Japan (Hasegawa *et al.* 1985; Oishi *et al.* 1985; Oishi & Hasegawa 1994b). Although the genus is widely distributed, only one sub-complete skeleton is known and allows significant comparison with *Piscobalaena*. This specimen (NSMT-PV 19540) is referred to *Herpetocetus sendaicus* (Hatai *et al.* 1963) and is from the Pliocene Yushima Formation of Japan (Hatai *et al.* 1963; Ichischima 1997; Oishi & Hasegawa 1994b). Therefore, referral to *Herpetocetus*, below, will be in

fact to this specimen (Oishi & Hasegawa 1994b: 159, fig. 2). The petrosal of this specimen is not isolated from the skull and therefore the petrosal of *Piscobalaena nana* has also been compared with the isolated petrosal (USNM 299652) referred to *Herpetocetus* by Geisler & Luo (1996).

Cetotherium rathkei Brandt, 1843 is the type species of *Cetotherium* (Kellogg 1931; Ichischima 1997). The holotype is an incomplete skull (lacking the rostrum) with associated tympanics and petrosals from the late Miocene of South Russia (Pilleri 1986).

Metopocetus durinasus Cope, 1896 is the type species of *Metopocetus*. The holotype (USNM 8518) and only known specimen is an incomplete braincase with the right petrosal *in situ* (Kellogg 1968; Ichischima 1997) and the auditory ossicles. This specimen is from the late Miocene of the Calvert Formation of Maryland, USA.

The specimens mentioned above have been examined by one of us (VB) except the partial skeleton of *Herpetocetus sendaicus*, a cast of which has been available during this study, and the holotype of *Cetotherium rathkei*, which has been studied from Brandt (1843), and Pilleri (1986) and from original photographs provided by M. Elstrup.

However, occasional comparisons have been also made with other fossil (*Aglaocetus patulus*, see Appendix 1; *Eomysticetus whitmorei*, see Appendix 1; *Cophocetus oregonensis*, see Appendix 1; *Diorocetus hiatus*, see Appendix 1; *Mauicetus* Benham, 1939 in Benham 1937, 1942; Marples 1956; *Mixocetus elysius*, see Appendix 1; *Parietobalaena palmeri*, see Appendix 1; *Pelocetus calvertensis*, see Appendix 1) and Recent baleen mysticetes (*Balaenoptera*, see Appendix 1; *Balaena*, see Appendix 1; *Eubalaena*, see Appendix 1; *Caperea marginata*, see Appendix 1; *Eschrichtius robustus*, see Appendix 1), with toothed mysticetes (*Aetiocetus*, see Appendix 1; *Chonecetus goedertorum* Barnes & Furasawa, 1994 in Barnes *et al.* 1994; *Mammalodon* Pritchard, 1939), and eventually with archaeocetes (*Dorudon*, see Appendix 1; *Zygorhiza*, see Appendix 1).

Comparison / skull

Size of the skull. The skull of *Piscobalaena nana* is very small compared to most other mysticetes. The range of bizygomatic width is 327-433 mm. However, the bizygomatic width of *Cetotherium rathkei* (bizygomatic width: 310 mm according to Brandt 1873: 81) and *Nannocetus eremus* (bizygomatic width: 240 mm) are smaller than in *Piscobalaena* and that of *Herpetocetus sendaicus* (bizygomatic width: 380 mm) is comparable to that of *Piscobalaena*. The skull of *Parietobalaena palmeri* (Kellogg, 1924) is also relatively small, but it is wider than the greatest width observed in *Piscobalaena* as its bizygomatic width ranges between 442 (estimated width) and 496 mm. The skull of *Piscobalaena* is distinctly smaller than that of *Metopocetus* (estimated bizygomatic width: 590 mm).

Nasal region. In *Piscobalaena*, the narial opening extends posteriorly, slightly posterior to the line joining the preorbital processes of the maxillae (the posterior end of the narial opening corresponds to the anterior edge of the nasals). A similar condition is present in *Cetotherium rathkei*. In *Herpetocetus sendaicus*, the preorbital processes of the maxillae of the only known specimen are not preserved. However, enough is preserved of the supraorbital process of the frontal to reasonably reconstruct the position of the preorbital process of the maxilla and to conclude that the posterior extremity of the narial opening was approximately at the level of (or slightly anterior to) the line joining the supraorbital processes of the maxillae. The condition of the poorly preserved holotypes of *Nannocetus eremus* and *Metopocetus durinasus* is unknown.

In Recent mysticetes, the posterior extension of the narial opening is well anterior to this line. A similar condition is present in Miocene mysticetes such as *Diorocetus* Kellogg, 1968, *Aglaocetus* Kellogg, 1934, and *Parietobalaena* Kellogg, 1924. It is absent in *Mixocetus* Kellogg, 1934, in which the narial opening distinctly extends posterior to the preorbital processes of the maxillae. Because the condition of Recent mysticetes is also present in aetiocetids (*Aetiocetus* Emlong, 1966 and *Chonecetus* Russel, 1968), it is apparently plesiomorphic and *Piscobalaena* is therefore more derived than the Recent mysticetes in this respect.

In *Piscobalaena*, the contact between the rostral and cranial bones is strongly V-shaped and forms a

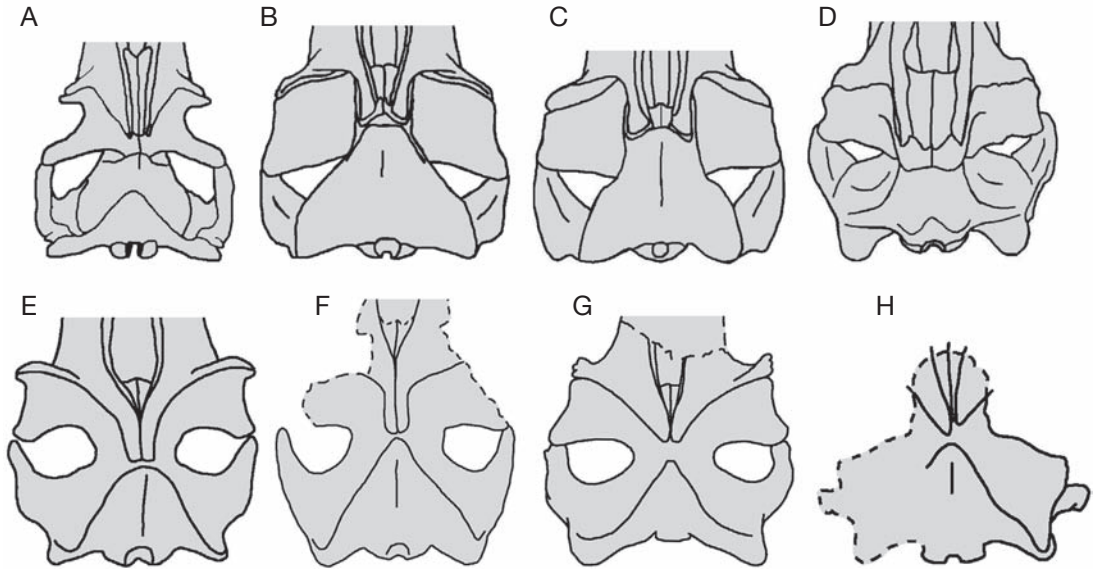

FIG. 28 — Schemas of skulls of various mysticetes taxa, bearing ascending processes of the maxilla: **A**, *Aetiocetus weltoni*; **B**, *Balaenoptera acutorostrata*; **C**, *Balaenoptera physalus*; **D**, *Eschrichtius robustus*; **E**, *Piscobalaena nana*; **F**, *Herpetocetus sendaicus*; **G**, *Cetotherium rathkii*; **H**, *Metopocetus durinasus*.

right to acute angle. A similar condition is present in *Herpetocetus*, *Cetotherium*, *Metopocetus*, and *Mixocetus*. In the Miocene mysticetes, *Parietobalaena*, *Diorocetus*, *Pelocetus* Kellogg, 1965, *Aglaocetus*, *Cophocetus* Packard & Kellogg, 1934, and in Recent balaenids, the contact between rostral and cranial bones is either transverse or forms a very obtuse angle. The contact is T-shaped in balaenopterids and eschrichtiids. In *Aetiocetus* and *Chonecetus*, the posterior edge of the rostral bones is also V-shaped but the condition of these genera is different from that of *Piscobalaena* in the smaller posterior process of the maxilla and the larger posterior process of the premaxilla. Furthermore, in aetiocetids (Fig. 28A), the telescoping of the skull is less advanced because the rostral bones are very distant from the parietal, while they contact it in *Piscobalaena*, *Herpetocetus*, *Cetotherium*, and *Metopocetus*.

The extremities of the ascending processes of the maxillae are preserved in *Metopocetus* (Fig. 28H), *Herpetocetus* (Fig. 28F) and *Cetotherium* (Fig. 28G). In *Nannocetus eremus* (Fig. 29), the processes are not preserved but their suture with the frontal is visible. The ascending processes of the maxillae of *Piscobalaena* are long and parallel; they extend well posterior to the nasals, and largely contact behind them. The condition is similar in *Herpetocetus*, although the processes are clearly longer in this genus than in *Piscobalaena*. In *Cetotherium*, although the processes extend posteriorly and approximate behind the nasals, they are much shorter than in *Piscobalaena* and not parallel. A condition similar to that of *Cetotherium* is present in *Metopocetus* (the premaxilla labelled in Kellogg 1968: fig. 51 is in fact the extremity of the ascending process of the maxilla). The skull of *Nannocetus* is poorly preserved. However, traces of the fronto-maxillar suture on the supraorbital process of the frontal suggest a condition similar to those of *Metopocetus* and *Cetotherium*.

In Recent mysticetes (Fig. 28B-D), the ascending processes of the maxillae are well developed but they do not extend and contact posteriorly to the nasals, which extend posteriorly as far as the maxillae. In Miocene mysticetes, *Diorocetus*, *Aglaocetus*, and *Cophocetus*, a distinct ascending process is not clearly individualised or it is very small. In these genera the fronto-maxillar suture tends to be roughly

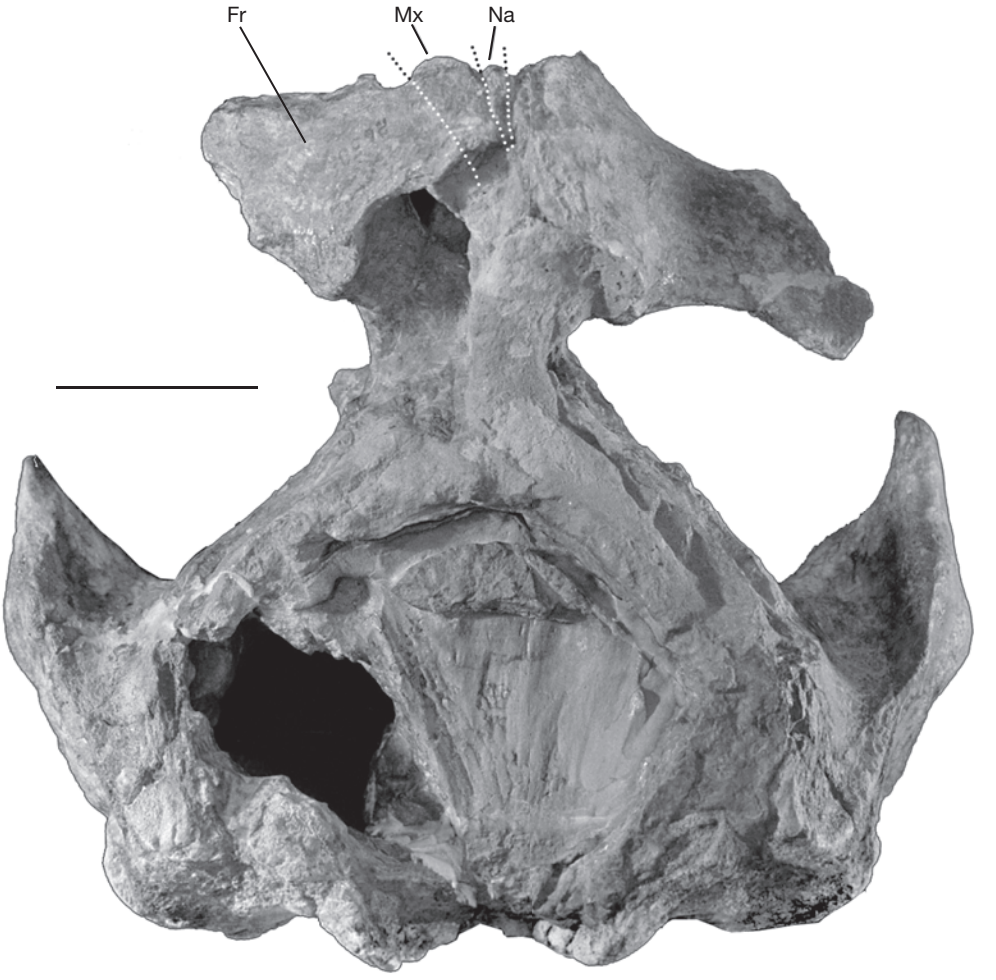

FIG. 29. — *Nannocetus eremus*, UCMP 26502 (holotype), skull in dorsal view showing the morphology of the apex of the ascending process of the maxilla (**Mx**), relatively to the nasal (**Na**) and frontal (**Fr**). Scale bar: 5 cm.

transverse. A distinct ascending process is present in *Mixocetus*, although not parallel-sided as in *Piscobalaena* and *Herpetocetus*.

In *Piscobalaena* (Fig. 28E) and *Herpetocetus* (Fig. 28F), the apex of the ascending process of the maxilla is relatively square. In this respect, they differ from *Cetotherium* and *Metopocetus*, in which the apex is rounded to pointed.

In *Piscobalaena* and *Herpetocetus*, the posterior apex of the premaxilla does not extend posterior to the anterior half of the nasal. The condition of *Cetotherium* is difficult to evaluate from the figure by Pilleri (1986: pl. 25, fig. 1), although it is probably similar to that of *Piscobalaena*. In *Metopocetus*, there is no premaxilla between the posterior part of the nasals and the ascending processes of the maxillae, which would indicate a similar condition to that of *Piscobalaena*. In Recent mysticetes, the premaxillae are wedged between the nasals and the ascending processes of the maxillae and reach the posterior extremities of the nasals posteriorly. A similar condition is present in the Miocene mysticetes (e.g., *Diorocetus*, *Aglaocetus*, *Cophocetus*, and *Mixocetus*). It is also present in

the Aetiocetidae and represents a plesiomorphic character state.

In *Piscobalaena*, the posterior extremity of the ascending process of the maxilla is at the level of (or slightly anterior to) the posterior edge of the temporal fossa, while in *Cetotherium* and *Herpetocetus* it is at the level of its anterior edge. The condition of *Metopocetus* is difficult to evaluate, although it is probably similar to that of *Piscobalaena*. A more posterior position of the rostral bone is indicative of a more developed telescoping of the skull and is regarded as apomorphic relatively to a less posterior position of the bones. However, the ascending processes of the maxillae of *Herpetocetus*, distinctly longer than those of *Piscobalaena*, *Cetotherium*, and *Metopocetus*, are regarded as derived, while the relative position of their apices is plesiomorphic when compared to *Piscobalaena*.

Supraorbital region. In *Piscobalaena*, *Cetotherium*, and *Herpetocetus*, the maxillo-frontal suture is regularly and slightly concave posteriorly. The condition of *Metopocetus* and *Nannocetus* are unknown. In Recent balaenopterids, the suture is deeply concave and the medial and lateral extremities of the suture are at a right to acute angle. The suture is almost straight to slightly sigmoid in *Diorocetus*, *Aglaocetus*, *Parietobalaena* and *Cophocetus*. The condition varies in the Aetiocetidae. It is V-shaped, opening posteriorly, in *Aetiocetus cotylalveus* and *A. weltoni*, but straight and oblique in *A. polydentatus*. In *Chonecetus*, the lacrimal is large, and wedged between the frontal and the maxilla on the lateral region of the skull, an archaeocete-like condition, which is probably plesiomorph. The condition of this character in *Piscobalaena* is difficult to evaluate, because the condition in the early diverging aetiocetids varies. However it is likely that the morphology of the balaenopterids is derived compared to that of *Piscobalaena*, *Herpetocetus*, *Cetotherium*, *Aglaocetus*, *Diorocetus*, *Parietobalaena* and *Cophocetus*.

The preorbital process of the maxilla is laterally developed and dorsally bulges as a thick and anteriorly protruding rim in *Piscobalaena*, *Cetotherium*, and *Diorocetus*. The process is small to absent in *Aglaocetus* and *Parietobalaena*. The large preorbital process of the maxilla is absent in archaeocetes but well developed in aetiocetids, a condition regarded as derived.

The preorbital notch of *Piscobalaena* is relatively deep and the anterior edge of the preorbital process is approximately at a right angle with the lateral edge of the maxilla. A similar condition is present in *Cetotherium*, although in this genus the preorbital notch is shallower than in *Piscobalaena* and the angle is slightly larger than 90°. A deep preorbital notch is also present in *Cophocetus* and *Diorocetus*. The preorbital notch is very shallow (i.e. the angle is much larger than 90°) or absent in Recent mysticetes, in Miocene taxa such as *Parietobalaena*, *Aglaocetus* and in Oligocene taxa such as *Mauicetus* Benham, 1939 and *Eomysticetus* Sanders & Barnes, 2002. In the Aetiocetidae, the preorbital notch is either reduced or absent, which suggests that the condition of *Piscobalaena* is apomorphic compared to that of the Recent mysticetes.

The posterior edge of the supraorbital process of *Piscobalaena* is distinctly concave and a similar condition is present in *Cetotherium* and *Nannocetus*. In fact, this morphology is present in most Miocene and Oligocene mysticetes (e.g., *Aglaocetus*, *Diorocetus*, *Parietobalaena*, *Mixocetus*, *Cophocetus*, *Eomysticetus*, aetiocetids). In *Herpetocetus*, the edge is only slightly concave, almost rectilinear. Within Recent mysticetes, the posterior edge of the process is roughly straight in balaenopterids and eschrichtiids and slightly concave in balaenids (*Eubalaena glacialis*). The condition of *Piscobalaena* is regarded as plesiomorphic.

In dorsal view, in *Piscobalaena*, the lines joining the pre- and postorbital processes of the supraorbital process of the frontal converge anteriorly. A similar condition, although less developed, is present in *Cetotherium*. In Recent balaenopterids and Miocene taxa (e.g., *Parietobalaena*, *Aglaocetus*, *Mixocetus*, *Diorocetus*, *Cophocetus*), the edges are approximately parallel, but they converge in Recent balaenids and eschrichtiids. The convergence is well pronounced in aetiocetids, which probably represents the plesiomorphic condition.

In dorsal view, the dorsal edge of the supraorbital process is concave in *Piscobalaena* and *Cetotherium* (the condition is unknown in *Herpetocetus*,

Metopocetus, and *Nannocetus*). The edge is roughly straight in Miocene taxa (e.g., *Parietobalaena*, *Aglaocetus*, *Mixocetus*, *Diorocetus*, *Cophocetus*). It is concave in aetiocetids, eschrichtiids and balaenids, which probably represents the plesiomorphic condition.

In lateral view, the orbit of *Piscobalaena nana* is shorter and more concave ventrally that in *Parietobalaena palmeri*, *Diorocetus hiatus*, and Recent balaenopterids. In this respect, *Piscobalaena nana* resembles *Cetotherium rathkei*, although this feature is more pronounced in the lattrer than in the former. A short and strongly arched orbit is present in archaeocetes and aetiocetids and is regarded here as a plesiomorphic condition.

Squamosal/Parietal/Pterygoid/Auditory region. In *Piscobalaena*, the parietals exposure on the vertex is reduced to an extremely thin strip of bones "pinched" between the frontals and the supraoccipital. The same condition is present in *Cetotherium*, *Metopocetus*, and *Herpetocetus*. It is also present in some Miocene taxa such as *Cophocetus* and *Mixocetus* and in Recent mysticetes (except in *Balaena mysticetus*, where the parietals are present on the vertex but their exposure is anteroposteriorly short). In these taxa, therefore, the posterior part of the rostral bones participates in the vertex. A relatively long exposure of the parietals on the vertex is present in many fossil mysticetes (e.g., aetiocetids, *Mauicetus*, *Mammalodon* Pritchard, 1939, *Eomysticetus*, *Parietobalaena*, *Diorocetus*, *Aglaocetus*). This condition is generally more pronounced in early taxa. The condition of *Piscobalaena* is an apomorphic character state, apparently highly homoplastic related to the telescoping of the skull, which is a characteristic of Autoceti (mysticetes and odontocetes).

In *Piscobalaena*, the fronto-parietal suture borders the posterior part of the temporal crest, and runs ventrally with a sigmoid morphology (concave anteriorly in its dorsal part and convex anteriorly in its ventral part). The vertical portion of the suture is located below the posterior third of the ascending process of the frontal and well anterior to the vertex. A similar morphology is apparently present in *Cetotherium* and *Mixocetus*. In *Herpetocetus*, the vertical part of the suture is also slightly sigmoid, but in a more posterior position than in *Piscobalaena*: it is located just below the vertex, posterior to the posterior extremity of the ascending process of the maxilla. As a consequence, a much larger portion of the frontal outcrops in the temporal fossa in *Herpetocetus* than in *Piscobalaena*. Such an anterior protrusion of the parietal, which extends anterior to the vertex is also present in Recent balaenopterids but is absent in balaenids. An anterior lobe of the fronto-parietal suture may be present in balaenids but it is not so anteriorly placed and located below the vertex. A large part of the frontal also participates in the construction of the temporal fossa in early mysticetes (aetiocetids, *Mauicetus*, *Eomysticetus*). Therefore, *Piscobalaena*, *Cetotherium* and *Mixocetus* bear an apomorphic character state, while *Herpetocetus* is plesiomorphic in this respect.

In *Piscobalaena*, *Herpetocetus* and *Metopocetus*, the parieto-squamosal suture passes on an elongated ridge of the braincase wall in the temporal fossa. The condition in *Cetotherium* is difficult to evaluate from the illustration provided by Pilleri (1986: pl. 25, fig. 1). Such a ridge is absent in Recent mysticetes and in the Miocene taxa such as *Aglaocetus*, *Diorocetus*, *Parietobalaena* and *Cophocetus*. A small ridge is apparently present in aetiocetids (*Chonecetus*), although less conspicuous than in *Piscobalaena* and *Herpetocetus*. It is therefore possible that *Piscobalaena* exhibits the plesiomorphic character state.

In *Piscobalaena*, the apices of the zygomatic processes are anterior to the anteriormost point of the occipital on the vertex. This condition is present in *Herpetocetus*, *Mixocetus*, *Eomysticetus*, *Diorocetus*, *Eschrichtius* and in aetiocetids. They are posterior in *Cophocetus*, *Aglaocetus*, *Parietobalaena* and in Recent balaenids and balaenopterids. The condition of *Piscobalaena* represents the plesiomorphic character state. The conditions of *Nannocetus* and *Metopocetus* are unknown.

In lateral view, the postglenoid process of *Piscobalaena* is strongly oriented posteriorly and, as a consequence, the ventral edge of the zygomatic and postglenoid processes is straight or slightly concave. This condition is related to the thickness of the postglenoid process at its base, which is relatively continuous with the zygomatic process. A similar condition is present in *Herpetocetus*, *Nannocetus* and *Cetotherium*, but also in *Eschrichtius* and balaenids.

In the two latter taxa, this morphology may be related to the strong reduction of the zygomatic process. It is absent in aetiocetids, *Eomysticetus*, *Parietobalaena*, and Recent balaenopterids, in which the postglenoid process is ventrally oriented and almost at a right angle with the zygomatic process. The condition of *Piscobalaena* is therefore likely to be apomorphic.

In lateral view, the zygomatic process of *Piscobalaena* is anteroposteriorly elongated and low at its base: with the posteriorly projected postglenoid process it forms approximately an isosceles triangle. In *Herpetocetus*, *Cetotherium* and *Nannocetus*, the process is much shorter and more elevated at its base and forms, with the postglenoid process, an equilateral triangle. As a consequence, in lateral view, the posterolateral angle of the temporal fossa is distinctly rounded in *Piscobalaena*, while it is acute in *Herpetocetus* and *Cetotherium*. The posterior region of the temporal fossa is not preserved in *Nannocetus*.

The postglenoid processes of *Piscobalaena* project posteroventrally and the anterior face of the process faces anteroventrally at an angle of approximately 45° with the horizontal plane of the skull. The apex of the process is a transversely oriented crest. The processes of *Herpetocetus* project posteroventrally but the posterior component is more reduced than in *Piscobalaena* and the posterior edge is sub-vertical. Furthermore, in *Herpetocetus*, the processes are twisted medially relatively to those of *Piscobalaena* (i.e. the left process is turned clockwise and the right is turned anticlockwise). Therefore, the posterior side of the process faces posterolaterally.

In posterior view, they also converge ventrally and the apices of the processes are posteromedially oriented and converge posteriorly. Because of this morphology, the glenoid fossa is much wider and shallower in *Piscobalaena* than in *Herpetocetus*, probably allowing a broader opening of the mouth. A twisted postglenoid process is also present in *Cetotherium* and *Nannocetus*. In other respects, a posteriorly projecting and non-twisted postglenoid process is present in *Diorocetus*, *Aglaocetus*, *Parietobalaena* and *Cophocetus*. In aetiocetids and *Eomysticetus*, the postglenoid process is not twisted but it projects ventrally (not posteroventrally), which is likely to represent the plesiomorphic condition. Therefore, *Piscobalaena* is plesiomorphic for the transversely oriented (i.e. non-twisted) process and apomorphic for its posterior extension. A twisted postglenoid process could be a synapomorphy of the genera *Herpetocetus*, *Cetotherium* and *Nannocetus*. In these genera, it is possible that the reduced posterior component of the projection of the processes as well as the stoutness and the equilateral triangular morphology of the postglenoid process are consequences of the twisting. In fact, the rotation of the postglenoid process is probably achieved by an anteroventral displacement of its lateral edge.

In dorsal view, the lateral border of the zygomatic process is slightly concave laterally in *Piscobalaena*, *Cetotherium*, and *Mixocetus*. In *Herpetocetus* and *Nannocetus*, the lateral edge of the zygomatic process is sub-rectilinear or slightly convex, a condition which is also present in the aetiocetids and in *Eomysticetus*, *Diorocetus*, *Aglaocetus*, *Parietobalaena*, *Eschrichtius* and Recent balaenids and balaenopterids.

The lateral edges of the zygomatic processes are convergent posteriorly in *Piscobalaena*, *Herpetocetus*, *Diorocetus* and *Aglaocetus*, whereas they are subparallel in *Cetotherium*, *Nannocetus*, *Parietobalaena*, *Cophocetus*, *Eomysticetus* and the aetiocetids, which represents the plesiomorphic condition.

In *Piscobalaena* and *Herpetocetus*, the apex of the zygomatic process is bent medially, and, to a greater extent, in *Cetotherium*. This condition is absent in aetiocetids, *Eomysticetus*, *Parietobalaena*, *Aglaocetus*, *Diorocetus*, *Cophocetus*, *Eschrichtius* and Recent balaenopterids and balaenids. The condition of *Piscobalaena*, *Herpetocetus* and *Cetotherium* probably represents the apomorphic character state.

The lateral edge of the zygomatic process of *Piscobalaena* bears a thick ridge, which is absent in *Herpetocetus*, *Cetotherium* and *Nannocetus*.

The dorsal zygomatic crest located above the sternomastoid fossa is laterally everted in *Piscobalaena* and sub-vertical in *Herpetocetus*, *Cetotherium*, and *Nannocetus*. Furthermore, in *Piscobalaena*, *Nannocetus* and *Cetotherium*, the crest is sigmoid, whereas it is straight in *Herpetocetus*. The two crests are subparallel in the juvenile individual of *Piscobalaena* and in *Herpetocetus* whereas they are slightly convergent

posteriorly in the adult specimens of *Piscobalaena* and in *Cetotherium*.

In *Piscobalaena* and *Herpetocetus*, the external opening of the foramen pseudovale is mainly formed by the squamosal posteriorly with a very small participation of the pterygoid anteriorly. In *Cetotherium*, the foramen is mainly formed by the squamosal with a little anteromedial participation of the pterygoid (Brandt 1873: pl. 1, fig. 2). In *Nannocetus*, due to the poor preservation of the specimen, it is impossible to say if Kellogg (1929: p. 455, and fig. 1, p. 452) statement is correct or not: "The foramen ovale pierces the external wall of the pterygoid fossa between the squamosal and the pterygoid". The foramen pseudovale could also be formed by the squamosal only. The condition in the aetiocetids is apparently more derived since the foramen ovale is opened ventrally and therefore is reduced to a notch confluent with the cranial hiatus (Barnes *et al.* 1994: fig. 17b, c and VB pers. obs.). In archaeocetes (*Dorudon* and *Zygorhiza* True, 1908), and in balaenids, the foramen pseudovale pierces the squamosal with apparently no participation of the pterygoid. In *Caperea*, the foramen pierces the pterygoid only. In the other fossils, in balaenopterids, and eschrichtiids, the condition of the foramen pseudovale is apparently similar to that of *Piscobalaena*. Therefore, the condition of *Piscobalaena* is probably plesiomorphic for the baleen mysticetes.

In *Piscobalaena* and *Nannocetus*, the longest axis of the tympanic is sub-parallel to the sagittal axis of the skull, while it is anteromedially oriented in *Cetotherium*, *Herpetocetus*, and *Eschrichtius*. The latter condition is related to the oblique orientation of the lateral edge of the basioccipital. The condition of *Piscobalaena* is also present in the aetiocetids, *Parietobalaena*, *Pelocetus*, and Recent balaenopterids.

In dorsal view, the tympanic of *Piscobalaena* is pear-shaped because its anterior third is narrower than its posterior two thirds. *Piscobalaena* approaches the condition observed in primitive mysticetes (aetiocetids and *Eomysticetus*). In *Nannocetus*, *Cetotherium*, *Herpetocetus*, *Diorocetus*, and *Aglaocetus*, the tympanic is roughly oval-shaped to rectangular. In Recent balaenopterids, the tympanic is conspicuously kidney-shaped.

In *Piscobalaena*, the anteromedial angle of the tympanic presents a small spiny protuberance, while in *Herpetocetus*, *Cetotherium* (Brandt 1873: pl. 3, figs 4, 5), and *Nannocetus*, this area exhibits a thick but smooth rim. The occurrence of an anterior spine is apparently unique in *Piscobalaena*. The anteromedial angle of the tympanic is smooth in most other mysticetes except *Eomysticetus* and, apparently, in the aetiocetids.

At the anterior extremity of the tympanic, the anterior border of the tympanic cavity, which corresponds to the anteroventral edge of the Eustachian tube, forms a narrow but smooth angle in *Piscobalaena*, whereas it is wider and rounded in *Cetotherium* (Brandt 1873: pl. 3, figs 4, 5), *Herpetocetus* and *Nannocetus*. This feature is apparently unique in *Piscobalaena*.

In *Piscobalaena* and *Herpetocetus*, the anterior third of the involucrum is marked by a distinct step and is narrower than the posterior two thirds. In *Nannocetus* and *Cetotherium* (Brandt 1873: pl. 3, fig. 4), as well as in most other mysticetes (e.g., aetiocetids, *Eomysticetus*, *Aglaocetus*, *Parietobalaena*, Recent balaenopterids and balaenids, the involucrum progressively decreases in width anteriorly.

In medial view, the posterior edge of the tympanic of *Piscobalaena* and *Herpetocetus* is bilobate. The dorsal lobe (i.e. medial lobe of archaeocetes and odontocetes) is in a more anterior position than the ventral one (i.e. lateral lobe of archaeocetes and odontocetes). This character is more pronounced in *Herpetocetus* than in *Piscobalaena*. The tympanic of *Nannocetus* is also bilobate but in this genus, the dorsal lobe extends as far posteriorly as the ventral lobe. According to Brandt's (1873) description, the tympanic of *Cetotherium* has no dorsal lobe and is, therefore, morphologically similar to that of a balaenopterid. The plesiomorphic condition is present in the aetiocetids and *Eomysticetus*, in which the two lobes are equally developed posteriorly.

The medial keel of the ventral lobe is more prominent in *Piscobalaena* and *Herpetocetus* than in *Nannocetus* and the notch between the lobes is deeper and more extended anteriorly.

In ventral view, in *Piscobalaena*, the sigmoid process of the tympanic is anterolaterally oriented whereas

it is posterolaterally oriented in *Cetotherium*, and laterally oriented in *Nannocetus*. Furthermore, the sigmoid process of *Piscobalaena* is twisted and its dorsolateral angle is shifted anteriorly. This condition is absent in *Cetotherium* and *Nannocetus*, and apparently unique to *Piscobalaena*.

In *Piscobalaena*, the conical process is markedly triangular and very salient laterally. In *Cetotherium*, the conical process is very low and reduced to a thin bony lip. The condition of *Nannocetus* is similar to that of *Piscobalaena*, although the process is less developed. Furthermore, the conical process of *Piscobalaena* is closely apressed against the posterior edge of the sigmoid process, while it is more posteriorly located in *Cetotherium* and *Nannocetus*.

The posterior process of the petrotympanic of *Piscobalaena* is transversely short and conical, with a well developed trapezoid surface in lateral view. Furthermore, the exposed surface of the process is roughly flat (the surface is slightly convex in juveniles or young adults) and sub-vertical and, therefore, faces laterally. The process is wedged between the squamosal and the exoccipital. In *Herpetocetus*, the process is similar to that of *Piscobalaena* but larger. It dorsally compresses the sternomastoid fossa, which is relatively smaller than in *Piscobalaena*. In *Nannocetus*, the process is similar in size to that of *Piscobalaena*. The posterior process of the petrotympanic is generally long and slender in most other mysticetes except in aetiocetids and *Eomysticetus*. The conical morphology of the posterior process of the petrotympanic of *Piscobalaena* is a derived character state shared with *Herpetocetus*, *Cetotherium*, *Metopocetus*, and *Nannocetus* (Fig. 30). In *Caperea*, the posterior process of the petrotympanic is relatively short and expands laterally as in *Piscobalaena*. However, in this taxon, the external exposure of the process is a curved surface ventrolaterally oriented. Furthermore, the process, although thickened, is dorsoventrally flattened as observed in the balaenids.

The stylomastoid notch or groove for the facial nerve exit is located on the ventral face of the posterior process of the petrotympanic. It is very deep in *Piscobalaena* and *Herpetocetus*, in which it is sometimes almost tubular and partially closed ventrally by an anterior expansion of the posterior process of the petrosal. The stylomastoid notch is much shallower in *Nannocetus*.

On the dorsal side of the petrosal, the suprameatal fossa is deep and distinctly concave in *Piscobalaena* and *Herpetocetus* whereas it is almost flat in *Nannocetus*, and slightly convex dorsally in *Metopocetus*. Furthermore, the lateral edge of the fossa is thickened in *Piscobalaena* and *Herpetocetus* while it is thin in *Nannocetus*.

The anterior process of the petrosal of *Piscobalaena* is short and compressed transversely to blade-like at apex. It is quadrate at apex (in lateral view) with a long vertical anterior border. A similar condition is present in *Herpetocetus*, *Nannocetus*, *Metopocetus*, and in the Oligocene baleen mysticete *Eomysticetus*. In *Diorocetus*, *Parietobalaena*, and *Aglaocetus*, the anterior process is shorter and dorsoventrally wider than in *Piscobalaena*. The petrosal of aetiocetids and *Cetotherium* is unknown. In the Recent balaenopterids, the anterior process of the petrosal is long, thick, and pointed at apex. In the Recent balaenids, it is very short and conical. In *Eschrichtius*, the process is thick and pointed and intermediate in length between that of balaenids and balaenopterids. In *Caperea*, the process is short but not atrophied and transversely compressed. The condition of *Piscobalaena* is regarded as plesiomorphic.

In *Piscobalaena* and *Metopocetus*, the anterior process of the petrosal is transversely thicker than in *Herpetocetus*, *Nannocetus* and *Parietobalaena*.

In ventral view, the anterior process of the petrosal of *Herpetocetus* bears a large lateral projection, which extends as a thick lamina of bone from the medial edge of the fossa incudis to the apex of the anterior process (Geisler & Luo 1996). This process imbricates between the squamosal and the anterolateral angle of the tympanic and bulges outside the skull laterally, anterior to the sigmoid process. Such a structure is also present in *Parietobalaena* but it is absent in *Piscobalaena* and *Nannocetus*.

On the dorsal face of the petrosal, the cranial foramen for the facial nerve canal and the fissure for the palatine branch of the facial nerve (hiatus fallopii) form a single external teardrop foramen in *Piscobalaena*, *Herpetocetus*, *Nannocetus*, and *Metopocetus*. This condition is also present in *Parietobalaena*. The endocranial opening for the

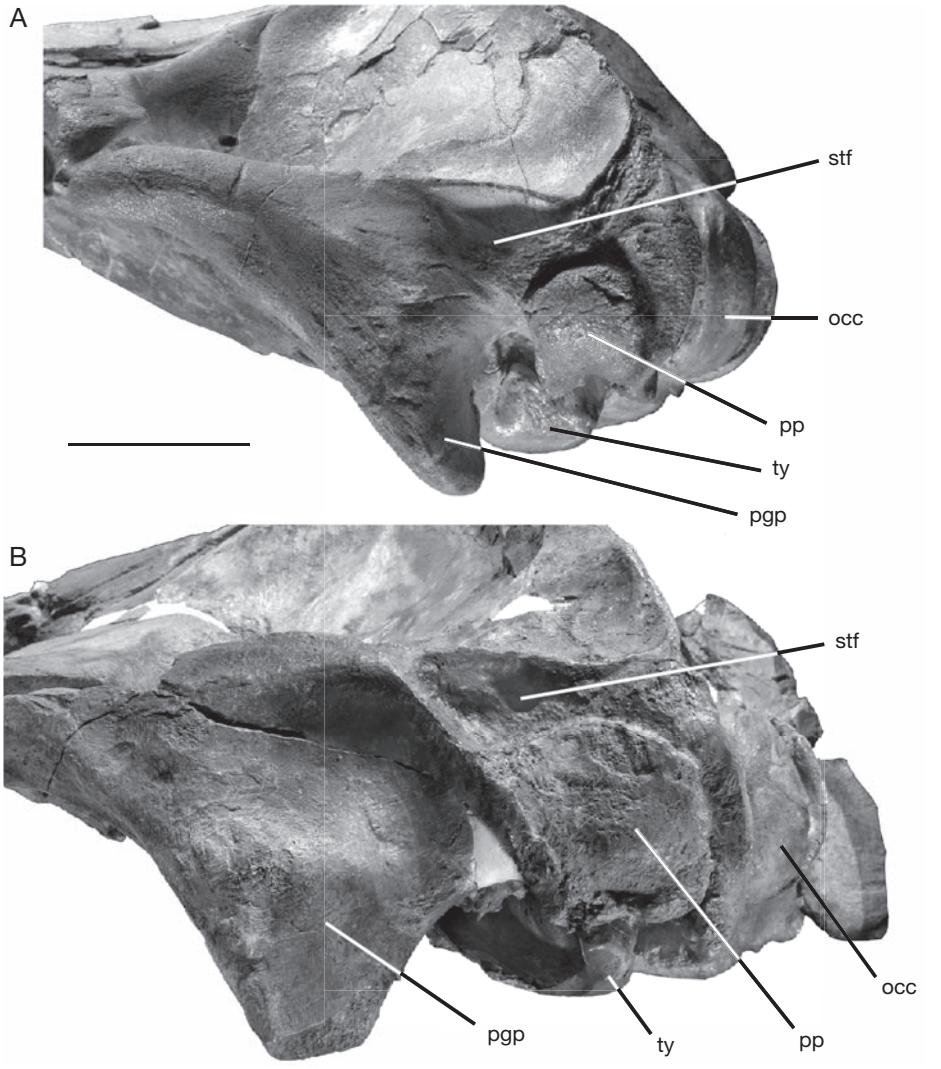

FIG. 30. — Lateral view of the skull in (**A**) *Piscobalaena nana* (MNHN SAS 1616) and (**B**) *Herpetocetus sendaicus* (cast of NSMP-PV 19540) showing the posterior process of the petrotypanic posterior process the petrotympanic. Abbreviations: see p. 322. Scale bar: 5 cm.

facial canal is circular in *Aglaocetus* (with a very small anterior fissure) and *Diorocetus*, but deep and tubular in *Balaenoptera*, *Eubalaena*, and *Eschrichtius*.

At the limit between the anterior region of the pars cochlearis and the base of the anterior process, the groove for the tensor tympani is wide and deep in *Piscobalaena*, *Metopocetus*, and *Herpetocetus*. The groove for the tensor tympani is extremely narrow in *Nannocetus* and forms a neck at the anteroventral base of the pars cochlearis.

The pars cochlearis is a smooth half-sphere in *Piscobalaena*, *Herpetocetus*, *Nannocetus*, *Metopocetus*, and *Parietobalaena*. It is mediolaterally compressed in *Aglaocetus* and *Diorocetus*. In the Recent balaenopterids, balaenids and *Eschrichtius*, the pars cochlearis is expanded dorsoventrally and higher than long. The condition of *Piscobalaena* is also

present in *Chonecetus* and *Eomysticetus*, although the pars cochlearis is less globular in these genera. Therefore, the condition of *Piscobalaena* is regarded here as plesiomorphic.

In *Herpetocetus* and *Metopocetus*, the fossa for the malleus is well defined whereas it is very shallow in *Piscobalaena* and *Nannocetus*. Because a deep malleus fossa is present in archaeocetes, aetiocetids and archaic baleen mysticetes (*Eomysticetus*), a shallow malleus fossa probably represents a derived character state.

In medial view, the internal auditory meatus and the facial nerve canal open rather dorsally in *Nannocetus* and *Herpetocetus*, whereas they open rather medially in *Piscobalaena* and *Metopocetus*. The internal auditory meatus is sub-circular in *Piscobalaena*, *Herpetocetus* and *Metopocetus* whereas it is oval-shaped in *Nannocetus*.

The crista transversa and the pyramidal process are extremely salient in *Piscobalaena*, *Herpetocetus* and *Metopocetus*. They are smooth on the holotype of *Nannocetus*. However, since the specimen may be a juvenile, the smooth morphology of the crista transversa and pyramidal process may be ontogenetic and/or an artefact due to fossilisation.

Occipital region. A distinct, elevated and thin sagittal crest is present on the occipital of *Piscobalaena*, *Cetotherium*, *Herpetocetus* and *Metopocetus*. In *Piscobalaena*, the crest is long and extends from the vertex on the dorsal three quarters of the supraoccipital. In *Herpetocetus*, the sagittal crest is shorter as it is present only on the dorsal half of the bone. A sagittal crest of the occipital is also present in *Aetiocetus*, *Eomysticetus*, *Parietobalaena*, *Diorocetus* (small), and *Caperea*. It is absent or limited to a smooth and extremely low ridge in balaenopterids, balaenids, and *Eschrichtius*. The presence of an occipital sagittal crest is therefore regarded as a plesiomorphic character state, although the condition of *Piscobalaena*, in which the crest is extremely developed, could be an autapomorphy of the genus.

The lambdoid crests form a wide and round crest at their junction on the vertex in *Piscobalaena*, while they meet at a sharp angle and are rectilinear in *Cetotherium* and *Herpetocetus*. In *Metopocetus*, they meet at an acute angle and are slightly concave laterally.

In lateral view, the vertex of *Piscobalaena* is more elevated than in *Herpetocetus* and *Cetotherium*.

Palatine/Vomer region. The maxillo-palatine suture of *Piscobalaena* is sigmoid (anteriorly concave medially and anteriorly convex laterally), while it is roughly anteriorly convex in all the other mysticetes.

Basioccipital region. In ventral view, in *Piscobalaena* and *Herpetocetus*, the basioccipital tubercle for the longus colli is sub-triangular and its lateral edge is sub-parallel to the sagittal axis of the skull. It is as long as the tympanic in *Piscobalaena* whereas it is shorter in *Herpetocetus*. In *Cetotherium*, the basioccipital tubercle is also triangular and shorter than the tympanic, but its lateral edge is oblique compared to the sagittal axis of the skull. In *Nannocetus*, the tubercle is oval-shaped and its length is approximately half of the length of the tympanic. The basioccipital tubercle extends medially to a greater extent in *Piscobalaena*, *Herpetocetus* and *Cetotherium* than in *Nannocetus*, where they are smaller and transversely narrower.

In posterior view, the notch between the basioccipital tubercles is markedly deeper in *Herpetocetus* and *Nannocetus* than in *Piscobalaena* and *Cetotherium*.

Dentary. The posterior two thirds of the right dentary of *Herpetocetus sendaicus* only are preserved and the dentary of the type specimen of the type species of the genus, *Herpetocetus scaldiensis*, is a posterior portion of a dentary (Fig. 31).

In *Herpetocetus sendaicus*, the skull is slightly larger and more massive than that of *Piscobalaena nana* MNHN SAS 1617 and the dentary of the referred specimen (the holotype is an isolated tympanic (Hatai *et al.* 1963) is much more slender than the dentary of MNHN SAS 1617. Although the ascending ramus of the dentary is similar in length in *Piscobalaena* and *Herpetocetus*, clear differences exist between the two genera. The coronoid process is not completely preserved on the specimen referred to *Herpetocetus sendaicus*; but it is fairly complete

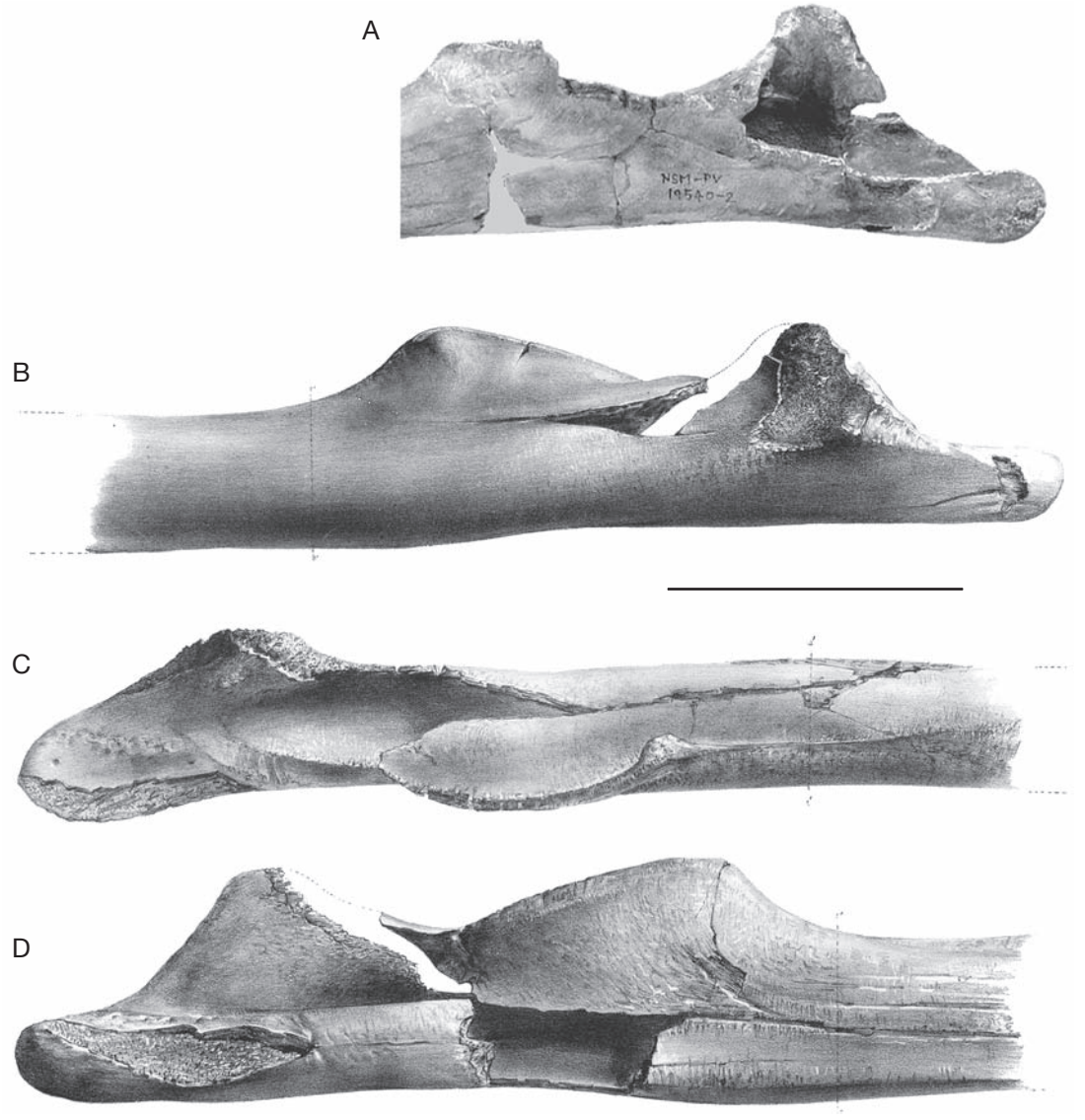

FIG. 31. — Dentary of *Herpetocetus*: **A**, *Herpetocetus sendaicus*, NSMT-PV 19540, dentary in medial view, detail of vertical ramus; **B**-**D**, *Herpetocetus scaldiensis* (holotype, from Van Beneden 1882); **B**, lateral view; **C**, dorsal view; **D**, ventral view. Scale bar: 10 cm.

in *H. scaldiensis*. It has the same elevation than in *Piscobalaena* but it is much more massive and triangular. It is however possible that the process in *H. sendaicus* was slightly more elevated than in *Piscobalaena*. The coronoid process of *Herpetocetus* (115 mm) is only slightly shorter than in *Piscobalaena* (125 mm). The mandibular canal opens approximately 50 mm anterior to the level of the anterior edge of the condyle in *Piscobalaena*, while in *Herpetocetus* it is 10 mm anterior. In fact, the portion of the dentary posterior to the opening of the mandibular canal is posteriorly extended in *Piscobalaena* relatively to the condition in *Herpetocetus*. The opening of the mandibular canal and

TABLE 7. — Vertebral formula of *Piscobalaena nana* (MNHN SAS 1617) and *Herpetocetus sendaicus* (NSMT-PV 19540).

Vertebrae	Cerv. V.	Dors. V.	Lomb. V.	Caud. V.
Piscobalaena nana (MNHN SAS 1617)	7	11	11?	?
Herpetocetus sendaicus (NSMT-PV 19540)	7	13?	9	?

the canal itself are much larger in *Herpetocetus* than in *Piscobalaena* in spite of the smaller size of the dentary of the former. Between the condyle and the angular process, the groove for insertion of the internal pterygoid is three times wider in *Herpetocetus* than in *Piscobalaena*. In *Herpetocetus*, this attachment area is a large fossa rather than a groove and it invades the medial side of the condyle.

The condyle of *Piscobalaena* is much larger and wider than in *Herpetocetus*. In *Piscobalaena*, it is slightly convex and almost flat in its dorsal portion and faces posterodorsally. In *Herpetocetus*, the condyle is strongly convex dorsally and its anterior region faces anterodorsally. The anterior region of the condyle is more elevated and broader (in lateral view) in *Herpetocetus* than in *Piscobalaena*.

In both genera, in lateral view, the dorsal side of the condyle is distinctly oblique relatively to the horizontal plane of the skull and not subvertical as in *Parietobalaena*, *Pelocetus*, *Cophocetus*, and Recent balaenopterids. Furthermore, in *Diorocetus*, the condyle is slightly oblique but to a lesser extent than in *Piscobalaena*. Eschrichtiids and balaenids also have a posterodorsally oriented condyle.

In *Piscobalaena*, the angular process is transversely thick and projects approximately 30 mm posteriorly to the condyle. In *Herpetocetus*, the apex of the angular process is much thinner, rounder and far more posteriorly projected (approximately 50 mm) than in *Piscobalaena*. In *Herpetocetus*, the dorsal edge of the angular process bears a strong crest approximately 40 mm long while in *Piscobalaena* a crest is hardly present and no longer than 10 mm. Furthermore, in posterior view, the angular process of *Herpetocetus* is small and circular, while it is twice larger, oval-shaped, and obliquely oriented in *Piscobalaena*.

Comparison / post-cranial skeleton

In the following section, comparisons will be made mainly with the holotype of *Herpetocetus sendaicus* because the postcranial skeleton of *Cetotherium*, *Metopocetus*, and *Nannocetus* is unknown.

Vertebrae. The skulls of *Piscobalaena nana* (MNHN SAS 1617) and that of *Herpetocetus sendaicus* (NSMT-PV 19540, referred specimen) are similar in size but the cervicals of *Herpetocetus* are smaller than those of MNHN 1617 and approach the size of those of MNHN SAS 1624, a juvenile individual or a young adult. However, the vertebral disks and centra of the cervical vertebrae of the holotype of *Herpetocetus sendaicus* are not perfectly fused, which suggests that the specimen was a young adult. Vertebral formula, see Table 7.

Cervicals. The axis, C3 and C4 are fused in *Herpetocetus*, contrary to the condition in *Piscobalaena*. In *Piscobalaena*, the centra of the first four cervical vertebrae are anteroposteriorly longer than in *Herpetocetus*. The condition of *Piscobalaena* is therefore more plesiomorphic than in *Herpetocetus*.

Atlas. The atlas of *Piscobalaena* is anteroposteriorly almost twice longer than that of *Herpetocetus*. Furthermore, in anterior view, the atlas of *Herpetocetus* is higher than that of *Piscobalaena*. Its neural arch is dorsoventrally thicker and its neural crest is more developed than in *Piscobalaena*. The ventral edge of the atlas is sub-rectilinear in *Herpetocetus* whereas it is ventrally convex in *Piscobalaena*.

In lateral view, the transverse foramen of *Herpetocetus* is located on the anterior edge of the neural arch, the right foramen being even partially open anteriorly, while it is approximately in the middle of the arch (slightly anterior) in *Piscobalaena*.

The transverse apophysis is dorsoventrally more elevated in *Piscobalaena* than in *Herpetocetus*.

In lateral view, the lateral margin of the transverse process is oblique (posterodorsal-anteromedial) and

TABLE 8. — Rib formula of *Piscobalaena nana* (MNHN SAS 1617) and *Herpetocetus sendaicus* (NSMT-PV 19540) (in mm).

	MNHN SAS 1617	NSMT-PV 19540
Number of left ribs	10	11 ?
Number of right ribs	11	13 ?

at an angle of approximately 45° with horizontal in *Piscobalaena*. In *Herpetocetus*, the margin is sub-vertical, at an angle of *c.* 80° with horizontal.

In posterior view, the lateral margin of the transverse process is oblique, facing dorsoventrally in *Piscobalaena*, contrary to the condition in *Herpetocetus*, where it is sub-vertical.

The transverse processes of *Piscobalaena* bear sub-equal thick dorsal and ventral tubercles. In *Herpetocetus*, the dorsal tubercle is thick as in *Piscobalaena*, while the ventral is very small.

In posterior view, the tubercle of the transverse process overhangs the lateral margin of the articular facet for the axis in *Piscobalaena*, while in *Herpetocetus* it is distinctly lateral to it.

Axis. In anterior view, the odontoid apophysis is higher in *Piscobalaena* than in *Herpetocetus*. The transverse foramen is not closed in *Herpetocetus* whereas it is in *Piscobalaena*.

C3-C7. The C3 and C4 of *Piscobalaena* are clearly more massive than those of *Herpetocetus*. Their centra are larger and anteroposteriorly thicker. On C4, the ventral half of the transverse apophysis is thicker in *Piscobalaena* than in *Herpetocetus*.

The C5 of *Herpetocetus sendaicus* is too incomplete to be compared to that of *Piscobalaena*.

The centra of C6 and C7 of *Herpetocetus* are approximately as thick as those of *Piscobalaena*. The neural arch of these vertebrae is shorter and more slender in *Herpetocetus* than in *Piscobalaena*. On the contrary, the dorsal part of the transverse process is clearly more massive in *Herpetocetus* and anteroposteriorly flattened and elevated, while it has a circular section in *Piscobalaena*. The apex of this portion is dorsoventrally twice thicker in *Herpetocetus* than in *Piscobalaena*. Furthermore, the dorsal transverse process of *Herpetocetus* is almost straight, whereas it is strongly recurved ventrally in *Piscobalaena*. As on the juvenile cervical vertebrae of *Piscobalaena* (MNHN SAS 1624), C6 has no ventral transverse process, while a process is distinctly present but small in MNHN SAS 1617. The absence of a ventral transverse process in *Herpetocetus sendaicus* is therefore probably related to the juvenile status of the specimen. On C7, the transverse process is similar in both genera, although less anteriorly oriented in *Herpetocetus*.

Thoracics. Contrary to the condition of the cervical vertebrae, the centra of the thoracic vertebrae are longer in *Herpetocetus* than in *Piscobalaena*. The neural arch is transversely wider and lower in *Piscobalaena* than in *Herpetocetus*. In *Herpetocetus*, the transverse processes are dorsoventrally flattened until their apices whereas they are regularly thick in *Piscobalaena* and expanded at apex. This character is conspicuous on the first three thoracic vertebrae. In *Herpetocetus*, the transverse process is sub-horizontal whereas it is slightly inclined ventrally in *Piscobalaena*. The pre- and postzygapophyses are more developed in *Piscobalaena* than in *Herpetocetus*. In *Piscobalaena*, they are clearly functional on the first six thoracics and articulate with the following vertebra, while in *Herpetocetus*, there is no contact between the zygapophyses, even between T1 and T2. In *Piscobalaena*, the prezygapophysis is close to the apex of the transverse process (except on T1, where it is located at the base of the process) from T1 to T7 and then become displaced medially on the arch from T8 to T11. In *Herpetocetus*, the prezygapophysis displaces medially from T1 to T11 but passes from the transverse process to the arch on T6. A well developed prezygapophysis is present on the neural arch from T8 to T11 in *Piscobalaena*, whereas it is present on the neural arch from T6 in *Herpetocetus*. The postzygapophysis is posteriorly developed on the first nine thoracic vertebrae of *Piscobalaena*, whereas in *Herpetocetus*, it is present

and much less developed on T1 only. Because of the presence of well developed postzygapophyses, the neural arch of the anterior thoracic vertebrae of *Piscobalaena* is anteroposteriorly longer than in *Herpetocetus*.

In lateral view, in *Piscobalaena*, the line joining the apices of the diapophyses is regularly convex dorsally whereas it is sigmoid in *Herpetocetus*: the line is sub-rectilinear until T6 and then inflects ventrally until the last thoracic vertebra.

Lumbars. The lumbar vertebrae of *Herpetocetus* and *Piscobalaena* are similar. The centra of *Piscobalaena* lumbars are thicker and wider than those of *Herpetocetus*. In *Piscobalaena*, the transverse process is more developed anteroposteriorly than in *Herpetocetus*.

Ribs. None of the ribs of *Herpetocetus* are complete. Although the skulls of *Herpetocetus* and *Piscobalaena* MNHN SAS 1617 are similar in size, the ribs of *Herpetocetus* are thinner and shorter than in *Piscobalaena*. On the fourth rib, the curved portion of the rib, located just laterally to the tuberculum, is much thicker in *Herpetocetus* than in *Piscobalaena*. In contrast with the first eight ribs, which are very similar in both specimens, the ninth rib is very different from a specimen to the other. The tuberculum and capitulum of the ninth rib are merged in *Piscobalaena*, whereas they are distinct, as on the anterior ribs, in *Herpetocetus*. Also, in *Piscobalaena*, the tuberculum of the ninth rib is quite developed whereas in *Herpetocetus* it is similar to that of the other ribs. In *Piscobalaena*, the curvature of the rib decreases on the seventh rib so that the next ribs become progressively rectilinear. In *Herpetocetus*, the curvature starts reducing on the ninth rib. In *Piscobalaena*, the capitulum of the 10th rib is atrophied and only the tuberculum is present, extremely developed sagittally and expanding posterolaterally on the rib. In *Herpetocetus*, the capitulum of the 10th rib is still present and has the same morphology as on the other ribs, whereas the articular facet of the tuberculum is atrophied. In *Piscobalaena*, the 11th rib is similar to the 10th but its vertebral extremity is thicker. In *Herpetocetus*, the vertebral extremities of the last two ribs are similar: the tuberculum appears atrophied and only the capitulum is present and sagittally slightly elongated. Rib formula, see Table 8.

Scapula. The scapula of *Piscobalaena* is trapezoidal and anteroposteriorly elongated, a condition apparently unique among mysticetes and which, therefore, probably represents an autapomorphy. It strongly differs from the scapula of *Herpetocetus*, which is triangular and morphologically similar to that of the other baleen mysticetes. The angle between the cranial and caudal edges of the scapula is about 130° in *Piscobalaena* and 90° only in *Herpetocetus*. The glenoid cavity is more circular in *Herpetocetus* than in *Piscobalaena*. The coracoid process is more medially oriented in *Herpetocetus* than in *Piscobalaena*.

Radius and ulna. The radius and the ulna in *Piscobalaena* do not fundamentally differ from those of *Herpetocetus*. In the latter genus, however, the radius and ulna are clearly less massive and transversely thinner than in *Piscobalaena*.

DISCUSSION AND PARSIMONY ANALYSIS

The new specimens of *Piscobalaena nana* described above represent an ontogenetic and probably sexually dimorphic series of mysticetes (Fig. 4). First, MNHN SAS 1616 and the isolated set of cervicals MNHN SAS 1624 are young adults. Second, according to the different sizes and various peculiarities of the four adults MNHN SAS 892, 1617, 1618 and 1623, the description suggests that MNHN SAS 892 could be a male, MNHN SAS 1617 and 1618 could be females with MNHN SAS 1618 slightly older than MNHN SAS 1617. Third, due to the degree of pachyostosis of MNHN SAS 1623 skull, this last specimen was most probably an old animal.

Consequently, these observations suggest that the intraspecific variation within the species *Piscobalaena nana* could be relatively limited and that it may be at least due to age and sexual dimorphism. Extension of this statement to other fossil mysticetes needs to

be confirmed by further studies of larger samples for instance on *Parietobalaena*, of which approximately 10 skulls (Kellogg 1968) have been reported from the Calvert Formation (Maryland).

The comparison of the new specimens of *Piscobalaena* with other fossil and living mysticetes also indicates that *Piscobalaena* cannot be referred to balaenids, neobalaenids or eschrichtiids. According to the following observations, *Piscobalaena* might belong to a family of fossil mysticetes phylogenetically closer to balaenopterids.

Piscobalaena lacks the synapomorphies of balaenids, neobalaenids and eschrichtiids, in which the rostrum is slightly to strongly bowed, whereas in *Piscobalaena*, the rostrum is rectilinear, a plesiomorphic condition observed in fossil and Recent balaenopterids, and all fossil mysticetes not referred to recent families. *Piscobalaena nana* also differs from balaenids and neobalaenids in having a well developed ascending process of the maxilla. Although different, this process is also present in balaenopterids, eschrichtiids, cetotheres (i.e. *Cetotherium*, *Herpetocetus*, *Metopocetus*), and aetiocetids. In some of these families and in *Piscobalaena*, the telescoping of the skull is achieved, in addition to a shortening of the cranial bones (frontal and parietal), by a posterior extension of the rostral bones (premaxilla, maxilla, and nasal), which overlap the cranial bones posteriorly. Such an overlapping does not occur in balaenids and neobalaenids, in which the rostro-cranial suture is sub-rectilinear. The condition of *Piscobalaena* is also present in several fossil baleen mysticetes (e.g., *Herpetocetus*, *Cetotherium*, *Metopocetus*, *Nannocetus*, and *Mixocetus*).

In balaenids and neobalaenids, the zygomatic process of the squamosal is reduced to a knob, while it is long (although variably) and well developed in *Piscobalaena*, balaenopterids, eschrichtiids, and in most fossil mysticetes.

Furthermore, in balaenids, neobalaenids and eschrichtiids, the coronoid process of the dentary is reduced or totally atrophied, whereas in *Piscobalaena* and balaenopterids, it is well developed, hook-like, and outwardly bent.

Although *Piscobalaena* shares these characters with balaenopterids, it cannot be included in this family, as it lacks the balaenopterids synapomorphies.

First, in balaenopterids, the supraorbital process of the frontal slopes abruptly downward from the vertex in its medial third to become sub-horizontal until the edge of the orbit. This apomorphic character state is present in all balaenopterids, and in *Eschrichtius*. In *Piscobalaena*, the supraorbital process slopes progressively from the vertex to the edge of the orbit.

Second, in balaenopterids, at the anterior edge of the supraorbital process, the maxillo-frontal suture is acutely convex anteriorly and consequently the supraorbital process is more than twice longer medially (at its base) than laterally (above the orbit). A strongly concave suture is also present in *Eschrichtius*, although in this genus the supraorbital process is only one third longer medially than laterally. In *Piscobalaena*, the maxillo-frontal suture is oriented obliquely (posteromedial-anterolateral) and gently convex anteriorly. Therefore, the supraorbital process is narrower medially than laterally. In other words, the anteriormost point of the maxillo-frontal suture is medial and anterior to the preorbital process of the frontal in balaenopterids and eschrichtiids, while it is lateral and at the level of the process in *Piscobalaena*.

Third, the posterior edge of the supraorbital process in balaenopterids is roughly straight, while it is acutely concave in *Piscobalaena*. As a consequence, the temporal fossa of balaenopterids is semicircular, whereas it is sub-circular to oval-shaped in *Piscobalaena*.

Fourth, in balaenopterids, the posterior extremities of the nasals and premaxillae project posteriorly as far as the apex of the ascending processes of the maxillae, whereas they end much anterior to them in *Piscobalaena*. In fact, in *Piscobalaena*, the ascending processes of the maxillae approximate and contact each other behind the nasals, which strongly taper posteriorly. Furthermore, in *Piscobalaena*, the premaxillae extend no further than mid-length of the nasals posteriorly.

Fifth, in balaenopterids, the degree of telescoping of the supraoccipital is higher than in *Piscobalaena*. In balaenopterids, the supraoccipital projects conspicuously beyond the line joining the apices of the zygomatic processes of the squamosals, whereas in *Piscobalaena*, the anteriormost limit of the supraoc-

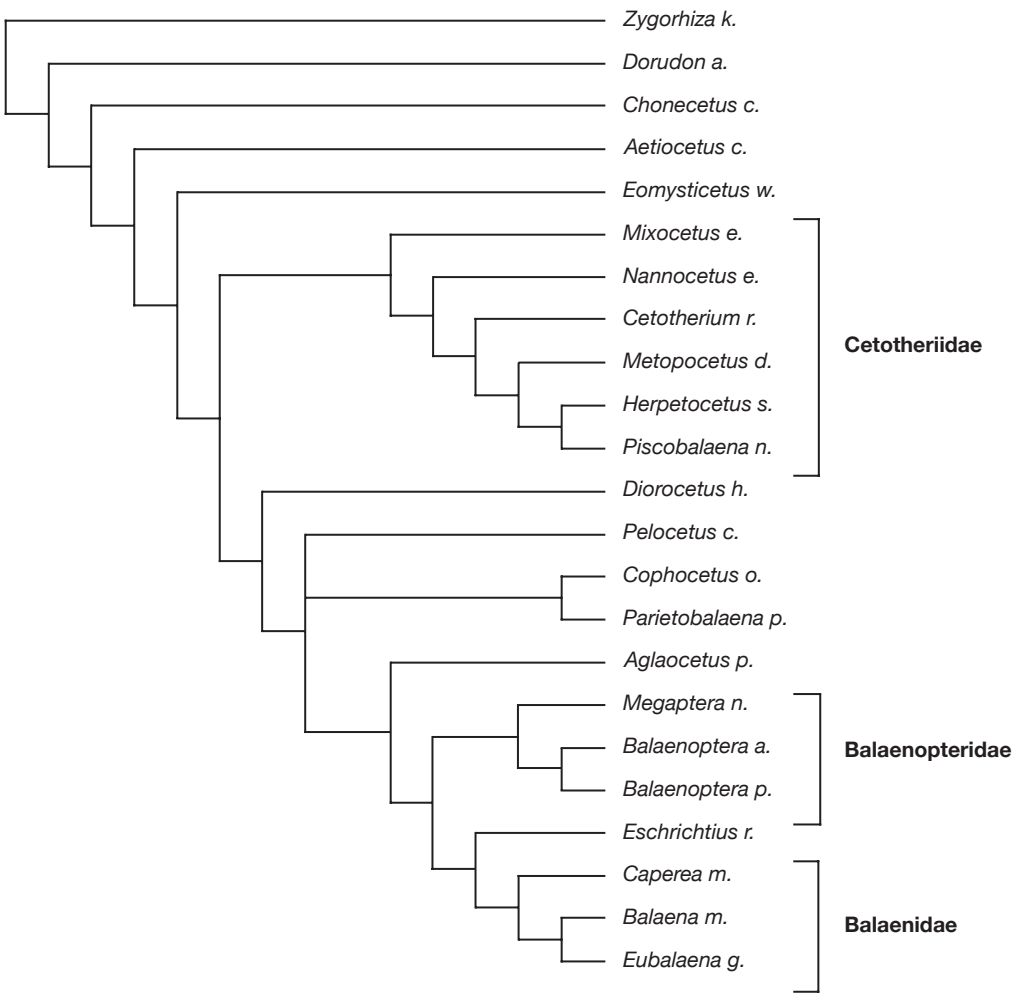

FIG. 32. — Strict consensus of the three trees obtained, after reweighting of the characters, via branch and bound analysis of the 23 taxa and 101 characters matrix (CI: 0.767; RI: 0.896; RC: 0.687; HI: 0.233).

cipital is well posterior to this line. The telescoping of the supraoccipital in balaenopterids is therefore achieved more by an anterior projection of the occipital, whereas in *Piscobalaena*, it is more induced by a posterior extension of the rostral bones.

As demonstrated above, *Piscobalaena* is clearly not a balaenopterid. However, several characters suggest closer relationships with this family than with balaenids and neobalaenids. As mentioned above, *Piscobalaena* shares with balaenopterids a strong posterior extension of the rostral bones, which overlap the cranial bones, a hook-like and laterally everted coronoid process of the dentary, and a slightly posteriorly developed angular process of the dentary, clearly separated from the mandibular condyle.

However, *Piscobalaena* also resembles *Eschrichtius* in the oblique (in lateral view) mandibular condyle, while it is vertical in balaenopterids.

Piscobalaena has been compared to several taxa traditionally included with many other taxa in the "Cetotheriidae" (*sensu* Simpson 1945 = *sensu lato*):

Cetotherium, *Nannocetus*, *Herpetocetus*, and *Metopocetus*. As stated above, the "Cetotheriidae" (*s.l.*) have not been securely demonstrated as monophyletic and very probably represent a polyphyletic taxon (Fordyce & Muizon 2001 and references therein). In fact, the comparison above suggests that *Cetotherium*, *Herpetocetus*, *Metopocetus*, *Nannocetus*, and *Piscobalaena* may constitute a monophyletic group, which should therefore represent the Cetotheriidae *sensu stricto*.

Parsimony analysis

The matrix (Appendix 3) of 101 morphological characters of the skull, auditory area and dentary (Appendix 2), observed in 23 terminal taxa: two outgroups (*Zygorhiza kochii*, *Dorudon atrox*), and 21 ingroups (Appendix 1). It was analysed by PAUP 4 (Swofford 1998), on Branch-and-Bound mode, and optimized by ACCTRAN. All characters were treated as unordered and no basal polarity was specified.

A first run proposed 66 equiparcimonious trees (length = 143.92 steps; CI = 0.713; RI = 0.863; RC = 0.616; HI = 0.287). In order to increase the degree of resolution of the trees, the characters have been rewheighted by maximum value of RC, which provided three equiparcimonious trees (length = 133.93 steps; CI = 0.767; RI = 0.896; RC = 0.687; HI = 0.233). The topology of the strict consensus tree (Fig. 32) suggests the following relationships.

– The monophyly of mysticetes is confirmed and supported by 19 characters: (6^1) the angle of the dorsal and ventral planes of the lateral edge of the maxilla (in anterior half), in cross section, is less than 45°; (18^1) the posterior extension of the premaxillae is at the same level as the posterior extremity of the maxillae; (22^1) the premaxillae are separated anterior to the bony nares; (23^1) the line joining the preorbital processes of the frontals passes through the nasals length; (30^1) the postorbital process of the frontal is long and finger-like; (34^1) deeply notched dorsal edge of the orbit (in dorsal view); (48^1) the postglenoid process (in lateral view) tapers ventrally to a point; (51^1) the basioccipital crest is wide and bulbous; (52^1) the foramen pseudovale perforates the squamosal only; (64^1) the apex of the anterior process of the periotic is deflected ventrally; (67^1) the posterior process of periotic is made of spongy bone, pitted and rugose, remaining portions are smooth and dense; (69^1) rounded or blade-like ventrolateral expansion (ventrolateral tubercle) at base of anterior process; (71^1) the suprameatal fossa is distinctly concave and the tegmen tympani is more elevated and thicker; (82^1) the caudal tympanic process of periotic is present as a prominent sharp crest; (88^1) the dentaries have no suture at their apices but are independent and connected by a ligament only attached on a short horizontal rim on the medial edge of the apex of the dentary; (90^1) the dentary is constant in height all along its length; (96^1) the notch for the insertion of the internal pterygoid muscle is present medially only; (97^1) the opening of the mandibular canal is approximately below the apex of the coronoid process; (101^1) the mandibular condyle is transversely narrow (distinctly narrower than long).

– Within this clade, the two toothed mysticetes (i.e. *Aetiocetus*, and *Chonecetus*) constitute the sister-group of the baleen mysticetes. Contrary to Barnes *et al.* (1994)'s statement, which regarded *Chonecetus* as a sub-family of the Aetiocetidae (i.e. Chonecetinae), in the present analysis, these two genera do not constitute a monophyletic clade.

– Baleen mysticetes are monophyletic and share 17 synapomorphies: (3^1) absence of maxillary teeth; (4^1) vascular foramina on the palate open in anterolaterally or anteroposteriorly directed grooves on the ventral surface of the maxilla, related (in Recent taxa) to the irrigation of the epithelium producing baleen; (7^1) extension of the posteroventral edge of the maxilla in a posteroventrally directed plate below the lacrimal; (8^1) presence of a preorbital notch of the maxilla; (16^1) the fronto-maxillar suture is long and reaches (or becomes close to) the vertex posteromedially; (17^1) the fronto-maxillar suture is slightly concave posterolaterally and oblique; (20^1) the frontal-nasal suture is approximately straight transversely; (22^0) the premaxillae are not separated or very close anterior to the bony nares; (27^1) the supraorbital process is slightly wider than long; (34^0) the postorbital process of the frontal is short and blunt; (40^1) the medial occipital crest is present and elevated; (41^1) the zygomatic process (in dorsal view) is transversely massive and relatively

long; (45[1]) the postglenoid process (in lateral view) is subvertical to slightly posteriorly projected; (49[1]) the glenoid cavity is very shallow, subcircular, and facing ventrally; (50[1]) presence of a basioccipital process (strong and massive tubercle on the basioccipital crest for the origin of the longus colli muscle); (53[1]) anterior edge of supraoccipital (in dorsoposterior view) triangular, sharply pointed anteriorly; (87[1]) dentary bowed medially (in dorsal view).

Among this clade, *Eomysticetus* is the sister-taxon of the all the other taxa.

– The rest of the taxa constitute two distinct clades. The first group includes six fossil taxa: [*Mixocetus* [*Nannocetus* [*Cetotherium* [*Metopocetus* [*Herpetocetus*, *Piscobalaena*]]]]], which monophyly is supported by 14 characters: (11[2]) the ascending process of the maxilla is as extended posteriorly as or posterior to the postorbital process of the frontal; (13[1]) the ascending processes of the maxillae contact medially or are very approximated at apex only; (18[0]) premaxillae not as extended posteriorly as posterior extremities of maxillae; (19[1]) lateral edges of nasals strongly convergent posteriorly (bones distinctly triangular and wedge-shaped); (21[1]) posterior limit of narial fossa posterior to or at same level as the line joining the preorbital processes of the frontals; (23[2]) the line joining the preorbital processes of the frontals is anterior to or on the same level as the anterior extremity of the nasals; (25[1]) supraorbital process of frontal anteriorly oriented (which gives an anteriorly opened V-shaped morphology of the posterior edge of the rostral bones); (36[2]) dorsal exposure of frontals (in the sagittal plane of the skull) totally covered by rostral bones; (37[1]) presence of a crest-like or ridge-like portion of the parieto-squamosal suture; (55[2]) lateral edge of paroccipital process (in ventral view) posterior to the posterior edge of the condyle; (64[0]) the apex of anterior process of periotic is straight (i.e. not deflected ventrally); (74[1]) thick crista transversa; (75[1]) the anterior edge of facial foramen, on the internal acoustic meatus, is notched (slightly to deeply) for the passage of the greater petrosal nerve; (85[1]) posterior processes of periotic and tympanic conical to tetrahedral, strongly widening distally; (86[1]) external exposure of posterior process of petrotympanic relatively flat (concave in juveniles), vertical, and facing roughly laterally. Characters 85[1] and 86[1] actually appear (in ACCTRAN optimization) before the node supporting both clades. Since state 1 of both characters 85 and 86 is present in the following taxa only: *Mixocetus*, *Nannocetus*, *Cetotherium*, *Metopocetus*, *Herpetocetus*, and *Piscobalaena*, it can be assumed that these character states support the monophyly of this clade. This distribution of the characters is attributable to an artefact of tree reconstruction in ACCTRAN optimization.

The second group includes the Recent mysticetes and the remaining fossil taxa (*Diorocetus*, *Pelocetus*, *Cophocetus*, *Parietobalaena*, and *Aglaocetus*). Within this clade, the monophyly of the Recent mysticetes is supported by 17 characters: (26[2]) medial portion of supraorbital process of frontal longer than lateral portion; (28[2]) dorsal surface of supraorbital process of frontal abruptly depressed medially; (35[2]) dorsal exposure of parietals in the sagittal plane of the skull totally covered by frontals and/or supraoccipital; (38[1]) supraoccipital as high as frontals and/or nasals; (48[0]) anterior and posterior sides of postglenoid process nearly parallel with squared-off end (in lateral view); (50[0]) absence of basoccipital process; (52[0]) the foramen pseudovale perforates the squamosal with a participation of the pterygoid; (53[2]) anterior edge of supraoccipital (in dorsoposterior view) triangular and rounded to squared anteriorly; (54[1]) lambdoidal crests of supraoccipital horizontal and directed anterolaterally, overhanging temporal fossae; (67[3]) most of the periotic is made of spongy bone, essentially the posterior and dorsal portions, the anterior process, and the dorsal region of the pars cochlearis; (70[1]) the anterior process is pointed and tapers until apex; (71[3]) indistinct suprameatal fossa due to extreme growth of tegmen tympani, which invades the fossa; (73[1]) tubular fundus of internal acoustic meatus; (76[0]) promontorium roughly hemispherical (in ventral view); (77[2]) pars cochlearis conspicuously expanded dorsally (width at base shorter than proximodistal length); (81[0]) absence of a groove on the medial side of the promontorium; (85[3]) posterior process of the petrotympanic anteroposteriorly flattened at apex.

The topology of the tree shows that Balaenopteridae is the sister-group of the other Recent taxa [*Eschrichtius* [*Caperea* [*Balaena*, *Eubalaena*]]]. The

monophly of the latter is supported by 14 characters: (1[1]) rostrum dorsally bowed (in lateral view); (15[1]) the posteromedial angle of the maxilla faces laterally; (39[0]) anteriormost limit of supraoccipital posterior to the line joining the apices of the zygomatic processes; (45[2]) postglenoid process strongly projecting posteriorly (in lateral view); (46[0]) postglenoid process ventrally oriented (in posterior view); (49[2]) glenoid cavity very shallow, subcircular to slightly elongated anteroposteriorly, and facing anteroventrally; (55[2]) the lateral edge of the paroccipital process (in ventral view) is posterior to the posterior edge of the occipital condyle; (60[1]) the tympanic is dorsoventrally compressed and mediolaterally expanded; (72[1]) cerebral opening for facial nerve and vestibulocochlear foramen separated by an elevated crista transversa; (85[4]) posterior process of petrotympanic dorsoventrally flattened at apex; (90[2]) the horizontal ramus of the dentary is expanded in height and arched dorsoventrally; (92[2]) coronoid process limited to a small hump or absent; (99[1]) mandibular condyle high on the posterior end of the dentary, facing posterodorsally with a dorsal component much more developed than the posterior one; (101[3]) mandibular condyle hemispherical and located at the posterodorsal end of the dentary.

The result of this analysis suggests two major comments:

1) First of all, the study has confirmed the paraphyly of the traditional Cetotheriidae *s.l.* and suggested that the Cetotheriidae *s.s.* consists in six of the fossil baleen mysticetes taxa observed. Consequently, in this paper, we propose the following new definition of the Cetotheriidae *s.s.*

Order CETACEA Brisson, 1762
Infraorder MYSTICETI Cope, 1891

Family CETOTHERIIDAE Brandt, 1872

INCLUDED GENERA

Piscobalaena Pilleri & Siber, 1989; *Herpetocetus* Van Beneden, 1872; *Metopocetus* Cope, 1896; *Cetotherium* Brandt, 1843; *Nannocetus* Kellogg, 1929; *Mixocetus* Kellogg, 1934.

So far, the following genera can reasonably be included in the Cetotheriidae *s.s.*: *Cetotherium*, *Herpetocetus*, *Nannocetus*, *Piscobalaena*. *Metopocetus* and *Mixocetus*. However, some genera are poorly known (*Nnanocetus*, *Metopocetus*), and better preserved specimens of these taxa are needed to confirm this statement. Furthermore, the holotype of *Mixocetus* is a fairly complete skull but the specimen is heavily reconstructed and some cetotheres characters are difficult to observe.

Kellogg (1941) described three species of cetotheres from Portugal previously figured by Vandelli (1831). Although the specimens were not available for this study, given the results above, some comments can be made on their affinities. *Metopocetus vandelli* is referred by Kellogg to this genus, but had been referred to the genus *Cetotherium* by Brandt (1872, 1873), and *Aulocetus* by Capellini (1901). Whether or not this specimen (the holotype) is congeneric with *Metopocetus durinasus* (the type species of the genus), it bears some clear synapomorphies of the Cetotheriidae *s.s.* The most characteristic feature is the oblique anterior edge of the supraorbital process of the frontal, which gives to the rostral bones a V-shaped protrusion in the cranial bones. Furthermore, the posteriorly salient lateral edge of the paroccipital processes is also characteristic of the Cetotheriidae. These features are also present in the two other cetotheres studied by Kellogg ("*Aulocetus*" *latus*, and *Cephalotropis nectus*). Therefore, these taxa, the taxinomic revision of which is much needed, are also probable Cetotheriidae *s.s.* but a detailed study of the type specimen of these species is needed to confirm this statement.

DIAGNOSIS OF THE FAMILY

For the list of characters, see Appendix 2.

(11[2]) ascending process of the maxilla as extended posteriorly as or posterior to the postorbital process of the frontal; (13[1]) ascending processes of the maxillae contacting medially or very approximated at apex only; (18[0]) premaxillae not as extended posteriorly as posterior extremities of maxillae; (19[1]) lateral edges of nasals strongly convergent posteriorly (bones distinctly triangular and wedge-shaped); (21[1]) posterior limit of narial fossa posterior to or at same level as the line joining; (23[2]) the line joining

the preorbital processes of the frontals is anterior to or on the same level as the anterior extremity of the nasal; (25[1]) supraorbital process of the frontal anteriorly oriented (which gives an anteriorly opened V-shaped morphology of the posterior edge of the rostral bones); (36[2]) dorsal exposure of frontals in the sagittal plane of the skull totally covered by rostral bones; (37[1]) presence of a crest-like or ridge-like portion of the parieto-squamosal suture; (55[2]) lateral edge of paroccipital process (in ventral view) posterior to the posterior edge of the occipital condyle; (64[0]) apex of anterior process of periotic straight (i.e. not deflected ventrally); (74[1]) thick crista transversa; (75[1]) the anterior edge of facial foramen on the internal acoustic meatus is notched (slightly to deeply) for the passage of the greater petrosal nerve; (85[1]) posterior processes of periotic and tympanic conical to tetrahedral, strongly widening distally; (86[1]) external exposure of posterior process of petrotympanic relatively flat (concave in juveniles), vertical, and facing roughly laterally.

2) The second statement concerns the status of Eschrichtiidae relatively to the other Recent taxa. The present analysis suggests that *Eschrichtius* is more closely related to Balaenidae and Neobalaenidae than to Balaenopteridae. This contradicts the traditional Eschrichtiidae-Balaenopteridae relationships (*sensu* Kimura & Osawa 2002: 698, "the Eschrichtiidae is traditionally considered to be more closely related to the Balaenopteridae"), a phylogeny often supported by morphological and molecular analyses (Àrnason & Gullberg 1996; Dooley *et al.* 2004; Geisler & Luo 1996; Kimura & Osawa 2002; Messenger & McGuire 1998; Milinkovitch *et al.* 1994, 1995).

The posterior expansion of the ascending processes of the maxillae, which contact (or almost) behind the nasals, and the V-shaped contact between the rostral and cranial bones are probably the most characteristic features of the Cetotheriidae *s.s.* As a matter of fact, the former has already been pointed out by Cabrera (1926), Miller (1923), and Kellogg (1928).

Although differently achieved, the posterior extension of the ascending processes of the maxillae approaches the condition observed in balaenopterids and is probably related to a similar "engulfment" feeding behaviour (Bouetel 2005). This could suggest a closer phylogenetic relationship of the Cetotheriidae *s.s.* with balaenopterids than with eschrichtiids or balaenids. Thus, the family could therefore represent the sister-group of the balaenopterids. However, the results of the parsimony analysis given above contradicts this hypothesis and the similar feeding behaviour suggested in the Cetotheriidae and the Balaenopteridae should be regarded as a convergent.

In other respects, the morphology of the posterior extremity of the dentary in Recent mysticetes varies greatly. In balaenopterids, the posterior extremity of the dentary is rectangular: the dorsal angle being the condyle and the ventral angle the angular process. Both processes form approximately a right angle. In *Eschrichtius*, the condyle is located on the dorsal edge of the posterior extremity of the dentary and the angular process is massive, rounded and projects posteriorly behind the condyle. The cetothere condition (i.e. *Piscobalaena* and *Herpetocetus*) approaches the condition of *Eschrichtius*. However, in these taxa, the angular process is more slender and projects further posteriorly. In balaenids and neobalaenids, the angular process is very reduced to absent. The morphology of the posterior extremity of the dentary represents another morpho-functional complex in relation with the feeding behaviour (Bouetel 2005) and the similarities observed between cetotheres and eschrichtiids do not fit the result of the analysis given above. Therefore, a careful functional analysis of the craniomandibular articulation of mysticete is urgently needed to clarify this point and its implication on mysticetes relationships.

PALEOBIOGEOGRAPHY

Among the numerous fossil taxa referred to the "Cetotheriidae", the five species cited above could represent the Cetotheriidae *s.s. Piscobalaena* is from the coast of Peru, *Herpetocetus* from Belgium, East Coast of the North America, and Japan, *Cetotherium* from Kertsch, near Azov Sea (Russia), *Nannocetus* from the West Coast of North America, and *Metopocetus* from the East Coast of North America.

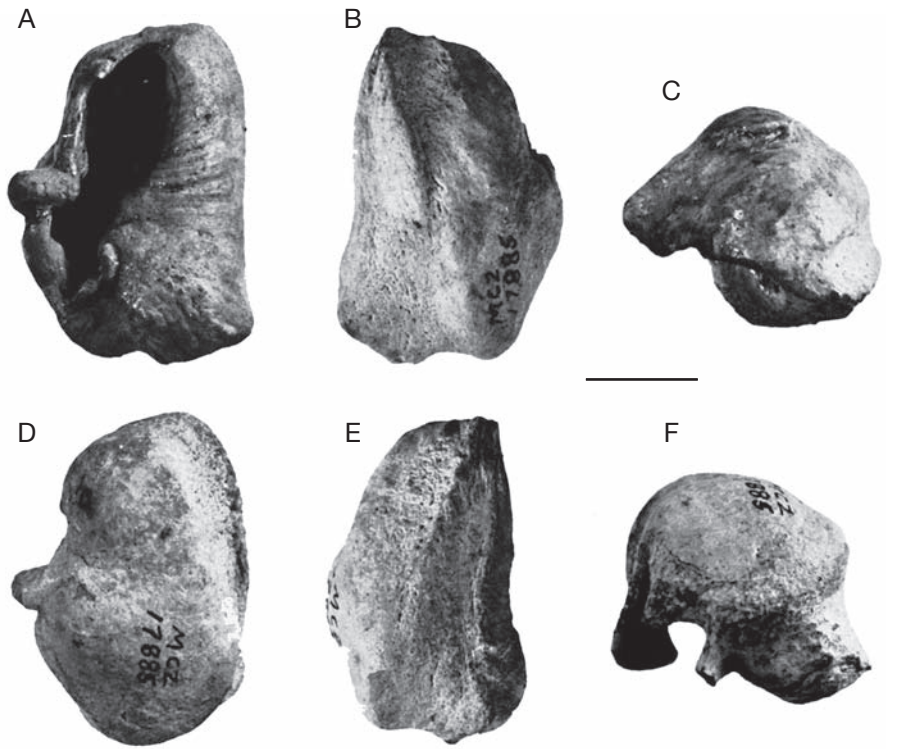

FIG. 33. — Tympanics of *Piscobalaena* sp. (MCZ 17885) referred to ?*Mesocetus* species indet. by Kellogg (reproduced from Kellogg 1944); **A**-**C**, left tympanic; **A**, dorsal view; **B**, medial view; **C**, anterior view; **D**-**F**, right tympanic; **D**, ventral view; **E**, medial view; **F**, posterior view. Scale bar: 2 cm.

Some specimens of another small whale from beds of the Pisco Formation (Peru) near Puerto Lomas on the southern coast (El Jahuay horizon, *c.* 10 to 9 Ma, according to Muizon & DeVries 1985) are present in the Museo de Historia natural de la Universidad Nacional mayor de San marcos (Lima, Peru). These specimens are referrable to a new species of the genus *Piscobalaena*. Although very similar to *Piscobalaena nana*, they mainly differ from the Pliocene species by the fact that the lateral edges of the maxillae are convergent anteriorly all along their length, whereas in *Piscobalaena nana*, they are sub-parallel on their posterior four-fifth and progressively converge anteriorly in their distal fifth. Furthermore, the mandibular condyle is only slightly oblique, (more resembling the condition of *Diorocetus* in this respect) and the angular process does not project posteriorly as it does in *Piscobalaena nana*. Also, these specimens are from a geologically older locality (10 Ma) than Sud-Sacaco (SAS, *c.* 5 Ma). Therefore *Piscobalaena* appear to be so far a genus known on the Pacific coast of South America, where it evolved at least during 5 Ma.

However, in 1944, Kellogg described an isolated tympanic from the Tertiary of Florida (Fig. 33). Although slightly smaller than that of *Piscobalaena nana*, this tympanic presents the diagnostic characters of the tympanic of the Peruvian taxon (i.e. pear-shaped bone; globose and dorsally developed dorsal lobe; medially keeled ventral lobe; ventrally swollen posterior two-thirds of the ventral lip). Kellogg referred this isolated bone to ?*Mesocetus*. Van Beneden (1886) defined *Mesocetus* upon various fragments of numerous specimens and assigned some portions to distinct species. Since he did not define a type species of the genus, as pointed out by Ichischima (1997), the genus *Mesocetus* needs revision and is regarded here as nomen

dubium. Consequently, since the isolated tympanic described by Kellogg is remarkably similar to that of *Piscobalaena*, this bone is referred here to this genus. Since it is not possible to assign a species name based on a single auditory bone, this isolated tympanic is referred to *Piscobalaena* sp. Therefore, *Piscobalaena* probably had a wider geographical distribution than the Peruvian coast only. This is possible because the Panama Isthmus was open until the late Pliocene (Marshall 1985). Stratigraphical data and faunal assemblages have permitted to confirm that migrations of cetaceans were then possible through the Isthmus from the northern Atlantic to the southern Pacific (Muizon 1984, 1988; Barnes 1985a, b). According to this, it seems that the Cetotheriidae *s.s.* have a relatively wide paleogeographic distribution, although mainly located in the northern hemisphere.

Acknowledgements
Special thanks are due to R. E. Fordyce (University of Otago, Dunedin, New Zealand) and anonymous reviewer for their very careful work, which greatly helped in improving the initial version of this work. Specimens were collected by CM with funds of the Institut français d'Études andines (IFEA) and of the Muséum national d'Histoire naturelle (MNHN). The "Société des Amis du Muséum national d'Histoire naturelle et du Jardin des Plantes" provided financial support to VB for two short term visits to the USNM and to the LACM. E. Frey (Staatlische Museum für Naturkunde, Karlsruhe, Germany) gave CM access to the holotype of *Piscobalaena nana* and provided, as usual, an extremely helpful and kind attention. M. Elstrup kindly provided original photographs of the holotypes of *Cetotherium rathkei* and *Metopocetus durinasus*. Thanks are due also to L. G. Barnes (LA county Museum), D. Bohaska (Department of Paleobiology, USNM), J. G. Mead and C. W. Potter (Marine Mammal Program, USNM), who provided VB access to the specimens of fossil and Recent mysticetes under their care. Photographs are by P. Loubry and D. Serrette (MNHN); line drawings are by VB except Figure 10, which is by F. Pilard.

REFERENCES

ADAMS J. I. 1908. —— An outline review of the geology of Peru. *Annual Report of the Smithsonian Institution*: 385-430.

ÀRNASON U. & GULLBERG A. 1996. — Cytochrome *b* nucleotide sequences and the identification of the five primary lineages of extant cetaceans. *Molecular Biology and Evolution* 13: 407-417.

BARNES L. G. 1985a. — Evolution, taxonomy and antitropical distribution of the porpoises (Phocoenidae, Mammalia). *Marine Mammal Science* 1: 149-165.

BARNES L. G. 1985b. — The late Miocene dolphin *Pithanodelphis* Abel, 1905 (Cetacea, Kentriodontidae) from California. *Contribution in Science, Natural History Museum of Los Angeles County* 363: 1-34.

BARNES L. G. & MCLEOD S. A. 1984. — The fossil record and phyletic relationships of gray whales, *in* JONES M. L., SWARTZ S. L. & LEATHERWOOD S. (eds), *The Gray Whale*: Eschrichtius robustus. Academic Press, Orlando: 3-32.

BARNES L. G. KIMURA M., FURUSAWA H. & SAWAMURA H. 1994. — Classification and distribution of the Oligocene Aetiocetidae (Mammalia; Cetacea; Mysticeti) from western North America and Japan. *The Island Arc* 3: 392-431.

BENHAM W. B. 1937. — Fossil Cetacea of New Zealand. II. On *Lophocephalus*, a new genus of zeuglodont Cetacea. *Transactions of the Royal Society of New Zealand* 67: 1-7.

BENHAM W. B. 1939. — *Mauicetus*: a fossil whale. *Nature* 143: 765.

BENHAM W. B. 1942. — Fossil Cetacea of New Zealand. V. *Mauicetus*, a generic name substituted for *Lophocetus* Benham. *Transactions of the Royal Society of New Zealand* 71: 260-270.

BOUETEL V. 2005. — Phylogenetic implications of skull structure and feeding behavior in balaenopterids (Cetacea, Mysticeti). *Journal of Mammalogy* 86 (1): 139-146.

BRANDT J. F. 1843. — De Cetotherio, novo balaenarum familiae genere, in Rossia meridionali anti aliquot annos effoso. *Bulletin de l'Académie impériale des Sciences de St Petersbourg* (2) 1: 145-148.

BRANDT J. F. 1872. — Bericht über den bereits vollendeten, druckfertigen Theil seiner Untersuchungen über die fossilen und subfossilen Cetaceen Europas. *Compte rendu de l'Académie impériale des Sciences de St Pétersbourg* tome 17: 407-408.

BRANDT J. F. 1873. — Untersuchungen über die fossilen und subfossilen Cetaceen Europas. *Mémoires de l'Académie de St Pétersbourg* 20 (1), sér. 7: 1-371.

CABRERA A. 1926. — Cetáceos fósiles del Museo de la Plata. *Revista del Museo de la Plata* 29: 363-411.

CAPELLINI G. 1901. — Balenottera miocenica del monte titano, Republica di S. Marino. *Memorie della reale*

Academia de scienze del'istituto di Bologna serie 5, 9: 237-260.

COPE E. D. 1896. — Sixth contribution to the knowledge of the Miocene fauna of North Carolina. *Proceedings of the American Philosophical Society* 35 (151): 139-146.

CUMMINGS W. C. 1985. — The right whales *Eubalaena glacialis* (Müller 1776) and *Eubalaena australis* (Desmoulins, 1822), *in* RIDGWAY S. H. & SIR HARRISON R. (eds), *Handbook of Marine Mammals.* Academic Press, New York: 275-304.

DOOLEY A. C. JR., FRASER N. C. & LUO Z. 2004. — The earliest known member of the rorqual-Gray whale clade (Mammalia, Cetacea). *Journal of Vertebrate Paleontology* 24 (2): 453-463.

EMLONG D. R. 1966. — A new archaic cetacean from the Oligocene of Northwest Oregon. *Bulletin of the Museum of Natural History*, University of Oregon 3: 1-51.

FORDYCE R. E. 1980. — Whale evolution and Oligocene Southern Ocean environments. *Palaeogeography Palaeoclimatology Palaeoecology* 55: 319-336.

FORDYCE R. E. 1989. — Origins and evolution of Antarctic marine mammals. *Special Publication of the Geological Society of London* 47: 269-281.

FORDYCE R. E. 1992. — *Mauicetus* and late Oligocene baleen-bearing primitive Mysticeti from the Southwest Pacific, *in Abstracts, 29th International Geological Congress, Kyoto, Japan* 2: 349.

FORDYCE R. E. 1994. — *Waipatia maerewhenua*, new genus and new species (Waipatiidae, new family), an archaic late Oligocene dolphin (Cetacea: Odontoceti: Platanistoidea) from New Zealand. *Proceedings of the San Diego Museum of Natural History* 29: 147-176.

FORDYCE R. E. & MUIZON C. DE 2001. — Evolutionary history of cetaceans: a review, *in* MAZIN J. M. & BUFFRÉNIL V. DE (eds), *Secondary Adaptation of Tetrapods to Life in Water*. Pfeil Verlag, Munich: 169-233.

FORDYCE R. E. & WATSON A. G. 1998. — Vertebral pathology in an early Oligocene whale (Cetacea, ?Mysticeti) from Wharekuri, North Otago, New Zealand. *Mainzer naturwissenschaftliches, Archiv/Beihefte* 21: 161-176.

FRASER F. C. & PURVES P. E. 1960. — Hearing in cetaceans: evolution of the accessory air sacs and the structure of the outer and middle ear in recent cetaceans. *Bulletin of the British Museum (Natural History)*, Zoology 7: 1-140.

GEISLER J. H. & LUO Z. 1996. — The petrosal and inner ear of *Herpetocetus* sp. (Mammalia: Cetacea) and their implications for the phylogeny and hearing of archaic mysticetes. *Journal of Paleontology* 70 (6): 1045-1066.

GEISLER J. H. & LUO Z. 1998. — Relationships of Cetacea to terrestrial Ungulates and the evolution of cranial vasculature in Cete, *in* THEWISSEN J. G. M. (ed.), *The Emergence of Whales*. Plenum Press, New York: 163-212.

GEISLER J. H. & SANDERS A. E. 2003. — Morphological evidence for the phylogeny of Cetacea. *Journal of Mammalian Evolution* 10: 23-129.

HASEGAWA Y., NOKARIYA H., SATO J. & OISHI M. 1985. — Part III. Fossil whale, the 1st specimen from Maesawa-cho, Iwate Prefecture, Japan, *in* OISHI M., ONO K., KAWAKAMY T., SATO J., NOKARIYA H. & HASHEGAWA Y. (eds), Pliocene baleen whales and bony-toothed bird from Iwate Prefecture, Japan (Parts I-VI). *Bulletin of the Iwate Prefectural Museum* 3: 148-150.

HATAI K., HAYASAKA S. & MASUDA K. 1963. — Some fossil tympanics from the Mizuno Period of northern Japan. *Saito Ho-on Kai Museum of Natural History, Research Bulletin* 32: 5-17.

ICHISCHIMA H. 1997. — *Systematics of the Latest Oligocene to the Earliest Miocene Mysticeti from New Zealand.* Dissertation, University of Otago, Dunedin, New Zealand, xx + 352 p.

KELLOGG R. 1924. — Description of a new genus and species of whalebone whale from the Calvert Cliffs Maryland. *Proceedings of the United States National Museum* 63: 1-14.

KELLOGG A. R. 1928. — History of whales – their adaptation to life in the water. *Quarterly Review of Biology* 3: 29-76, 174-208.

KELLOGG R. 1929. — A new cetothere from southern California. *University of California Publications, Bulletin of the Department of Geological Sciences* 18: 449-457.

KELLOGG R. 1931. — Pelagic mammals from the Temblor formation of the Kern River region, California. *Proceedings of the Californian Academy of Science* series 4, 19: 217-297.

KELLOGG R. 1934. — The patagonian fossil whalebone whale *Cetotherium moreni* (Lydekker). *Carnegie Institution of Washington Publication* 447: 64-81.

KELLOGG R. 1936. — A review of the Archaeoceti. *Carnegie Institute of Washington Publication* 482: 1-366.

KELLOGG R. 1941. — On the cetotheres figured by Vandelli. *Boletim do museu de mineralogia e geologia da universidade de Lisboa* 7-8: 1-12.

KELLOGG 1944. — Fossil cetaceans from the Florida Tertiary. *Bulletin of the Museum of Comparative Zoology* 94: 433-471.

KELLOGG R. 1965. — Fossil marine mammals from the Miocene Calvert Formation of Maryland and Virginia. *Bulletin of the United States National Museum* 247: 1-63.

KELLOGG R. 1968. — Fossil marine mammals from the Miocene Calvert Formation of Maryland and Virginia. *Bulletin of the United States National Museum* 247: 103-201.

KELLOGG R. 1969. — Cetothere skeletons from the

Miocene Choptank Formation of Maryland and Virginia. *Bulletin of the United States National Museum* 294: 1-40.

KIMURA T. 2002. — Feeding strategies of an early Miocene cetothere from the Toyama and Akeyo Formations, Central Japan. *Paleontological Research* 6 (2): 179-189.

KIMURA T. & OSAWA T. 2002. — A new cetothere (Cetacea: Mysticeti) from the early Miocene of Japan. *Journal of Vertebrate Paleontology* 22: 684-702.

LAMBERTSEN R. H. 1983. — Internal mechanism of rorqual feeding. *Journal of Mammalogy* 64: 76-88.

LINDOW B. E. K. 2002. — Bardehvalernes indbyrdes slaegtskabsforhold – en forelobig analyse [= The internal relationships of the baleen whales – preliminary analysis], *in* LINDOW B. E. K. (ed.), *Résumé-haefte. Hvaldag, 2002, 24 september 2002.* Midtsonderjyllands Museum, Gram: 12-19.

LUO Z. 1998. — Homology and transformation of cetacean ectotympanic structures, *in* THEWISSEN J. G. M. (ed.), *The Emergence of Whales*. Plenum Press, New York: 269-301.

LUO Z. & GINGERICH P. D. 1999. — Terrestrial Mesonychia to aquatic Cetacea: transformation of the basicranium and evolution of hearing in whales. *University of Michigan Papers on Paleontology* 31: 1-98.

MARPLES B. J. 1956. — Cetotheres (Cetacea) from the Oligocene of New Zealand. *Proceedings of the Zoological Society of London* 126: 565-580.

MCDONALD H. G. & MUIZON C. DE 2002. — The cranial anatomy of *Thalassocnus* (Xenarthra, Mammalia), a derived nothrothere from the Neogene of the Pisco Formation (Peru). *Journal of Vertebrate Paleontology* 22: 349-365.

MARSHALL L. 1985. — Geochronology an land-mammal biochronology of the transamerican faunal interchange, *in* STEHLI F. G. & WEBB S. D. (eds), *The Great American Biotic Interchange*. Plenum Press, New York: 49-85.

MAROCCO R. & MUIZON C. DE 1988. — Los Vertebrados del Neogeno de la Costa Sur del Perú: Ambiente Sedimentario y Condiciones de Fosilización. *Bulletin de l'Institut français d'Études andines* 17 (2): 105-117.

MCINTYRE G. T. 1967. — Foramen ovale and Quasi mammals. *Evolution* 21: 834-841.

MCKENNA M. C. & BELL S. K. 1997. — *Classification of Mammals Above the Species Level*. Columbia University Press, New York, 631 p.

MCLEOD S. A., WHITMORE F. C. & BARNES L. G. 1993. — Evolutionary relationships and classification, *in* BURNS J. J., MONTAGUE J. J. & COWLES C. J. (eds), *The Bowhead Whale*. Society for Marine Mammalogy, Lawrence, Kansas: 45-70.

MESSENGER & MCGUIRE 1998. — Morphology, molecules, and the phylogenetic of Cetaceans. *Systematic Biology* 47: 90-124.

MILINKOVITCH M. C., MEYER A. & POWELL J. R. 1994. — Phylogeny of all major groups of cetaceans based on DNA sequences from 3 mitochondrial genes. *Molecular Biology and Evolution* 11: 939-948.

MILINKOVITCH M. C., ORTI G. & MEYER A. 1995. — Novel phylogeny of whales revisited but not revised. *Molecular Biology and Evolution* 12: 518-520.

MILLER G. S. 1923. — The telescoping of the cetacean skull. *Smithsonian Miscellaneous Collections* 76: 1-71.

MILLER M. E., CHRISTENSEN G. C. & EVANS H. E. 1964. — *Anatomy of the Dog*. W. B. Saunders, Philadelphia; London, 941 p.

MITCHELL E. 1989. — A new cetacean from the late Eocene La Meseta Formation, Seymour Island, Antarctic Peninsula. *Canadian Journal of Fisheries and Aquatic Sciences* 46: 2219-2235.

MUIZON C. DE 1981. — Les vertébrés fossiles de la Formation Pisco (Pérou). Première partie : deux nouveaux Monachinae (Phocidae, Mammalia) du Pliocène inférieur de Sud-Sacaco. *Travaux de l'Institut français d'Études andines* 22: 1-22.

MUIZON C. DE 1984. — Les odontocètes (Cetacea, Mammalia) du Pliocène inférieur de Sud-Sacaco. *Travaux de l'Institut français d'Études andines* 50: 1-188.

MUIZON C. DE 1988. — Les odontocètes (Cetacea, Mammalia) du Miocène. *Travaux de l'Institut français d'Études andines* 78: 1-244.

MUIZON C. DE & DEVRIES T. J. 1985. — Geology and paleontology of late Cenozoic marine deposits in the Sacaco area (Peru). *Sonderdruck aus der Geologische Rundschau* 74: 547-563.

MUIZON C. DE & MCDONALD H. G. 1995. — An aquatic sloth from the Pliocene of Peru. *Nature* 375: 224-227.

OISHI M. & HASEGAWA Y. 1994a. — Diversity of Pliocene mysticetes from eastern Japan. *The Island Arc* 3: 436-452.

OISHI M. & HASEGAWA Y. 1994b. — A list of fossil cetaceans in Japan. *The Island Arc* 3: 493-505.

OISHI M., ONO K., KAWAKAMY T., SATO J., NOKARIYA H. & HASHEGAWA Y. 1985. — Pliocene baleen whales and bony-toothed bird from Iwate Prefecture, Japan (Parts I-VI). *Bulletin of the Iwate Prefectural Museum* 3: 143-162.

ORTON L. S. & BRODIE P. F. 1987. — Engulfing mechanics of fin whales. *Canadian Journal of Zoology* 65: 2898-2907.

PACKARD E. L. & KELLOGG R. 1934. — A new cetothere from the Miocene Astoria Formation of Newport, Oregon. *Carnegie Institution of Washington, Publication* 447: 1-62.

PILLERI G. 1986. — *Beobachtungen an den Fossilen Cetaceen des Kaukasus*. G. Pilleri Berne, Hirnananatomisches Institut, Ostermundingen, 40 p.

PILLERI G. & SIBER H. J. 1989. — Neuer spättertiärer

cetotherid (Cetacea, Mysticeti) aus der Pisco-Formation Perus. *Beiträge zur Paläontologie der Cetacean Perus*. G. Pilleri. Berne, Hirnanatomisches Institut, Ostermundigen: 108-115.

PIVORUNAS A. 1977. — The fibrocartilage skeleton and related structure of the ventral pouch of balaenopterid whales. *Journal of Morphology* 151: 299-314.

RALLS K. & MESNICK S. L. 2002. — Sexual dimorphism, *in* PERRIN W. F., WÜRSIG B. & THEWISSEN J. G. M. (eds), *Encyclopedia of Marine Mammals*. Academic Press, San Diego, 1414 p.

REEVES R. R. & LEATHERWOOD S. 1985. — Bowhead whale *Balaena mysticetus* Linnnaeus, 1758, *in* RIDGWAY S. H. & SIR HARRISON H. (eds), *Handbook of Marine Mammals*. Academic Press, New York: 305-344.

RICE D. W. 1998. — *Marine Mammals of the World. Systematics and Distribution*. Society for Marine Mammalogy, Lawrence, KS, 231 p.

SANDERS A. E. & BARNES L. G. 2002. — Paleontology of the late Oligocene Ashley and Chandler Bridge Formations, a new family of primitive mysticetes (Mammalia, Cetacea), *in* EMRY R. J. (ed.), Cenozoic mammals of land and sea: tribute to the career of Clayton E. Ray. *Smithsonian Contributions to Paleobiology* 93: 313-356.

SCHULTE H. V. W. 1916. — Monographs of the Pacific Cetacea. The Sei whale (*Balaenoptera borealis* Lesson). Part 2: Anatomy of a foetus of *Balaenoptera borealis*. *Memoirs of the American Museum of Natural History*, New York 1 (6), part 1: 391-502.

SIMPSON G. G. 1945. — The principles of classification, and a classification of mammals. *Bulletin of the American Museum of Natural History* 85: 1-350.

SLIJPER E. J. 1979. — *Whales*. Hutchinson, London, 511 p.

SWOFFORD D. L. 1998. — *PAUP*. Phylogenetic Analysis Using Parsimony (*and Other Methods)*. Version 4. Sinauer Associates, Sunderland, Massachusetts, software.

TRUE F. W. 1904. — The whalebone whales of the Western North Atlantic compared with those occuring in European waters with some observations on the species of the North Pacific. *Smithsonian Contribution to knowledge* 33: 1-332.

UHEN M. D. 2004. — Form, function, and anatomy of *Dorudon atrox* (Mammalia, Cetacea): an archaeocete from the middle to late Eocene of Egypt. *University of Michigan Papers on Paleontology* 34:1-222.

VAN BENEDEN P. J. 1882. — Description des ossements fossiles des environs d'Anvers. Part. 3 : genres *Megaptera*, *Balaenoptera*, *Burtinopsis* et *Erpetocetus*. *Annales du Musée royal d'Histoire naturelle de Belgique*, sér. Paléontologie 7: 1-90.

VAN BENEDEN P. J. 1886. — Description des ossements fossiles des environs d'Anvers. Part. 5 : cétacés. Genres *Amphicetus*, *Heterocetus*, *Mesocetus*, *Idiocetus* et *Isocetus*. *Annales du Musée royal d'Histoire naturelle de Belgique*, sér. Paléontologie 13: 1-139.

VAN BENEDEN P. J. & GERVAIS P. 1868-1880. — *Ostéographie des cétacés vivants et fossiles, comprenant la description et l'iconographie du squelette et du système dentaire de ces animaux ; ainsi que des documents relatifs à leur histoire naturelle*. Arthus Bertrand, Paris, 2 volumes: text, 634 p.; atlas, 64 pls.

VANDELLI A. A. 1831. — Additamentos ou notas a memoria geognostica ou golpe de vista do perfil das estratificações das differentes rochas que compõem os terrenos desde a Serra de Cintra até a de Arrabida. *Historia e memorias da Academia real das sciencias de Lisboa* 2 (1): 281-306.

WATSON L. 1981. — *Sea Guide to Whales of the World*. Hutchinson, London, 302 p.

WIBLE J. R. 1990. — Petrosals of Late Cretaceous marsupials from North America, and a cladistic analysis of the petrosal in therian mammals. *Journal of Vertebrate Paleontology* 10 (2): 183-205.

Submitted on 14 December 2005;
accepted on 24 April 2006.

APPENDIX 1

SYSTEMATICS OF THE OUTGROUP

Order CETACEA Brisson, 1762
Infraorder ARCHAEOCETI Flower, 1883
Family BASILOSAURIDAE Cope, 1868
Subfamily BASILOSAURINAE Cope, 1868

Genus *Zygorhiza* True, 1908

TYPE SPECIES. — *Basilosaurus kochii* Reichenbach, 1847.

Zygorhiza kochii (Reichenbach, 1847)

HOLOTYPE. — Geologisch-Paläontologisches Institut and Museum der Universität Berlin no. 15324, partial skull.

LOCALITY AND HORIZON. — Clark County, Alabama, USA, late Eocene.

REFERRED SPECIMEN. — USNM 11962.

REFERENCE. — Kellogg 1936.

Subfamily DORUDONTINAE Miller, 1923

Genus *Dorudon* Gibbes, 1845

TYPE SPECIES. — *Dorudon serratus* Gibbes, 1845.

Dorudon atrox (Andrews, 1906)

HOLOTYPE. — CGM 9319, cranium with right ramus of the lower jaw.

LOCALITY AND HORIZON. — Birket Qarun Formation, Fayum, Egypt, Bartonian to early Priabonian.

REFERRED SPECIMENS. — Those figured by Uhen 2004.

REFERENCE. — Uhen 2004.

SYSTEMATICS OF THE INGROUP

Infraorder MYSTICETI Cope, 1891
Superfamily AETIOCETOIDEA
Sanders & Barnes, 2002
Family AETIOCETIDAE Emlong, 1966
Subfamily AETIOCETINAE Emlong, 1966

Genus *Aetiocetus* Emlong, 1966

TYPE SPECIES. — *Aetiocetus cotylalveus* Emlong, 1966.

Aetiocetus cotylalveus Emlong, 1966

HOLOTYPE. — USNM 25210, sub-complete skull, both auditory areas and post-cranial elements.

LOCALITY AND HORIZON. — Yaquina Formation, Lincoln County, Oregon, USA, latest Oligocene.

REFERENCES. — Barnes *et al.* 1994; Emlong 1966; Sanders & Barnes 2002.

Subfamily CHONECETINAE Barnes, Kimura, Furusawa & Sawamura, 1994

Genus *Chonecetus* Russel, 1968

TYPE SPECIES. — *Chonecetus sookensis* Russel, 1968.

Chonecetus goedertorum
Barnes & Furasawa, 1994

HOLOTYPE. — LACM 131146, partial skull, dentary and post-cranial elements.

LOCALITY AND HORIZON. — Pysht Formation, Clallam County, Washington, USA, latest Oligocene.

REFERENCE. — Barnes *et al.* 1994.

REMARKS
As Ichishima (1997) mentioned it, the systematics of fossil mysticetes is far from clear in some cases (e.g., *Cetotherium*...). This is due to the fact that some taxa "are represented by non-diagnostic skeletal elements". According to this, and in order to minimize the number of missing data and to avoid

problems of uncertain taxa, when possible, only type species were used in the present study.

Infraorder MYSTICETI Cope, 1891

Genus *Aglaocetus* Kellogg, 1934

TYPE SPECIES. — *Cetotherium moreni* Lydekker, 1894.

Aglaocetus patulus (Kellogg, 1968)

HOLOTYPE. — USNM 23690, sub-complete skull (lacking both lachrymals and jugals, and pterygoids), both tympanics, left petrosal, and post-cranial elements.

LOCALITY AND HORIZON. — Calvert Formation, Virginia, USA, middle Miocene.

REFERRED SPECIMENS. — (1) USNM 13472, (2) USNM 23049.

REFERENCE. — Kellogg 1968.

Genus *Cetotherium* Brandt, 1843

TYPE SPECIES. — *Cetotherium rathkei* Brandt, 1843.

Cetotherium rathkei Brandt, 1843

HOLOTYPE. — Paleontological Institute of the Academy of Science, Moscow (uncatalogued), sub-complete skull lacking rostrum, left tympanic.

LOCALITY AND HORIZON. — South of Russia, late Miocene.

REFERENCES. — Brandt 1843, 1873; Pilleri 1986.

Genus *Cophocetus* Packard & Kellogg, 1934

TYPE SPECIES. — *Cophocetus oregonensis* Packard & Kellogg, 1934.

Cophocetus oregonensis
Packard & Kellogg, 1934

TYPE SPECIMEN. — CMUO, No. 305, sub-complete skull with tympanic and petrosal, both mandibles lacking the anterior end, and post-cranial elements.

LOCALITY AND HORIZON. — Astoria Formation, Newport, Oregon, USA, Miocene.

REFERRED SPECIMENS. — (1) USNM 13646, (2) CMUO 305, skull studied from Packard & Kellogg 1934.

REFERENCE. — Packard & Kellogg 1934.

Genus *Diorocetus* Kellogg, 1968

TYPE SPECIES. — *Diorocetus hiatus* Kellogg, 1968.

Diorocetus hiatus Kellogg, 1968

HOLOTYPE. — USNM 16783, sub-complete skull lacking its left half and the right petrosal, both mandibles lacking condyles and adjacent portion of the vertical ramus behind coronoid process, and post-cranial elements.

LOCALITY AND HORIZON. — Calvert County, Calvert Formation, Maryland, USA, middle Miocene.

REFERRED SPECIMENS. — (1) USNM 16871, (2) USNM 23494, (3) USNM 16567.

REFERENCE. — Kellogg 1968.

Genus *Eomysticetus* Sanders & Barnes, 2002

TYPE SPECIES. — *Eomysticetus whitmorei* Sanders & Barnes, 2002.

Eomysticetus whitmorei Sanders & Barnes, 2002

HOLOTYPE. — ChM PV 4253, sub-complete skull, both petrosals, both tympanics, both dentaries, post-cranial elements.

LOCALITY AND HORIZON. — Chandler Bridge Formation, South Carolina, USA, late Oligocene.

REFERENCE. — Sanders & Barnes 2002.

Genus *Herpetocetus*
Van Beneden, 1872

TYPE SPECIES. — *Herpetocetus scaldiensis* Van Beneden, 1872.

Herpetocetus sendaicus
(Hatai, Hayasaka & Masuda, 1963)

HOLOTYPE. — NSMT-PV 19540, sub-complete skull lacking anterior third of rostrum, with left tympanic and both petrosals still in situ in the skull, and prepared sub-complete right tympanic, and sub-complete post-cranial skeleton.

LOCALITY AND HORIZON. — Yushima Formation, Japan, Pliocene.

REFERRED SPECIMENS. — (1) NSMT-PV 19540, cast of the type specimen, (2) USNM 299652, right petrosal, Yorktown Formation, North Carolina, USA, Pliocene, from Geisler & Luo 1996, (3) ChM PV 5028, right petrosal, Yorktown Formation, North Carolina, USA, Pliocene, from Geisler & Luo 1996.

REFERENCES. — Geisler & Luo 1996; Oishi *et al.* 1985.

REMARKS

Since *Herpetocetus sendaicus* (NSMT-PV 19540) is not the type species of the genus *Herpetocetus*, the specimen NSMT-PV 19540 was used, and referred petrosal were studied. The choice of using these petrosals was supported by the fact that they noticeably resemble those that are still *in situ* in the skull of NSMT-PV 19540.

Genus *Metopocetus* Cope, 1896

TYPE SPECIES. — *Metopocetus durinasus* Cope, 1896.

Metopocetus durinasus Cope, 1896

HOLOTYPE. — USNM 8518, an incomplete cranium with right petrosal in situ in the skull and left petrosal prepared.

LOCALITY AND HORIZON. — Calvert Formation, Maryland, USA, middle Miocene.

REFERENCES. — Cope 1896; Kellogg 1968.

Genus *Mixocetus* Kellogg, 1934

TYPE SPECIES. — *Mixocetus elysius* Kellogg, 1934.

Mixocetus elysius Kellogg, 1934

HOLOTYPE. — LACM, Cat. No. 882, sub-complete skull, imperfectly preserved tympanics and petrosals, both mandibles, and post-cranial elements.

LOCALITY AND HORIZON. — Modelo Formation, Los Angeles County, California, USA, late Miocene.

REFERENCE. — Kellogg 1934.

Genus *Nannocetus* Kellogg, 1929

TYPE SPECIES. — *Nannocetus eremus* Kellogg, 1929.

Nannocetus eremus Kellogg, 1929

HOLOTYPE. — UCMP 26502, incomplete cranium, right tympanic and petrosal in situ in the skull, left tympanic and petrosal prepared.

LOCALITY AND HORIZON. — Towsley Formation, California, USA, late Miocene.

REFERENCE. — Kellogg 1929.

Genus *Parietobalaena* Kellogg, 1924

TYPE SPECIES. — *Parietobalaena palmeri* Kellogg, 1924.

Parietobalaena palmeri Kellogg, 1924

HOLOTYPE. — USNM 10668, sub-complete cranium lacking rostrum, with both petrosals and tympanic.

LOCALITY AND HORIZON. — Calvert Formation, Maryland, USA, middle Miocene.

REFERRED SPECIMENS. — (1) USNM 7424, (2) USNM 10677, (3) USNM 10909, (4) USNM 11535, (5) USNM 12697, (6) USNM 13874, (7) USNM 13903, (8) USNM 15576, (9) USNM 16119, (10) USNM 16568, (11) USNM 16570, (12) USNM 16667, (13) USNM 16838, (14) USNM 20376, (15) USNM 23015, (16) USNM 23022, (17) USNM 23055, (18) USNM 23203, (19) USNM 23448, (20) USNM 23725.

REFERENCES. — Kellogg 1924, 1968.

Genus *Pelocetus* Kellogg, 1965

TYPE SPECIES. — *Pelocetus calvertensis* Kellogg, 1965.

Pelocetus calvertensis Kellogg, 1965

HOLOTYPE. — USNM 11976, sub-complete skull, with both tympanics and petrosals, both mandibles, and post-cranial elements.

LOCALITY AND HORIZON. — Calvert Formation, Maryland, USA, late Miocene.

REFERRED SPECIMENS. — (1) USNM 14693, (2) USNM 21306, (3) USNM 23058, (4) USNM 23059.

REFERENCE. — Kellogg 1965.

Genus *Piscobalaena* Pilleri & Siber, 1989

TYPE SPECIES. — *Piscobalaena nana* Pilleri & Siber, 1989.

Piscobalaena nana Pilleri & Siber, 1989

HOLOTYPE. — SMNK 4050, incomplete skull lacking the dorsal part of the braincase, both premaxillae and one tympanic.

LOCALITY AND HORIZON. — Pisco Formation, Peru, early Pliocene.

REFERRED SPECIMENS. — (1) MNHN SAS 1616, (2) MNHN SAS 1617, (3) MNHN SAS 1618, (4) MNHN SAS 1623, (5) MNHN SAS 892, (6) MNHN SAS 1624, (7) MNHN PPI 259.

REFERENCE. — Pilleri & Siber 1989.

Family BALAENOPTERIDAE Gray, 1864
Subfamily BALAENOPTERINAE Gray, 1864

Genus *Balaenoptera* Lacépède, 1804

TYPE SPECIES. — *Balaenoptera gibbar* Lacépède, 1804 (junior synonym of *Balaena physalus* Linnaeus, 1758).

Balaenoptera acutorostrata Lacépède, 1804

AGE. — Ranging from late middle Miocene to Present.

REFERRED SPECIMENS. — (1) MNHN 1881-1225 (A11683), (2) MNHN 1886-328, (3) MNHN 1885-729

REFERENCES. — Reeves & Leatherwood 1985; True 1904; Van Beneden & Gervais 1880; Watson 1981.

Balaenoptera physalus (Linnaeus, 1758)

AGE. — Ranging from late middle Miocene to Present.

REFERRED SPECIMENS. — (1) MNHN 1889-403, (2) MNHN 1983-108, (3) MNHN 1894-36

REFERENCES. — Reeves & Leatherwood 1985; True 1904; Watson 1981.

Subfamily MEGAPTERINAE Gray, 1864

Genus *Megaptera* Gray, 1846

TYPE SPECIES. — *Balaena novaeangliae* Borowski, 1781.

Megaptera novaeangliae (Borowski, 1781)

AGE. — Ranging from late middle Miocene to Present.

REFERRED SPECIMEN. — MNHN A2931.

REFERENCES. — Reeves & Leatherwood 1985; True 1904; Van Beneden & Gervais 1880; Watson 1981.

Family ESCHRICHTIIDAE
Ellerman & Morrison-Scott, 1951

Genus *Eschrichtius* Gray, 1864

TYPE SPECIES. — *Balaenoptera robusta* Lilljeborg, 1861.

Eschrichtius robustus (Lilljeborg, 1861)

AGE. — Ranging from late Pleistocene (Barnes & McLeod, 1984) to Present.

REFERRED SPECIMENS. — Specimens figured by Barnes & McLeod 1984, and (1) USNM 364970, tympanic, (2) USNM 364975, tympanic, (3) USNM 364979, tympanic, (4) USNM 571931, petro-tympanic.

REFERENCES. — Barnes & McLeod 1984; Reeves & Leatherwood 1985; True 1904; Watson 1981.

Family BALAENIDAE Gray, 1821

Genus *Balaena* Linnaeus, 1758

TYPE SPECIES. — *Balaena mysticetus* Linnaeus, 1758.

Balaena mysticetus Linnaeus, 1758

AGE. — Ranging from early Miocene to Present.

REFERENCES. — Reeves & Leatherwood 1985; Van Beneden & Gervais 1880; Watson 1981.

Genus *Eubalaena* Gray, 1864

TYPE SPECIES. — *Eubalaena glacialis* Müller, 1776.

Eubalaena glacialis Müller, 1776

AGE. — Ranging from early Miocene to Present.

REFERRED SPECIMENS. — (1) MNHN 1921-123, (2) MNHN 1903-1795, (3) MNHN 1877-93, (4) MNHN 1921-123 (A2929).

REFERENCES. — Cummings 1985; Reeves & Leatherwood 1985; True 1904; Van Beneden & Gervais 1880; Watson 1981.

Family NEOBALAENIDAE Gray, 1873

Genus *Caperea* Gray, 1864

TYPE SPECIES. — *Balaena marginata* Gray, 1846.

Caperea marginata (Gray, 1846)

AGE. — Present, lacking fossil register.

REFERRED SPECIMENS. — (1) MNHN 1879-259, (2) USNM 550146.

REFERENCE. — Watson 1981.

APPENDIX 2

Characters list. See Appendix 3 for the data matrix.

SKULL

1. Rostrum shape in lateral view: 0, sub-rectilinear; 1, dorsally bowed.

2. Part of the rostrum anterior to the anterior end of the nasals in lateral view: 0, depressed; 1, not depressed.

3. Maxillary teeth: 0, present; 1, absent.

4. Vascular foramina on the palate: 0, small and few; 1, open in anterolaterally or anteroposteriorly directed grooves on the ventral surface of the maxilla, related (in Recent mysticetes) to irrigation of the epithelium producing baleen (modified from Geisler & Sanders 2003: K 17).

5. Palatal surface of the rostrum: 0, flat or gently concave; 1, bears pronounced longitudinal keel (formed by the vomer and maxillae) along the midline of the rostrum (McLeod *et al.* 1993; Geisler & Sanders 2003: K 16).

6. Angle of the lateral edge of the maxilla (in anterior half) in cross section: 0, more than 45°; 1, less than 45° (Geisler & Sanders 2003: K 4 modified).

7. Extension of the posteroventral edge of the maxilla in a posteroventrally directed plate below the lacrimal: 0, absent; 1, present (modified from Geisler & Sanders 2003: K 59).

8. Preorbital notch of maxilla (a pronounced preorbital notch is a consequence of a conspicuous lateral expansion of the preorbital process of the maxilla and supraorbital process of the frontal relatively to the base of the rostrum): 0, absent; 1, present.

9. Oblique groove (posteroventrolateral-anterodorsomedial) on the anterolateral face of the zygomatic process of maxilla for the passage of the facial nerve from the ventral face of the skull to the dorsal side of the rostrum: 0, absent; 1, present (modified from Geisler & Sanders 2003: K 13).

10. Preorbital process of the maxilla: 0, absent; 1, knob-like and rounded with a variably developed short crest extending anteromedially on the maxilla; 2, elongated, extending posteromedially in a crest on the posterior edge of the maxilla along the anteromedial edge of the supraorbital process of the frontal.

11. Posterior extension of the ascending process of maxilla: 0, does not extend posterioly beyond the anterior edge of the supraorbital process; 1, apex of the ascending processes are posterior to the preorbital process of the frontal and anterior to the postorbital process; 2, at the same level as or posterior to the postorbital process of the frontal; 3, absent (the maxilla does not have a true process and the Mx-Fr suture is roughly perpendicular to the axis of the skull).

12. Morphology of the ascending process of maxilla: 0, subtriangular (edges converging posteriorly) with pointed or rounded posterior end; 1, elongated with subparallel edges and squared apex; -, non applicable (Geisler & Sanders 2003: K 14).

13. Medial contact of the ascending processes of the maxillae: 0, contact absent, processes widely separated; 1, processes contacting or very approximated at apex only; 2, long contact posteriorly; -, not applicable.

14. Position of the posterior end of the ascending process of the maxilla relatively to the posterior extremity of the nasal: 0, anterior; 1, approximately at the same level or slightly posterior; 2, strongly posterior.

15. Orientation of the posteromedial angle of the maxilla (whether an ascending process is present or not): 0, faces dorsally; 1, faces laterally.

16. Fronto-maxillar suture length: 0, short and not reaching the level of the vertex posteromedially; 1, long and reaching (or close to) the vertex posteromedially.

17. Shape of the fronto-maxillar suture: 0, straight or slightly V-shaped posteriorly and oblique; 1, slightly concave posterolaterally and oblique; 2, strongly concave posterolaterally and forming an acute angle; 3, roughly straight and transverse, or slightly convex posteriorly; 4, roughly straight and oblique posteriorly.

18. Posterior extension of the premaxillae relative to the posterior extremity of the maxillae: 0, anterior; 1, at the same level; 2, posterior.

19. Lateral edges of the nasals: 0, subparallel or tapering anteriorly (bones rectangular or trapezoid) or slightly convergent posteriorly; 1, strongly convergent posteriorly (bones distinctly triangular and wedge-shaped).

20. Frontal-nasal suture: 0, frontal has anterior wedge between posterior ends of the nasals; 1, approximately straight transversely (modified from Muizon 1988; Geisler & Sanders 2003: K 121).

21. Posterior limit of the narial fossa: 0, conspicuously anterior to the line joining the preorbital processes of the frontals; 1, posterior or at the same level as the line joining the preorbital processes of the frontals.

22. Separation of the premaxillae anterior to the bony nares: 0, absent or very close; 1, present (modified from Geisler & Sanders 2003: K 67).

23. Position of the line joining the preorbital processes of the frontals: 0, posterior or on the same level as the posterior extremity of the nasals; 1, passing through the nasals length; 2, anterior or on the same level as the anterior extremity of the nasals.

24. Position of the temporal crest: 0, on posterior edge of the supraorbital process of the frontal; 1: on dorsal surface of the supraorbital process; 2, absent or hardly discernible on the dorsal surface of the supraorbital process (modified from Geisler & Sanders 2003: K 131).

25. Orientation of the supraorbital process of the frontal: 0, roughly transverse; 1, anteriorly oriented (which gives an anteriorly opened V-shaped morphology of the posterior edge of the rostral bones); 2, posteriorly oriented.

26. Shape of the supraorbital process of the frontal in dorsal view: 0, medial portion shorter than lateral; 1, medial portion as long as lateral; 2, medial portion longer than lateral.

27. Width of the supraorbital process: 0, roughly as long (at the dorsal edge of the orbit) as wide transversely; 1, slightly wider than long; 2, distinctly wider than long (more than twice its length above the orbit).

28. Morphology of the dorsal surface of the supraorbital process: 0, subhorizontal; 1, gradually sloping ventrally and laterally; 2, abruptly depressed medially (modified from Miller 1923; Lindow B. E. K. 2002).

29. Posterior edge of the supraorbital process of the frontal: 0, concave posteriorly; 1, roughly straight and transversely oriented.
30. Shape of postorbital process of frontal: 0, short and blunt; 1, long and finger-like.
31. Postorbital process of the frontal and zygomatic process: 0, widely separated; 1, very close or contacting.
32. Temporal fossa: 0, anteroposteriorly elongated; 1, transversely elongated.
33. Position of the orbit in lateral view relative to a plane joining the apex of the rostrum and the occipital condyles: 0, dorsal; 1, at the same level or ventral.
34. Shape of the dorsal edge of the orbit in dorsal view: 0, roughly straight or slightly concave; 1, deeply notched.
35. Dorsal exposure of parietals in the sagittal plane of the skull: 0, long; 1, short; 2, totally covered by frontals and/or supraoccipital.
36. Dorsal exposure of frontals in the sagittal plane of the skull (modified from Dooley *et al.* 2004): 0, long; 1, short; 2, totally covered by rostral bones.
37. Crest-like or ridge-like portion of the parieto-squamosal suture: 0, absent; 1, present.
38. Height of the supraoccipital relatively to the frontal and/or nasals: 0, higher; 1, at the same level (modified from Geisler & Sanders 2003: K 128).
39. Telescoping of the supraoccipital (position of the anteriormost limit of the supraoccipital): 0, posterior to the line joining the apices of the zygomatic processes; 1, at the same level as the line joining the apices of the zygomatic processes; 2, anterior to the line joining the apices of the zygomatic processes but posterior to the line joining the preorbital processes of the frontals; 3, anterior to the line joining the preorbital processes of the frontals.
40. Medial occipital crest: 0, absent or ridge only; 1, present and elevated.
41. Shape of zygomatic process in dorsal view: 0, transversely thin and long; 1, transversely massive and relatively long; 2, very short and knob-like (modified from Lindow 2002).
42. Orientation of zygomatic process in dorsal view: 0, anteromedially oriented; 1, subparallel to the sagittal axis of the skull; 2, anterolaterally oriented.
43. Dorsal crest of the zygomatic process: 0, present; 1, absent; -, non applicable.
44. Morphology of the postglenoid process in lateral view: 0, thin; 1, thick; 2, extremely reduced to absent.
45. Orientation of the postglenoid process in lateral view: 0, subvertical to anteriorly projected; 1, subvertical to slightly posteriorly projecting; 2, strongly projecting posteriorly; -, non applicable.
46. Orientation of the postglenoid process in posterior view: 0, ventrally oriented; 1, ventrolaterally oriented.
47. Twisting of the postglenoid process in ventral view: 0, not twisted and roughly transverse to the sagittal axis of the skull; 1, twisted clockwise on the right side and anticlockwise on the left side.
48. Postglenoid process in lateral view: 0, anterior and posterior sides nearly parallel with squared-off ventral end; 1, tapers ventrally to a point (modified from Geisler & Sanders 2003: K 151).
49. Glenoid cavity: 0, deeply concave, transverse, and facing anteriorly; 1, very shallow, subcircular, and facing ventrally; 2, very shallow, subcircular to slightly elongated anteroposterioly, and facing anteroventrally; 3, circular, almost flat, facing almost ventrally, and located on all the anterior edge of the postglenoid process; 4, circular almost flat facing anteriorly.
50. Basioccipital process (strong and massive tubercle on the basioccipital crest for the origin of the longus colli): 0, absent; 1, present.
51. Basioccipital crest: 0, narrow transversely; 1, wide and bulbous (Geisler & Sanders 2003: K 191).
52. Foramen pseudovale: 0, perforating the squamosal with a participation of the pterygoid; 1, perforating the squamosal only; 2, perforating the pterygoid only.
53. Anterior edge of supraoccipital in dorsoposterior view: 0, semicircular; 1, triangular, sharply pointed anteriorly; 2, triangular and rounded to squared anteriorly (modified from Geisler & Sanders 2003: K 152).
54. Orientation of the lambdoid crests of supraoccipital: 0, dorsally directed (posterodorsally in posterolateral portion); 1, horizontal and directed anterolaterally, overhanging temporal fossae (modified from Geisler & Sanders 2003: K 153).
55. Posterior extension of the lateral edge of the paroccipital process in ventral view: 0, anterior to the posterior edge of the condyle; 1, level with the posterior edge of the condyle; 2, posterior to the posterior edge of the condyle (modified from Geisler & Sanders 2003: K 197).

TYMPANIC

56. Orientation of the main axes of the tympanics: 0, parallel; 1, diverging posteriorly; 2, diverging anteriorly.
57. Posterior end of the tympanic: 0, bilobate; 1, unilobate.
58. Relative position of the dorsal and ventral lobes: 0, equally project posteriorly; 1, the ventral lobe projects further posteriorly than the dorsal; -, non applicable.
59. Median groove: 0, in posterior view, the two lobes are separated by a deep groove; 1, the two lobes are separated by a flat area; -, non applicable.
60. Dorsoventral compression and mediolateral expansion of the tympanic: 0, absent; 1, present. State 1 is especially obvious on the involucrum, which is wider than the total width of the bulla at the level of the sigmoid process.
61. Orientation of the "lip" of the tympanic: 0, faces laterally; 1, faces ventrolaterally to ventrally.

PERIOTIC

62. Posterior processes of the tympanic and periotic: 0, unfused; 1, fused.
63. Morphology of the anterior process of the petrosal: 0, distinctly shorter than the pars cochlearis; 1, approximately as long as the pars cochlearis or slightly longer; 2, long (distinctly longer than the pars cochlearis); 3, knob-like.
64. Apex of the anterior process of the periotic: 0, straight (not deflected ventrally); 1, deflected ventrally (modified from Geisler & Sanders 2003: K 202; Fordyce 1994).
65. Sulcus for capsuloparietal emissary vein: 0, present, forms a dorsoventral groove on lateral side of anterior process immediately anterior to lateral tuberosity; 1, absent (Geisler & Sanders 2003: K 206).
66. Ventrolateral ridge of periotic: 0, absent; 1, present; 2, present and expanded (Geisler & Luo 1996: K 16;

Geisler & Sanders 2003: K 215).

67. Bone structure of the periotic: 0, the periotic is made of dense bone (osteosclerotic) and its surface is smooth; 1, posterior process of periotic is made of spongy bone and is pitted and rugose, remaining portions are smooth and dense; 2, posterior and superior processes are made of spongy bone, the dorsal part of the anterior process is also made of spongy bone but the lateral and ventral parts are relatively dense; 3, most of the periotic is made of spongy bone essentially the posterior, the dorsal, and the anterior processes and the dorsal region of the pars cochlearis (modified from Geisler & Sanders 2003: K 216).

68. Fenestra rotunda: 0, oval; 1, shaped like a teardrop with a fissure directed towards the perilymphatic foramen (Geisler & Sanders 2003: K 222).

69. Ventrolateral expansion (ventrolateral tubercle) at base of the anterior process: 0, absent; 1, rounded or blade-like; 2, long process.

70. Morphology of the apex of the anterior process: 0, quadrate or rounded; 1, pointed and tapering until the apex; -, non applicable.

71. Suprameatal fossa and tegmen tympani: 0, relatively flat (or slightly concave) with a low tegmen tympani; 1, the fossa is distinctly concave and the tegmen tympani is more elevated and thicker; 2, the fossa expands laterally and its surface is still somehow concave but rugose irregular, this morphology being related to the great thickening and enlargement of the tegmen tympani; 3, because of its extreme growth, the tegmen tympani totally invades the suprameatal fossa, which is indistinct.

72. Internal auditory meatus: 0, cerebral opening for the facial nerve and vestibulocochlear foramen separated by a low crista transversa; 1, cerebral opening for the facial nerve and vestibulocochlear foramen separated by an elevated crista transversa.

73. Fundus of internal acoustic meatus: 0, funnel-like, smaller at the blind end and wide near the rim; 1, tubular (Geisler & Sanders 2003: K 234).

74. Crista transversa: 0, thin; 1, thick.

75. Morphology of the facial foramen on the internal acoustic meatus: 0, roughly circular; 1, the anterior edge of the foramen is notched (slightly to deeply) for the passage of the greater petrosal nerve. This condition corresponds to a confluence of the internal facial foramen and the hiatus Fallopii.

76. Promontorium morphology in ventral view: 0, roughly hemispherical; 1, transversely narrow, rim-like; 2, roughly circular and little convex.

77. Dorsal expansion of the pars cochlearis: 0, not expanded dorsally (width at base longer than proximodistal length); 1, little expanded dorsally (width at base approximately similar to proximodistal length); 2, conspicuously expanded dorsally (width at base shorter than proximodistal length).

78. Mallear fossa: 0, present and well defined; 1, shallow or absent.

79. Fossa incudis: 0, present and deep; 1, poorly defined or absent.

80. Attachment for the tensor tympani muscle: 0, deep fossa with well defined edges; 1, notch on the anterior edge only, with distinct edges; 2, shallow and wide depression without edges (no groove, sulcus or fossa) (modified from Geisler & Sanders 2003: K 217).

81. Groove on the medial side of the promontorium: 0, absent; 1, present.

82. Caudal tympanic process of the periotic: 0, low, rounded ridge; 1, prominent and sharp crest, its ventral and posterior edges form a right or acute angle in medial view (modified from Geisler & Sanders 2003: K 225).

83. Facial nerve sulcus on the posterior process of the petrotympanic: 0, does not extend on the posterior process of the periotic; 1, deep and tubular all along the process; 2, deep at base and progressively shallowing and little marked on the distal two thirds of the process.

84. Length of the posterior processes (periotic + tympanic): 0, shorter than or approximately as long as the rest of the periotic (pars cochlearis + anterior process); 1, distinctly longer than the rest of the periotic.

85. Morphology of the posterior processes of the periotic and tympanic (whether fused or not): 0, roughly oval-shaped and nodular; 1, conical to tetrahedral, strongly widening distally; 2, roughly cylindrical; 3, anteroposteriorly flattened at apex; 4, dorsoventrally flattened at apex.

86. Orientation of the external exposure of the posterior processes of the petrotympanic (the ventral edge of the surface is limited by the lateral end of the facial groove): 0, distal surface small, irregular and not clearly defined; 1, relatively flat (concave in juveniles), vertical and facing roughly laterally; 2, oblique and facing conspicuously ventrolaterally to ventrally; -, surface poorly defined and rugose with no precise edges or apex totally tapered and no proper surface is observable (in these cases the character is not applicable).

DENTARY

87. Morphology of the dentary in dorsal view: 0, straight; 1, bowed medially.

88. Mandibular symphysis: 0, the two dentaries are connected medially by a bony suture; 1, the dentaries have no suture at their apices but are independent and connected by a ligament only attached on a short horizontal rim on the medial edge of the apex of the dentary.

89. Anterior extremity of the dentary: 0, vertical; 1, twisted with the ventral edge shifted medially (i.e. the apex is twisted clockwise on the right dentary and anticlockwise on the left); 2, apex of the dentary almost horizontal.

90. Height of the horizontal ramus of the dentary: 0, slightly increasing in height posteriorly; 1, height constant all along its length; 2, expanded and arched dorsoventrally.

91. Cross-section of the horizontal ramus: 0, both edges are convex; 1, lateral edge is convex and medial edge is flat.

92. Coronoid process: 0, well developed, elevated and blade-like; 1, short, hook-like and outwardly bent; 2, limited to a small hump or absent.

93. Morphology of the angular process: 0, bony blade ventral to the condyle; 1, knob-like.

94. Posterior expansion of the angular process: 0, located below the condyle or slightly anterior; 1, projects posteriorly posterior to the condyle.

95. Relationships of the condyle and angular process: 0, individualized from the condyle; 1, merged to the condyle in a single nodular region at the posterior

edge of the dentary.

96. Notch for the insertion of the internal pterygoid muscle: 0, absent; 1, present medially only; 2, deep groove on the posterior separating the condyle and angular process medially or/and laterally.

97. Position of the opening of the mandibular canal: 0, anterior to the apex of the coronoid process; 1, approximately below the apex of the coronoid process; 2, well posterior.

98. Mandibular fossa: 0, small (half the height of the dentary, or less) or absent; 1, large cavity (more than half the height of the dentary) posterior to mandibular foramen (modified from Geisler & Sanders 2003: K 43).

99. Position of the condyle: 0, facing almost posteriorly with a slight dorsal component and off set laterally; 1, high on the posterior end of the dentary, facing posterodorsally with a dorsal component much more developed than the posterior; 2, facing posteriorly on most of the posterior end of the dentary; 3, facing almost dorsally on most of the posterior end of the dentary.

100. Dorsal surface of the condyle: 0, elevated above the dorsal edge of the horizontal ramus of the mandible; 1, at the level of or below the dorsal edge of the horizontal ramus (Geisler & Sanders 2003: K 45).

101. Shape of the condyle: 0, small and triangular, transversely wide and dorsoventrally narrow; 1, transversely narrow (distinctly narrower than long); 2, wide, massive, and rounded and forming the two thirds of the posterior end of the dentary; 3, hemispherical and located at the posterodorsal end of the dentary.

APPENDIX 3

Data matrix of the distribution of the character states of 101 characters of the skeleton in 23 taxa of cetaceans. See appendix 2 for character list. **?**, missing; **-**, non applicable.

```
12345678911111111112222222222333333333344444444445555555555666666666677777777778888888888999999999911
         01234567890123456789012345678901234567890123456789012345678901234567890123456789012345678900
                                                                                                   01
```

Zygozhiza k.
```
00000000001001000000000000000000000000000000000000000000000000000000000000000000000000000000000000000
```
Dorudon a.
```
00000000000000000000000000000000000000000000000000000001000000000000000000000000000000000000000000000
```
Chonecetus c.
```
000001000010000002000110000000100010010000000000010011000?00000001?0?????????000??0??000010100000?10001
```
Aetiocetus c.
```
000001001110010001000110000001100101000001000001001100100000000??????????????????????0??0??100????????
```
Eomysticetus w.
```
001?01?????????1?10100100010010000?010001121010?11111101?000000110010101000000000001000011010000?0?10001
```
Nannocetus e.
```
???????????????????????????1???1?????????101101121 1????00010?11001101011011111?0011011???????????????
```
Mixocetus e.
```
011111?1?1?0??011??110211?110111101211011101110?11112?2??????1????????????????1?????11????????????????
```
Cetotherium r.
```
011?1?1112211101101 11?211010111?111000111012011211010210010111 0??1010?1???01?001110111??111?????????
```
Metopocetus d.
```
???????????01101?011???????????????2210?1???????1????100???????10111010110110 11?011?011???????????????
```
Herpetocetus s.
```
0111111?1?21220110111?2010110??11?2210111101201121101021010011101110101101101110111 0111??111110101101
```
Piscobalaena n.
```
0111111112212201101110201011011111221001120121012110201001001110111010110110110011101111111111 0121101
```
Pelocetus c.
```
01111111111001013101011101110111111100101101110111111 0201--011?1?2?0??2101?11110?1212-111111100121212
```
Cophocetus o.
```
011111??1?????0???01?01?0?110?????11?0?0110111011111?1022???0111??2???0?1001011???1?1??1??111100?20212
```
Parietobalaena p.
```
0111111?1?3-0101310100010111011110110010110110001111 10121--01111122010210000111111212-11111100110212
```
Aglaocetus p.
```
01111111113-010131010002011100111011002012011101111 1101?01101111122110200001111011212-???????????????
```
Diorocetus h.
```
011111111110010131000111001101111011001112011101111110120110111111201021000 1111111212-1111111101?1202
```
Megaptera n.
```
011111111101010121010122021210111022012012111100101021101--011111231113010002112012 13-11111100221212
```
Balaenoptera a.
```
011111111111010121010122021210111022012011111100101021101--0112112311130100021120121 3-11111100221212
```
Balaenoptera p.
```
011111111111010121011112021210111022012011111100101021101--0112112311130100021120121 3-11111100221212
```
Eschrichtius r.
```
111111111111011111010112021201110121010011012000211020201--11111?231113110002111012142111212110121113
```
Caperea m.
```
11111111113-01114101010220210011102101302--1---14011212?1--111111231003111021112012142111202101121313
```
Balaena m.
```
11111111113-01113100010200210011102101302--2---0301121111--1113--2312-310000111101214211211210 1121303
```
Eubalaena g.
```
11111111113-01113100010200210011102101302--2---0301221111--1113--2312-310000111101214211211210 1121303
```

APPENDIX 4

TABLE 9. — Measurements of the tympanic of *Piscobalaena nana* (in mm).

	SMNK PAL 4050	MNHN SAS 892	MNHN SAS 1616	MNHN SAS 1617	MNHN SAS 1618	MNHN SAS 1623
Greatest width	51	51	54	55	50	59
Greatest length	65	63	63	65	60	67

TABLE 10. — Measurements of the malleus of *Piscobalaena nana* (in mm).

	MNHN SAS 892	MNHN SAS 1617	MNHN SAS 1618
Distance between the lateral most edge of the head to the apex of the manubrium	17	16	16
Distance between the anterior- and posteriormost edges of the articular head	12	12	12

TABLE 11. — Measurements of the skull of *Piscobalaena nana* (in mm). Abbreviation: **e**, estimated.

	SMNK PAL 4050	MNHN SAS 892	MNHN SAS 1616	MNHN SAS 1617	MNHN SAS 1618	MNHN SAS 1623
Greatest length of premaxilla	–	–	–	790	785e	–
Greatest width of rostrum	251	221	197	246	240	–
Width of the two ascending processes of maxillae at posterior apex	–	42	35	41	41	50
Length of nasal	–	–	–	114	–	148
Anterior width of nasal	–	–	–	21	–	18
Height of skull from plane of preorbital notch of maxilla to vertex	–	134	77	83	109	131
Greatest width of external nares	–	81	68	79	92	99
Distance between preorbital notch	255	240	21	275	253	270
Distance between preorbital processes of maxillae	370	357	291	380e	380e	369
Greatest length of orbit	84	87	75	77	86	86
Intertemporal width	118	134	107	130	122	130
Greatest length of temporal fossa	91	90	62	85	80	92
Greatest width of temporal fossa	129	150	88	113	128	124
Bizygomatic width	410	397	324	403	418	432
Maximum length of zygomatic process from apex of process to extremity of postglenoid process	178	158	142	167	182	194

Distance between lateral edges of paroccipital processes of exoccipital	262	278	218	286	290	313
Dorsal margin of foramen magnum to vertex	–	133	115	130	128	133
Transverse diameter of foramen magnum	–	43	36	40	37	39
Vertical diameter of foramen magnum	–	52	40	45	47	60
Greatest distance between lateral edges of occipital condyles	120	120	99	113	151	131
Vertical diameter of occipital condyle	–	64	61	73	88	80
Distance between medial edge of occipital condyle to lateral edge of paroccipital process of exoccipital	115	124	101	128	132	139
Distance between medial edges of foramina pseudovale	149	154	123	146	143	160
Distance between medial edges of basioccipital processes	39	39	21	20	31	41
Distance between lateral edges of basioccipital processes	114	111	82	100	108	122
Distance between apex of postglenoid processes	308	297	248	305	287	330e
Greatest internal height of braincase	–	–	–	–	–	83
Greatest thickness of vertex	–	–	–	–	–	57
Greatest thickness of basioccipital	–	–	–	–	–	38

TABLE 12. — Measurements of the dentary of *Piscobalaena nana* (in mm). Abbreviation: **e**, estimated.

	MNHN SAS 892	**MNHN SAS 1617**	**MNHN SAS 1618**
Total length in straight line	989	1023e	1024
Height at coronoid process level	80	83	85
Distance between coronoid process and mandibular condyle	140	153	134
Height at anterior apex	67	71	73
Greater width	43	43	45

TABLE 13. — Measurements of the hyoid of *Piscobalaena nana* (in mm).

	MNHN SAS 1617	MNHN SAS 1618
Distance in straight line between the two long cornuas	175	190
Height measured from the posteroventral edge of the hyoid to the apex of the best preserved little cornua	59	62

TABLE 14. — Measurements of the atlas and axis of *Piscobalaena nana* (in mm).

	MNHN SAS 1624	MNHN SAS 1617	MNHN SAS 892	MNHN SAS 1618
Atlas width	136	151	153	157
Atlas height	95	101	106	115
Axis width	175	191	189	199
Axis height	91	104	113	120

TABLE 15. — Measurements of the scapula of *Piscobalaena nana* (in mm).

	MNHN SAS 892	MNHN SAS 1617	MNHN PPI 260
Greatest length	416	-	358
Greatest height	196	200	191

TABLE 16. — Measurements of the humerus of *Piscobalaena nana* (in mm).

	MNHN SAS 1617	MNHN SAS 892
Proximodistal length	175	182
Anteroposterior length of proximal epiphysis	104.1	104.8
Transverse length of proximal epiphysis	81	76.7
Anteroposterior length of distal epiphysis	80.5	90.9
Transverse width of distal epiphysis	36	34.6

TABLE 17. — Measurements of the radius of *Piscobalaena nana* (in mm).

	MNHN SAS 1617	MNHN SAS 892
Greatest length of the radius	262	247

TABLE 18. — Measurements of the ulna of *Piscobalaena nana* (in mm).

	MNHN SAS 1617	MNHN SAS 892
Greatest length of the ulna	278	267